R-06-22

Evaluation of hydrogeological properties for Hydraulic Conductor Domains (HCD) and Hydraulic Rock Domains (HRD)

Laxemar subarea – version 1.2

Ingvar Rhén, Torbjörn Forsmark,
Ingela Forssman, Miriam Zetterlund
SWECO VIAK

April 2006

Svensk Kärnbränslehantering AB
Swedish Nuclear Fuel
and Waste Management Co
Box 5864
SE-102 40 Stockholm Sweden
Tel 08-459 84 00
+46 8 459 84 00
Fax 08-661 57 19
+46 8 661 57 19

ISSN 1402-3091
SKB Rapport R-06-22

Evaluation of hydrogeological properties for Hydraulic Conductor Domains (HCD) and Hydraulic Rock Domains (HRD)

Laxemar subarea – version 1.2

Ingvar Rhén, Torbjörn Forsmark,
Ingela Forssman, Miriam Zetterlund
SWECO VIAK

April 2006

Keywords: Hydrogeology, Hydrogeological model, Hydrogeological properties, Fracture zones, Fractures, Crush, Hydraulic tests, Difference flow measurements, Injection tests.

Abstract

The Initial Site Investigations (ISI) at Oskarshamn finished in 2005. A number of new boreholes were drilled and investigated during ISI (core holes: KSH01A, KSH02, KSH03A, KLX03, KLX04, KLX05, KLX06 and KAV04A and B) some old core holes were tested with new methods (KAV01, KLX02), and a number of new percussion holes were drilled and investigated (HSH01–03, HAV09–10 and 9 HLXxx boreholes). In some boreholes (KLX05, KLX06), only preliminary tests during drilling were available for analysis, and in KLX03 not all data planned for the borehole were available for the analysis in this report. Different types of investigations have been performed in the boreholes and the data for the analysis are based on data freeze for Laxemar model version 1.2 (November 2004).

The analysis done for Laxemar model version 1.2 comprises estimates of hydraulic properties based on data from the Simpevarp and Laxemar subareas, including data from the Äspö HRL. The estimates of hydraulic properties and conditions for Laxemar model version 1.2 in this report are the base for the Site Description Model L1.2 and the numerical groundwater flow simulations, reported elsewhere.

Sammanfattning

De inledande platsundersökningarna (IPLU) i Oskarshamn slutfördes under 2005. Ett flertal nya borrhål borrades och undersöktes under IPLU (kärnborrhål: KSH01A, KSH02, KSH03A, KLX03, KLX04, KLX05, KLX06 och KAV04A and B) några äldre borrhål testades på nytt med nya metoder (KAV01, KLX02), och ett antal nya hammarborrhål borrades och undersöktes (borrhålen HSH01–03, HAV09–10 och 9 HLXxx). I några borrhål (KLX05, KLX06), fanns endast preliminära resultat från borrningen, och i KLX03 fanns ej alla data som planerats för borrhålet tillgängliga för analysen i denna rapport. Olika typer av undersökningar har utförts i borrhålen och dataunderlaget för analysen baseras på datafrysen för Laxemar modelversion 1.2.

Analysen utförd för Laxemar modelversion 1.2 innehåller skattningar av hydrauliska egenskaper baserat på data från Simpevarp och Laxemar delområden samt data från Äspölaboratoriet. Skattningarna av de hydrauliska egenskaperna och förhållanden för Laxemar modellversion 1.2 är basen för den platsbeskrivande modellen Laxemar 1.2 och de utförda numeriska grundvattenflödesmodelleringarna, rapporterade i andra rapporter.

Summary

The Initial Site Investigations (ISI) at Oskarshamn finished in 2005. A number of new boreholes were drilled and investigated during ISI (core holes: KSH01A, KSH02, KSH03A, KLX03, KLX04, KLX05, KLX06 and KAV04A and B) some old core holes were tested with new methods (KAV01, KLX02), and a number of new percussion holes were drilled and investigated (HSH01–03, HAV09–10 and 9 HLXxx boreholes). In some boreholes (KLX05, KLX06), only preliminary tests during drilling were available for analysis, and in KLX03 not all data planned for the borehole were available for the analysis in this report. Different types of investigations have been performed in the boreholes and the data for the analysis are based on data freeze for Laxemar model version 1.2 (November 2004).

The analysis done for Laxemar model version 1.2 comprises estimates of hydraulic properties based on data from the Simpevarp and Laxemar subareas, including data from the Äspö HRL. The estimates of hydraulic properties and conditions for Laxemar model version 1.2 in this report are the base for the Site Description Model L1.2 and the numerical groundwater flow simulations, reported elsewhere.

HCD (Hydraulic Conductor Domains)

HCD are large planar fracture zones defined deterministically in the regional model that generally, but not always, more conductive than the surrounding rock. HCD may also act as hydraulic barriers, but no such HCDs have yet been identified. Most of the HCD are subvertical, a few with dip around 60–45 degree. So far no major subhorizontal HCD have been found in the model area, but cannot be excluded to exist.

Probably the transmissivity (T) in the HCDs is decreasing by depth. The heterogeneity within a specified HCD is probably large, and so far not estimate of the heterogeneity is available. The geometric mean transmissivity of HCDs is near surface ca $2 \cdot 10^{-5}$ m^2/s and in the elevation interval –300 to –600 m ca $2 \cdot 10^{-5}$ m^2/s. These values are highly uncertain due to few samples.

HRD (Hydraulic Rock Domains)

The hydraulic conductivity (K) of the rock between the larger deformation zones is probably decreasing by depth, at least is the hydraulic conductivity higher in the uppermost 200–300 m compared to rock deeper than this. Possibly is this difference related to the lower rock stress near the surface, which may cause more fractures to be open for flow. The hydraulic conductivity is also coupled to rock type and to identified rock domains; the more basic rock, the less conductive. The difference in hydraulic conductivity by depth or rock domain is probably more related to the intensity of flowing fractures than the transmissivities of the individual fractures. So far these results are uncertain, due to few samples. Some rock domains are only represented by one borehole. The hydraulic properties of the HRDs are described in more detail below.

The geometric mean hydraulic conductivity of HRD, based on test scale 100 m, all data (all rock domains in the regional area) but with borehole sections with HCDs excluded, is near surface ca $8 \cdot 10^{-8}$ m/s, in the elevation interval –200 to –400 m ca $2 \cdot 10^{-8}$ m/s and in elevation interval –400 to –600 m ca $3 \cdot 10^{-9}$ m/s.

The 100 m results do not indicate any depth-dependence in the 0–500 m interval of the Äspö HRL data. In the data from the Laxemar subarea and the Simpevarp peninsula, there seem to be a decrease in hydraulic conductivity with depth, similar to the entire data set as described above. There are hardly any data at depth from the Ävrö Island, but the few existing data indicate a depth trend such that values below 100 m are lower than that above 100 m.

There is a clear difference in mean hydraulic conductivity between rock types. The Granite and Fine-grained granite (rock type codes 501058, 511058) are the most permeable. Ävrö granite (rock code 501044) has a lower hydraulic conductivity and the lowest hydraulic conductivity is found in the more basic rock types (rock type codes 501030, 501033, 501036, 505102).

The rock domains defined in the geological model have different geometric mean hydraulic conductivity when comparing groupings based on geological rock domains with similar K; (A and BA) have the highest K for rock domains; (B, C and M(A)) have lower K for rock domains than (A and BA); (D and M(D)) are the least conductive rock domains.

There seems to be approximately a linear correlation between the frequencies of open fractures and the flow anomalies, except for KAV04B, which is the only borehole where data have been collected in the uppermost 100 m of the bedrock. The reason for this difference may be that near the surface there is a lower effective rock stress that affects the open fractures. One can expect 0.02–0.1 flow anomalies per mapped open fracture above a transmissivity about $1 \cdot 10^{-9}$ m^2/s (the approximate measurement limit for PFL-f) for rock between 100 to 1,000 m depth.

Transmissivity distributions for the PFL-f flow anomalies are rather similar in different boreholes and at different depth. It seems that the difference in intensity of flow anomalies is the main causes for the difference in average properties as hydraulic conductivity show for rock domains and depth dependency. Geometric mean transmissivity of the PFL-f flow anomalies is generally between $1 \cdot 10^{-8}$ m^2/s and $1 \cdot 10^{-7}$ m^2/s, with a standard deviation of Log10(T) around 0.5 to 1. The frequency of PFL-f anomalies varies between ca 0.01 and 0.3 No/m below 100 m depth. Near surface the intensity is higher; 0.7 No/m, though based on just one borehole (KAV04B).

Sections in the boreholes mapped as crush, seem to have a higher permeability than single fractures. The simple reason is probably that it is generally a few fractures in a crush, and the transmissivity of the crush is the sum of the transmissivities of several fractures. These borehole sections may, at least some of them, represent clusters of fractures that interconnect for some distance to form larger hydraulic features.

About 1/3 of the crush zones are conductive and about 2/3 are non-conductive, or rather below the measurement limit for PFL-f. In two of the boreholes (KSH01A and KAV01) the geometric mean transmissivity is ca 10 times greater for crush zones (as individual features) than for individual flow anomalies outside the mapped crush zone, with a bit less difference noted for KLX04 and KSH02.

Water table

The numerous small streams, small lakes and peat lands in the Simpevarp regional model confirms that the small discharge areas are well spread over the area, and also indicating a lower possible level for the water table (Water table-base). The elevation of this “Water table-base” follows that topography well, indicating that the level of the water table probably follows the topography in the area.

Contents

1 Introduction

The Simpevarp area is located in the province of Småland, within the municipality of Oskarshamn, and immediately adjacent to the Oskarshamn nuclear power plant and the Central interim storage facility for spent fuel (Clab), cf Figure 1-1. The Simpevarp area (including the Simpevarp and Laxemar subareas) is located close to the shoreline of the Baltic Sea. The easternmost part (Simpevarp subarea) includes the Simpevarp peninsula (which hosts the power plants and the Clab facility, cf Figure 1-1) and the islands Hålö and Ävrö. The island of Äspö, under which the Äspö Hard Rock Laboratory (Äspö HRL) is developed, is located some two kilometres north of the Simpevarp peninsula. The area of the Laxemar subarea covers some 12.5 km^2 whereas the Simevarp subarea is approximately 6.6 km^2.

Figure 1-2 shows the regional model area selected for Laxemar1.2. The figure also shows the local models areas for Laxemar version 1.2 and the previous model; version Simpevarp 1.2.

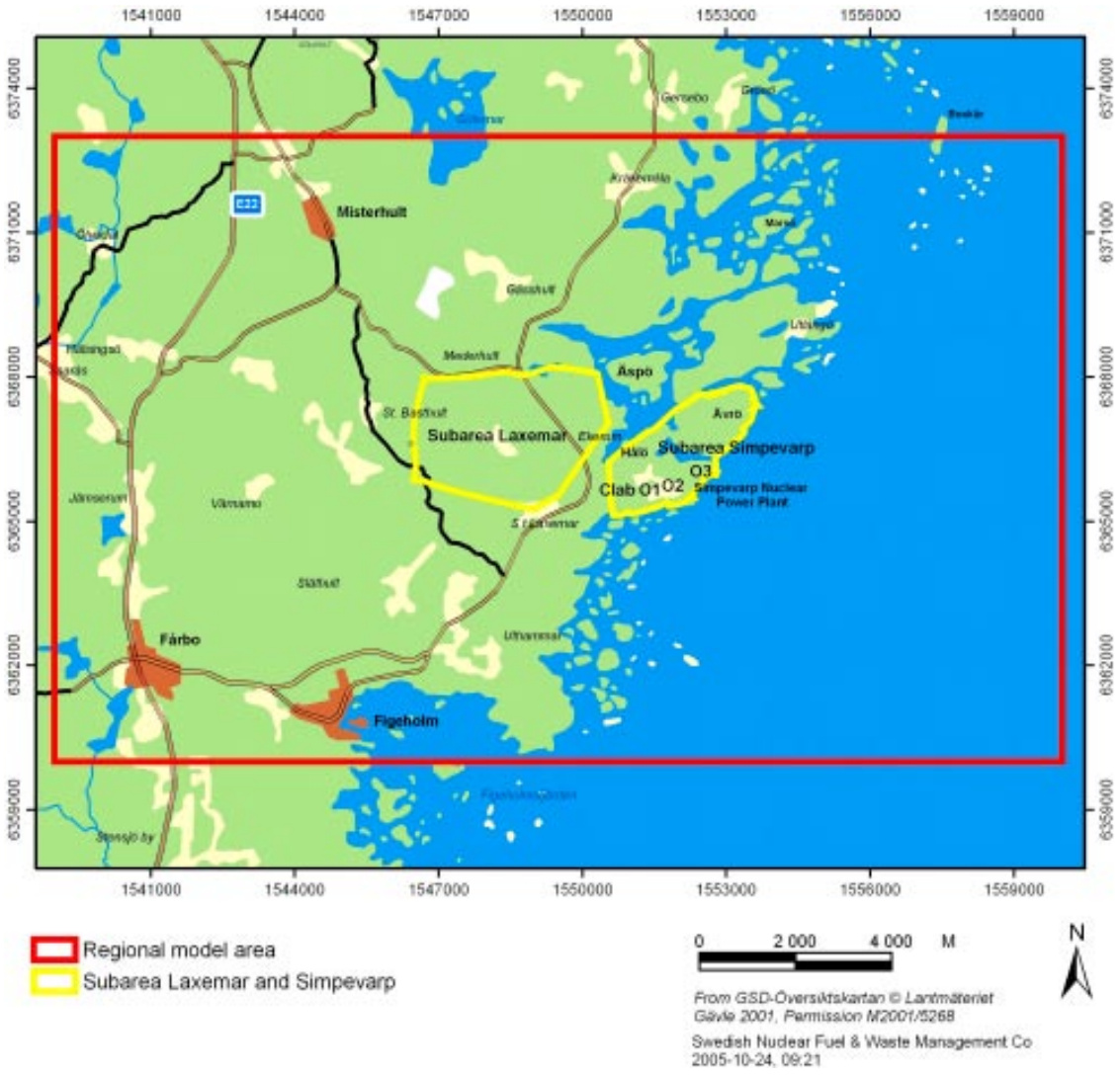

Figure 1-1. *Overview of the Simpevarp regional model area and identification of the Simpevarp and Laxemar subareas, cf Figure 1-3.*

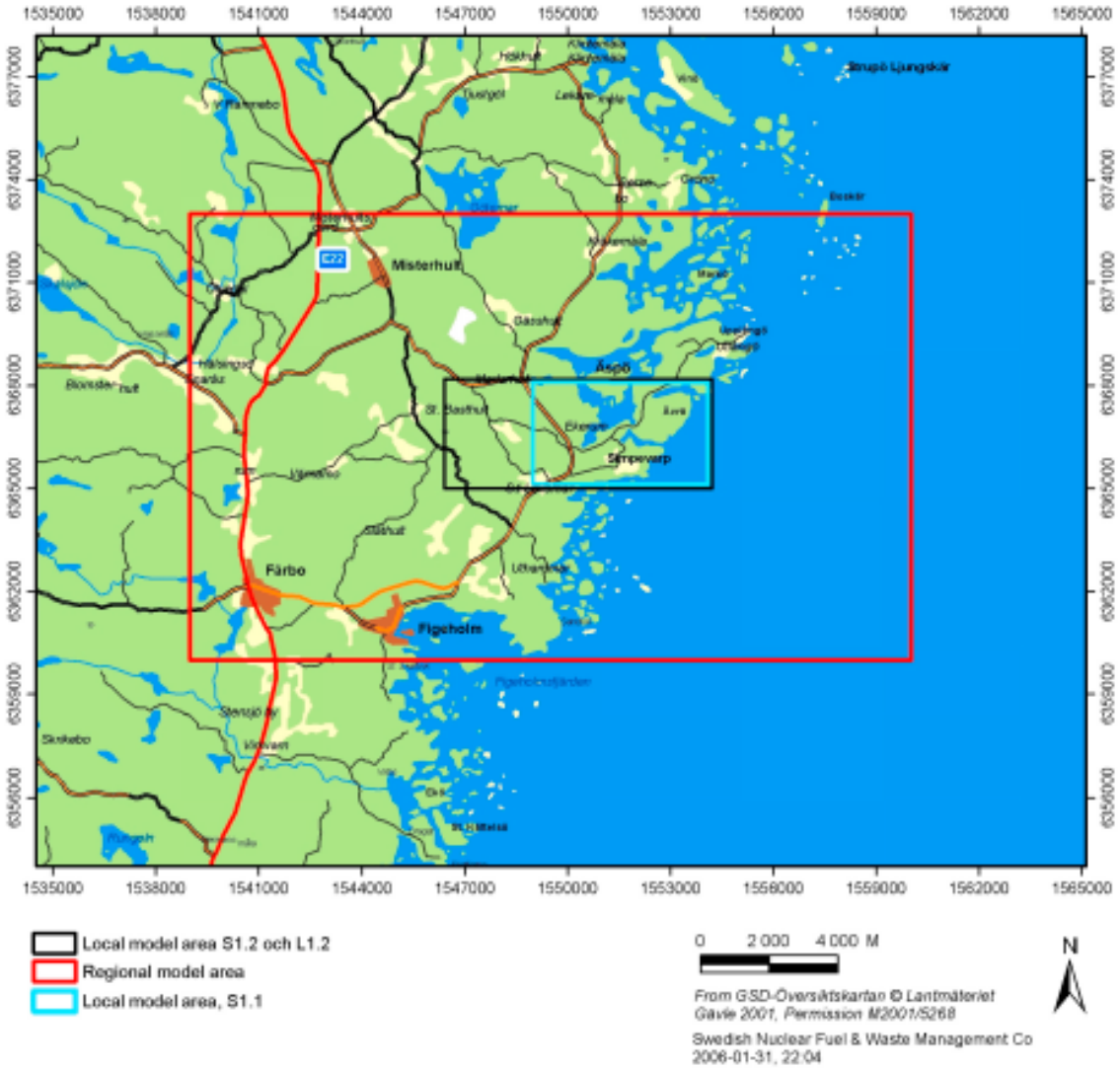

Figure 1-2. *Regional and local model areas used for Laxemar 1.2. The areal coverages of the local and regional models are the same as those employed in version Simpevarp 1.2.*

The Initial Site Investigations (ISI) at Oskarshamn finished in 2005. A number of new boreholes were drilled and investigated during ISI (core holes: KSH01A, KSH02, KSH03A, KLX03, KLX04, KLX05, KLX06 and KAV04A and B) some old core holes were tested with new methods (KAV01, KLX02), and a number of new percussion holes were drilled and investigated (HSH01–03, HAV09–10 and 9 HLXxx boreholes), see Figure 1-3. In some boreholes (KLX05, KLX06), only preliminary tests during drilling were available for analysis, and in KLX03 not all data planned for the borehole were available for the analysis in this report. Different types of investigations have been performed in the boreholes and all intended investigations for a particular borehole were not reported or performed in time to be included in this report. A description of the available data for the Site Descriptive Modelling (SDM) of Laxemar model version 1.2 (L1.2) is described in /Rhén et al. 2006ab/.

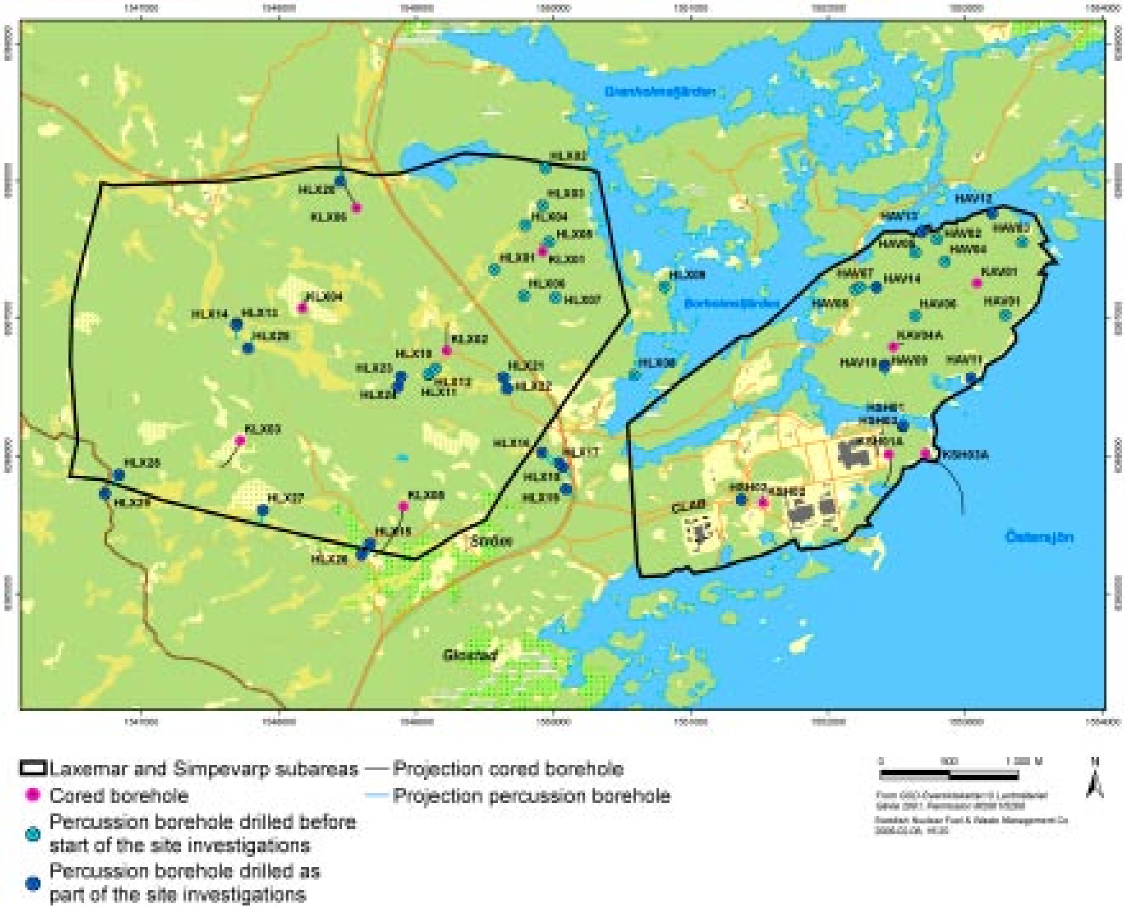

Figure 1-3. *Overview map of core-drilled and percussion-drilled boreholes in the Laxemar and Simpevarp subareas at stage model version Laxemar 1.2. Location of the core-drilled boreholes with new site investigation data available for model version Laxemar 1.2: KSH01A, KSH02, KSH03A, KAV01, KLX02, KLX03, KLX04 and KAV04A,B.*

2 Objective and scope

The hydrogeological descriptive model should provide a hydraulic parameterisation of interpreted deterministic deformation zones and the rock mass between the interpreted deformation zones. The Hydrogeological DFN models are in this context of particular important. A key user of this information is Safety Assessment.

The hydrogeological descriptive model also provides data used for variable-density groundwater flow modelling. The flow models should be able to simulate groundwater flow within a given volume under natural (undisturbed) conditions, to provide a general understanding of the natural groundwater flow system, and disturbed system with a deep repository. The flow paths to the potential repository volyme are of interest, as they provide a description of the rate at which potential corrodants are introduced. Likewise, the flow paths from the recharge areas of the potential repository volume within the modelled volume are important for estimation of the paleohydrogeological and hydrogeochemical evolution. Of importance in this context is the shoreline displacement which must be taken into account when modelling the long-time evolution of the groundwater flow (and groundwater chemistry). The established flow paths from the repository volume to discharge areas are important for Safety Assessment.

The numerical groundwater flow modelling serves three main purposes:

- Model testing: Simulations of different major geometric alternatives or boundary conditions in order to disprove a given geometric interpretation, material property assignment, or boundary condition, and thus reduce the number of alternative conceptual models of the system.
- Calibration and sensitivity analysis: to explore the impact of different assumptions as to hydraulic properties, boundary and initial conditions.
- Description of flow paths and flow conditions: useful for the general understanding of the groundwater flow system (and hydrogeochemistry) at the site.

The numerical groundwater flow simulations are thus helpful for the assessing the interplay between geological structures (domains) and hydrogeological properties and conditions (hydraulic properties, boundary and initial conditions), as well as for improving the general understanding of the site. The close interaction between the geological and hydrogeological interpretations, together with the integration of the hydrochemical, transport and surface systems information, is critical to interpret the available hydrogeological data and also essential for obtaining consistent conceptual models that can be used in the numerical groundwater flow modelling

A given version of the site description, with its groundwater flow model, subsequently forms the basis for further analysis by Repository Design and Safety Assessment and for the planning of new investigations. Exploratory groundwater flow simulations are considered when planning field investigations or addressing specific Repository Engineering and Safety Assessment questions.

2.1 Objectives for this report

The purpose of this report is to analyse data available for assessing useful Hydrogeological concepts and assessing hydraulic properties to identified hydrogeological domains. The report provides details useful for the Site Descriptive Model (SDM) and in particular the numerical groundwater flow modelling. The report does not include Hydrogeological DFN (Discrete Fracture Network) modelling.

2.2 Overview of work done for Laxemar 1.2

The data for the hydrogeological model Laxemar version 1.2 presented in the subsequent sections is based on the current Laxemar version 1.2 geological descriptive model.

The modelling done for Laxemar 1.2 comprises estimates of hydraulic properties based on data from the Simpevarp and Laxemar subareas, including data from the Äspö HRL. The new data based on the site investigations in the Simpevarp and Laxemar subareas for Laxemar model version 1.2 (L1.2) are described in /Rhén et al. 2006ab/. Different types of investigations have been performed in the boreholes and the data for the analysis are based on data freeze for Laxemar model version 1.2 (November 2004).

3 Data used for the hydrogeological evalution

In this chapter a brief overview is given of the data used for the modelling presented in this report.

3.1 Geological data

The geological data available for Laxemar model version 1.2 is in detail described in /Wahlgren et al. 2005/. The main data that have been used for the Hydrogeological modelling are:

- Boremap data for core holes.
- The 3D rock domain model /Wahlgren et al. 2005/ to define rock domains along core holes and percussion boreholes.
- Deterministic deformations zones /Wahlgren et al. 2005/, generally referred as RVS-DZ in this report, to define intercepts between boreholes and RVS-DZ.

3.1 Hydro-test data

Hydraulic data comprises a wide range of data from different hydraulic tests. Some data are from the on-going site investigations (SI) and some are from SKB investigations before SI.

During SI generally a set of standard methods are applied in each core hole and in each percussion hole (different from the core holes). As the investigations are ongoing during the evaluation for Laxemar model version 1.2, it was not possible to have access to complete data sets for all boreholes. The available data is presented in /Rhén et al. 2006ab/.

To estimate the hydraulic properties of the by the geologists deterministically defined deformations zones, data from the SI is used as well as for the investigations made before and during the construction of the Äspö Hard Rock Laboratory (Äspö HRL). An overview of data and model parameters based on the Äspö HRL investigations is given in /Rhén et al. 1997abc/. The data used are mainly the ones performed in boreholes drilled from surface. To estimate the properties of a few of the RVS-DZ, some data from the Äspö HRL tunnel is also used. Tests from boreholes drilled from the surface of Äspö island with test scale 100 m is also used in the analysis of the rock domains.

Before the investigations started for Äspö HRL, SKB performed some drilling and hydraulic tests in core holes drilled on Ävrö (KAV01, KAV02, KAV03) and in the Götemar granite (KKR01, KKR02, KKR03). These tests have also been used.

These tests, performed before SI, are not of the same standard as the on-going site investigations, but still considered to give valuable data.

4 General conditions and concepts

The Simpevarp area is dominated by a crystalline bedrock covered by a fairly thin overburden mainly consisting of till /Wahlgren et al. 2005/. The crystalline bedrock is fractured and it is interpreted that there are a number of major deformation zones within the area. The existence of these deformations zones have to some extent been confirmed by surface geophysics and drilling. Hydraulic tests have confirmed, in most cases, that the deformation zones are more conductive than the surrounding rock, as further elaborated in Chapter 6

Different geological and geophysical investigations have resulted in a description of the spatial distribution of rock types, and interpreted larger geological entities (rock domains) consisting of rock types with similar geological properties, see /Wahlgren et al. 2005/. The deformation zone model developed for SDM L1.2 is presented in Chapter 5, and is further detailed by /Wahlgren et al. 2005/. Observations of the general character of the hydraulic tests, as shown in /Rhén et al. 2006ab/ indicate that the defined geological rock domains also exhibit distinct and significant hydraulic characteristics. In Section 6.4 it is shown that if the rock domains defined along each corehole, is used for analysing the difference in hydraulic properties related to rock domain, there seems to be significant differences in hydraulic properties of the rock domains that should be taken into account in the hydrogeological description. However, it is also noted that the current database is sparse, and the conclusion that the geologically defined rock domains constitute a basis for defining hydraulic domains is uncertain.

The overburden constitute mainly of till, but glacifluvial sediments, peat and clay are also found. The hydraulic conductivity of these components is generally higher than for the crystalline bedrock. Depending on the modelling task, the hydrogeology of the overburden requires attention and quantification.

Based on the above deliberation, the conceptual model for the Simpevarp area, including the Laxemar subarea, can be illustrated as in Figure 4-1. The conceptual model consists of the following entities:

- The geometry of large, deterministically modelled deformation zones, here included as Hydraulic Conductor Domains (HCD) and the bedrock in between the deterministic zone (the rock mass), here included as Hydraulic Rock Domains (HRD).
- The distribution of Quaternary deposits (overburden), here included as Hydraulic Soils Domains (HSD) (including genesis, composition, material properties, stratification and thickness).

As the Simpevarp area is dominated by the fractured crystalline basement, the hydrogeological description of the HRDs, also used for flow modelling, may be either discrete (hydraulic DFN) or continuous (equivalent porous medium, EPM) depending on the DFN properties, the scale of resolution, and the modelling objectives. The basis for the assignment of hydraulic properties to the HSD model is the hydraulic testing conducted in the monitoring wells (soil pipes) in the Quaternary deposits. Details of the Quarternary deposits and the hydrogeological description of the overburden are provided in /Lindborg (ed) 2006/.

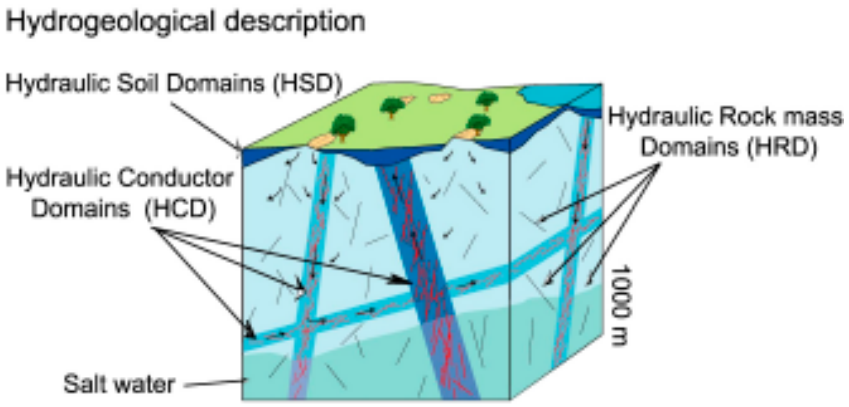

Figure 4-1. *Division of the crystalline bedrock and the overburden (Quaternary deposits) into hydraulic domains representing the overburden,(HSD) and the rock mass volumes (HRD) between major fracture zones (conductors, HCD). Within each domain, the hydraulic properties are represented by mean values, or by spatially distributed statistical distributions /Rhén et al. 2003/.*

4.1 General modelling strategy

The hydrogeological models representing the HRDs, the HCDs, and the HSDs are combined into a regional scale groundwater flow model, see Figure 4-2. The derivation of block scale parameters from hydraulic DFN is requested by Repository Engineering, but the underlying principle for the derivation, the equivalent porous medium (EPM) (or equivalent continuum porous medium, ECPM) approach, is also used in the regional flow modelling.

The regional flow model is calibrated against hydraulic test data and hydrogeochemical data, e.g. chemical composition including; salinity, different water types and isotopic signatures. The calibrated regional flow model is used for sensitivity analysis of groundwater flow and advective transport of solutes using particle tracking. Conceptual models, assumptions and details on the modelling approaches used are presented in /Hartley et al. 2006/.

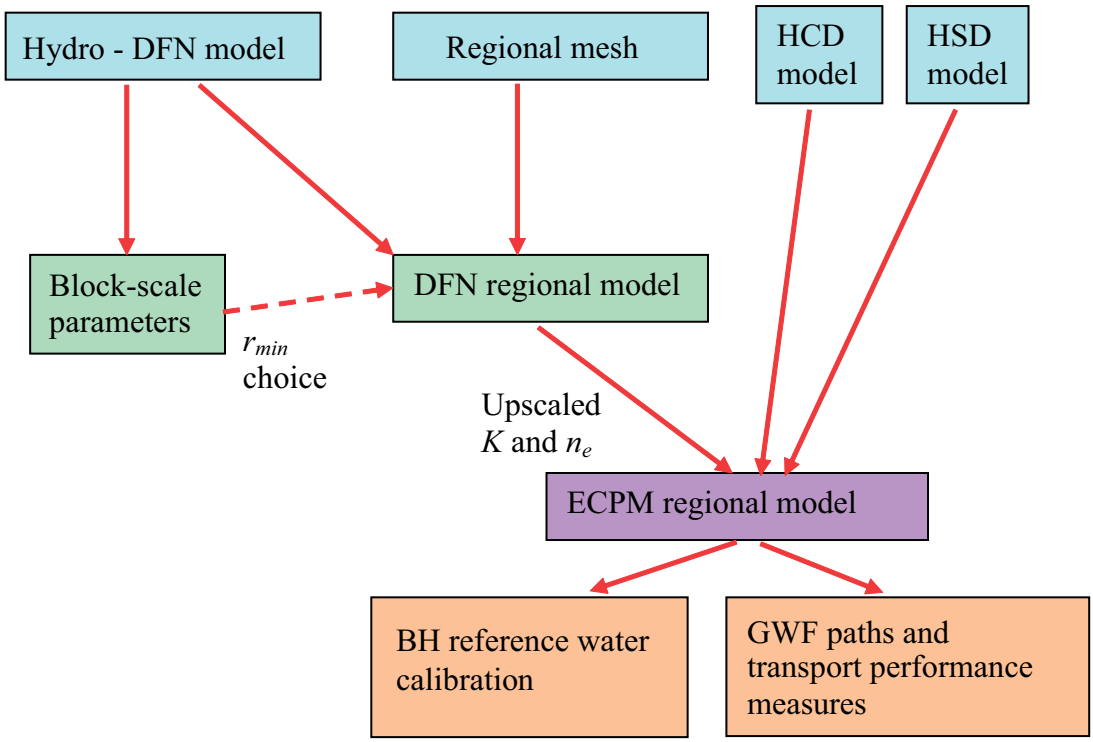

Figure 4-2. *A schematic workflow for the modelling /Hartley et al. 2006/.*

4.2 Evaluation presented in this report

The evaluation in this report covers assessment of useful concepts for defining hydraulic domains and interpreted properties of hydraulic domains HCDs and HRDs, based on hydraulic test data. Properties of HSD are summarized in this report, but the analysis is presented in other reports. The present, probable, upper hydraulic boundary conditions are also presented in this report.

Hydro-DFN (Discrete Fracture Network) and Block-scale modelling results, as well as ECPM regional modelling results, are presented in other reports. These results are based on data from this report and /Rhén et al. 2006ab/.

4.2.1 Statistics of single hole test results

Data from the hydraulic tests performed in the boreholes have been compiled and univariate statistics have been calculated and compared with data from other cored boreholes in the Simpevarp area, where similar tests have been conducted.

Hydraulic conductivity (or transmissivity) evaluated from hydraulic tests with the same test section length often fit rather well to a lognormal distribution. When the test section length decreases, the number of tests below the lower measurement limit of the equipment increases. The data set is hence "censored", which has to be taken into account when choosing a statistical distribution that should describe the measured values above the measurement limit as well as possible. A data set is said to be truncated if the number of unmeasured values is unknown and it is censored if this number is known /Jensen et al. 2000/. For censored data below the measurement limit, the fitted distribution can be used to estimate the properties below the measurement limit, but these estimates are of course associated with uncertainty. When performing modelling based on the fitted distribution it has to be

decided if extrapolation below the measurement limit is reasonable and whether there is a definite lower limit (below the lower measurement limit) for the property in question due to e.g. conceptual considerations. In crystalline rock, the matrix permeability sets the physical lower limit, cf /e.g. Brace 1980/. The matrix hydraulic condictivity of crystalline rock is generally found to be ca 1E–14 to 1E–13 m/s.

The standard procedure for describing the hydraulic material properties from single-hole test data is to fit the logarithm of the data to a normal distribution, also taking the censored data into account. The associated statistics normally include the mean and standard deviation (std) of Y, $Y = \log_{10}(X)$, X = hydraulic conductivity (K) or transmissivity (T), where the mean of $\log_{10}(X)$ corresponds to the geometric mean of X. Occasionally, the number of measurements below the lower measurement limit is greater than the number above the measurement limit, see Figure 4-3 . However, it is here argued that the above methodology (the fitting of the statistical distribution to values above the lower measurement limit – the "known values") is the appropriate way to describe a dataset with censored values. This while measured values above the measurement limit are fairly well reproduced by the distribution which also indirectly accounts for the values below the measurement limit. A power law distribution may work equally well, but this has not been tested here.

4.2.2 Best choice of T and K

Generally different hydraulic tests (WLP, PFL and PSS, see /Rhén et al. 2006a/) and with different test scales (= length of tested borehole section) are performed in each core hole. In percussion boreholes there may be different hydraulic tests and with different test scales, but generally tests are performed as pumping tests with submersible pump or airlift tests of the entire borehole.

The tests from WLP and PSS are evaluated as transient tests giving Transmissivity (T_T) and skin factor (assuming a storage coefficient S = 1E–6). T_T is evaluated for the first seen radial flow period in a test. Steady state evaluation of transmissivity (T_M) based on /Moye 1967/ is also made. If it was not possible to evaluate T_T, the T_M values are used as "best choice" (BC) for the test section in question, otherwise T_T is used as best choice value.

When assigning properties to the HCDs, there are sometimes options to use results from different hydraulic tests and with different test scales. As "best choice" (BC) for an observation in a HCD, transient test results (T_T) are preferred and tests that straddles the entire HCD and have long test duration are used if they are available. If no single test straddles the entire HCD, smaller test section, transmissivities are summed up to represent the HCD at the borehole section, still preferring transient tests with as long test sections as possible and long test duration.

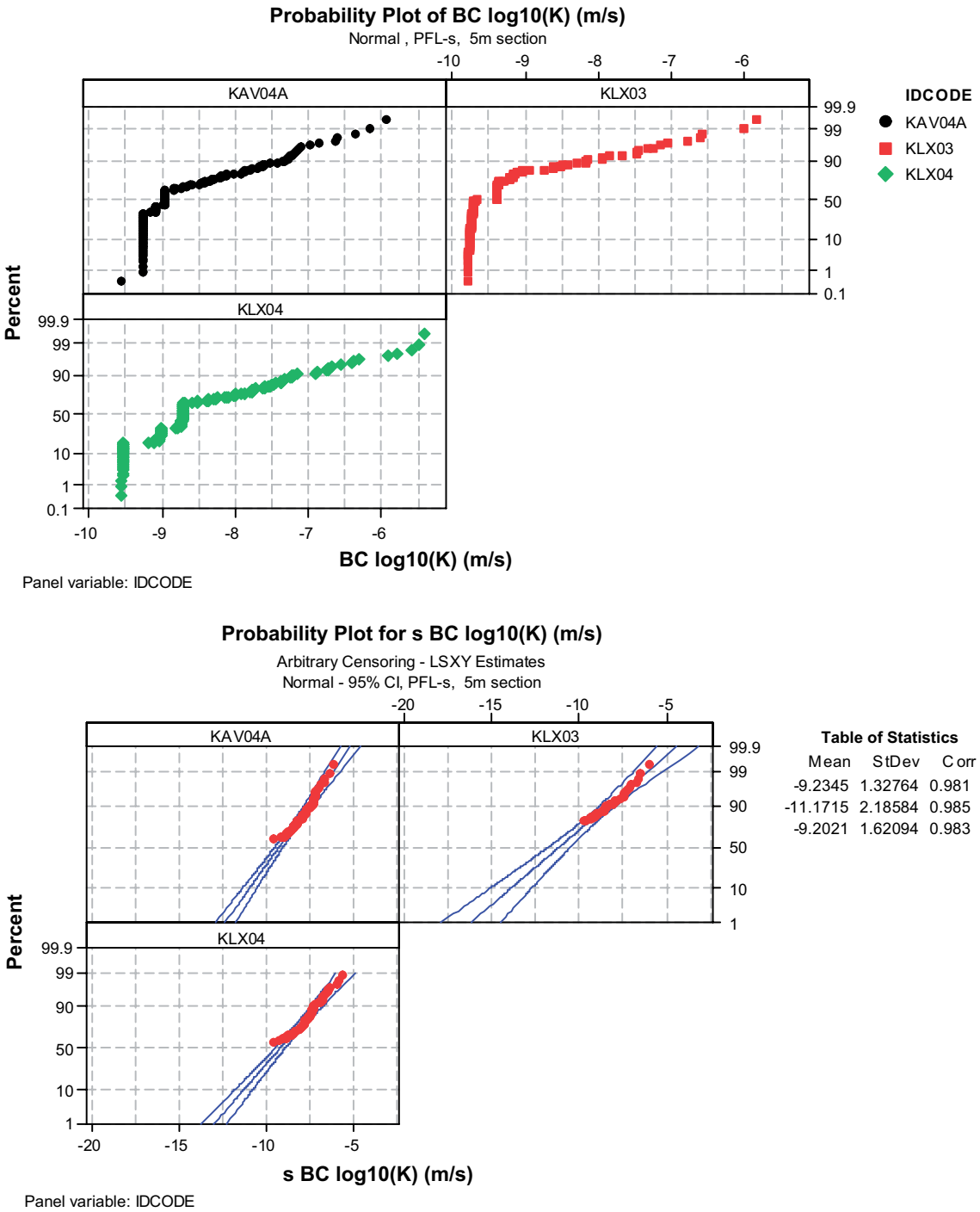

Figure 4-3. *Example of statistical distributions plotted as Normal distributions. Top: All data including measurement limit values are plotted. Bottom: Statistical analysis of the values shown in the top figure, setting all measurement limit values as Censord values result in the matched mean and standard deviations shown in the caption.*

5 Hydraulic conductor domains (HCD)

The basis for the interpretation of the HCD properties is the 3D deformation zone model in the RVS (Rock Visualisation System) and the intersections between boreholes and deformation zones in the RVS model. The judgement of the geologists as to where the deformation zones intersect the boreholes has guided the search for relevant hydraulic information. The hydrogeological properties extracted from transient pumping or injection tests have been used to estimate the HCD parameters. If a single hydraulic test section covers the entire part of a deformation zone defined in a borehole, the corresponding test results have been used, instead of summing up transmissivities for shorter test sections.

The deterministic deformation zone model is in detail described in /Wahlgren et al. 2005/ and in Figure 5-1 and Figure 5-2 the identified zones are shown. The model is based on airborne and surface based geophysics, topography, borehole data and tunnel data. Depending on the information available for each zone, the existence of a particular zone is classified as having: High confidence, Medium confidence or Low confidence, see Figure 5-1. Most zones are assumed to be vertical as no information is available to estimate the dip of the zone.

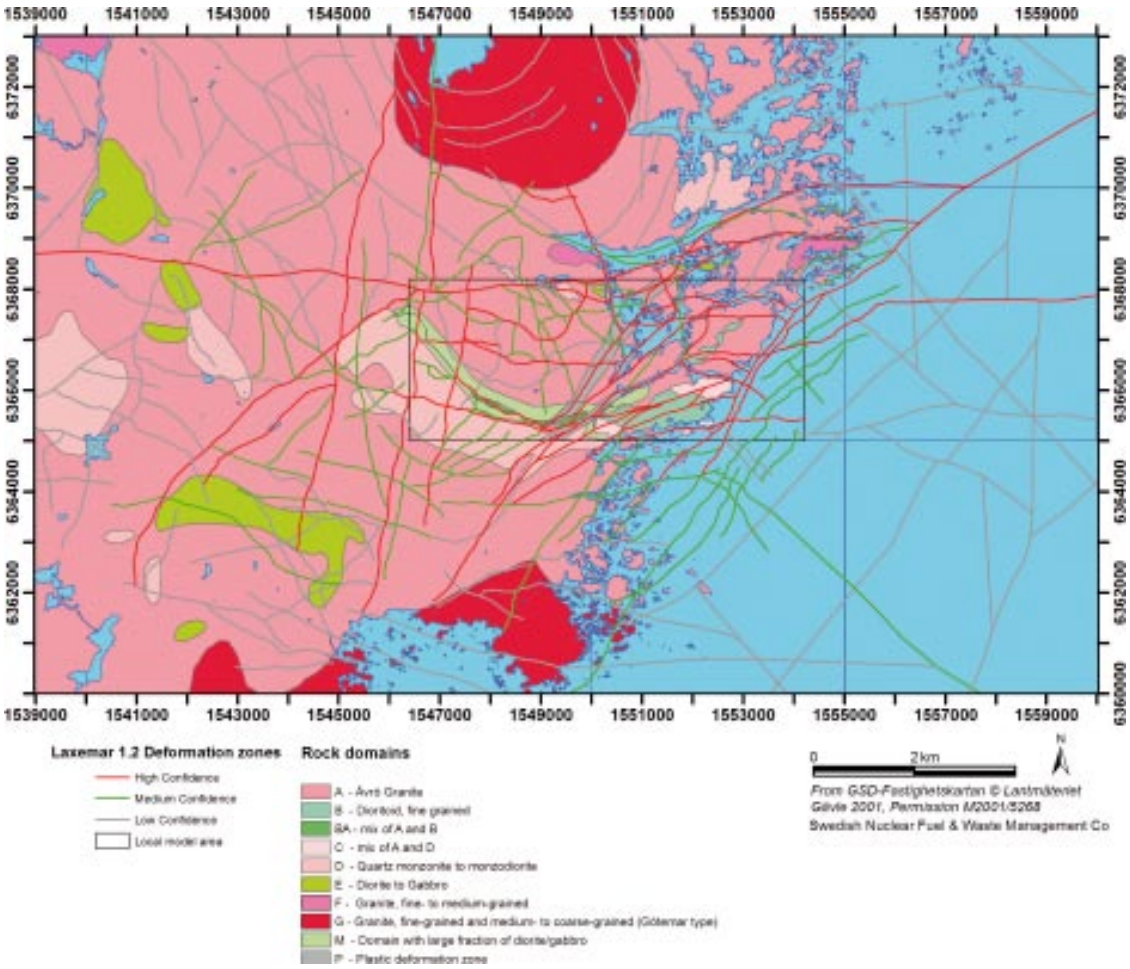

Figure 5-1. *The interpreted thirty-five high confidence deformation zones in the Laxemar 1.2 regional model area (red) together with interpreted medium and low confidence deformation zones (green and grey respectively) /Wahlgren et al. 2005/.*

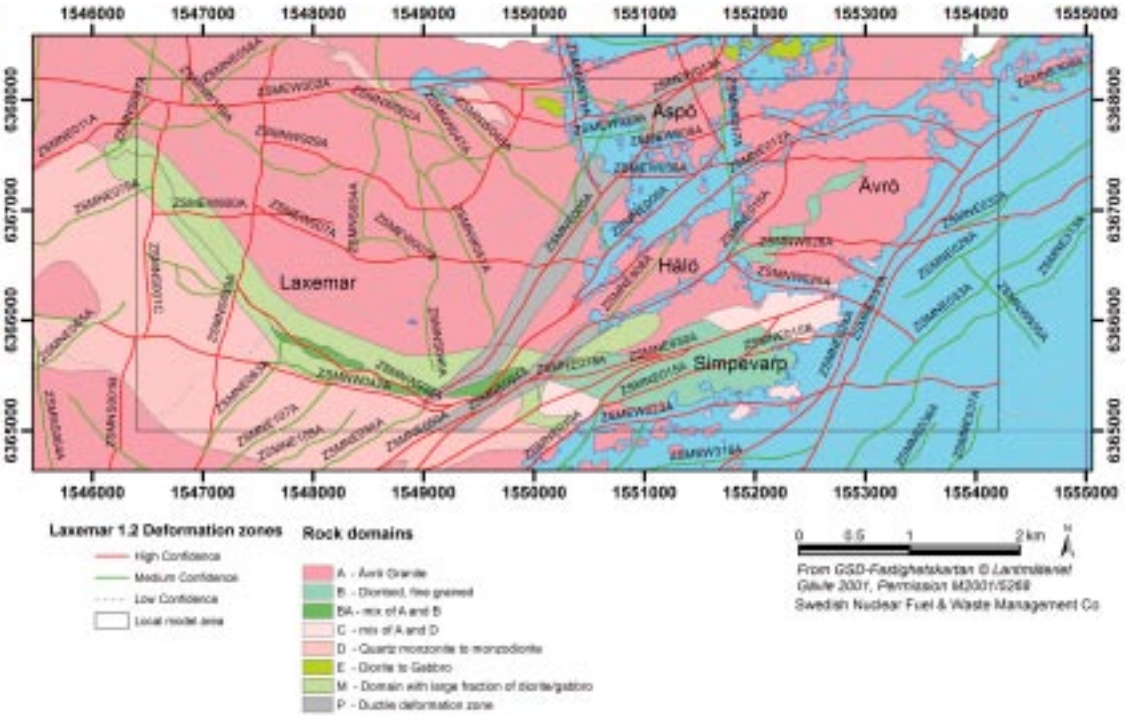

Figure 5-2. *The interpreted high, medium and low confidence deformation zones in the Laxemar 1.2 local model area (red) including medium and low confidence zones (green and grey respectively) /Wahlgren et al. 2005/.*

As pointed out in Chapter 4, the deterministically defined deformation zones that are included in the hydrogeological model are called Hydraulic Conductor Domain (HCD) and are considered to be mainly planar objects. Thus relevant hydraulic properties are transmissivity (T) and storage coefficient (S). Deformation zones certainly have a thickness, that also can be useful when applied in a numerical model, which in the report is based on the "geological thickness" – that is the thickness estimated in /Wahlgren et al. 2005/.

5.1 Interference tests

The cross-hole interference test constitutes a good tool to confirm the presence and continuity of deformation zones. So far, only a limited number of interference tests have been made and consequently the present model of zone connectivity is mainly a product of geological interpretation. However, a number of deformation zones near Äspö HRL were studied by hydraulic testing /Rhén et al. 1997abc/ and hydraulic interference tests along the extent of zone ZSMEW007A (not yet reported) will be used to confirm the existence, near-surface geometry and extent of the zone in future model versions.

During the initial site investigation a few interference tests have been reported, with pumping in HSH03 and observation in HSH01 /Ludvigson et al. 2003/, as well as pumping in HLX10 and monitoring in KLX02 and a few other boreholes in the area /Gustafsson and Ludvigson 2005/ to assess the connectivity through a potential deformation zone between HLX10 and KLX02. The response characteristics of the latter test can be seen in Figure 5-4, Figure 5-5 and Table 5-1. The response classification is explained in Figure 5-3.

Index $(s/Q_p)*(r/r_0)$	Index(s/Qp)	Est. Criteria (test) Value>x	
E: Excellent		1.00E+06	E
H: High		1.00E+05	H
M: Medium		1.00E+04	M
L: Low		1.00E+03	L
N: No response		s < 0.1 m	N

Index(r^2/tL)		Est. Criteria (test) Value > x	
E: Excellent		100	E
H: High		10	H
M: Medium		1	M
L: Low		0.1	L
N: No response			N

Figure 5-3. *Response classification for interference tests. Classification scheme.*

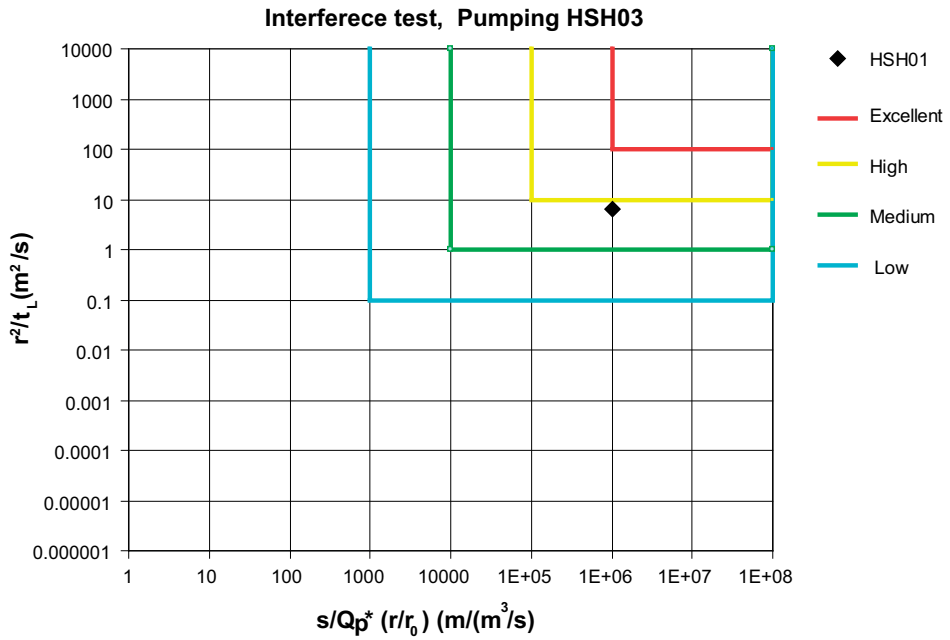

Figure 5-4. *Response classification for interference tests. Pumping well: HSH03. The rectangles represents judgements of the responses: within Red: Excellent, within Yellow (outside red rect.): High, within Green (outside yellow rect.): Medium, within Blue (outside green rect.): Low, No response is plotted as s = 0.01 m and t_L = 1E8 s. s/Q_p: drawdown at the end of the pumping phase divided with the final pumping rate. r: The distance, r, between different borehole sections has been calculated as the spherical distance using coordinates for the mid-point for each test section or the point of application calculated from the hydraulic conductivity distribution in the observation or pump section. r_0 is set to 1. t_L: The time lag t_L is defined as the time after pumping stop when the pressure response in an observation section is greater than 0.1 m.*

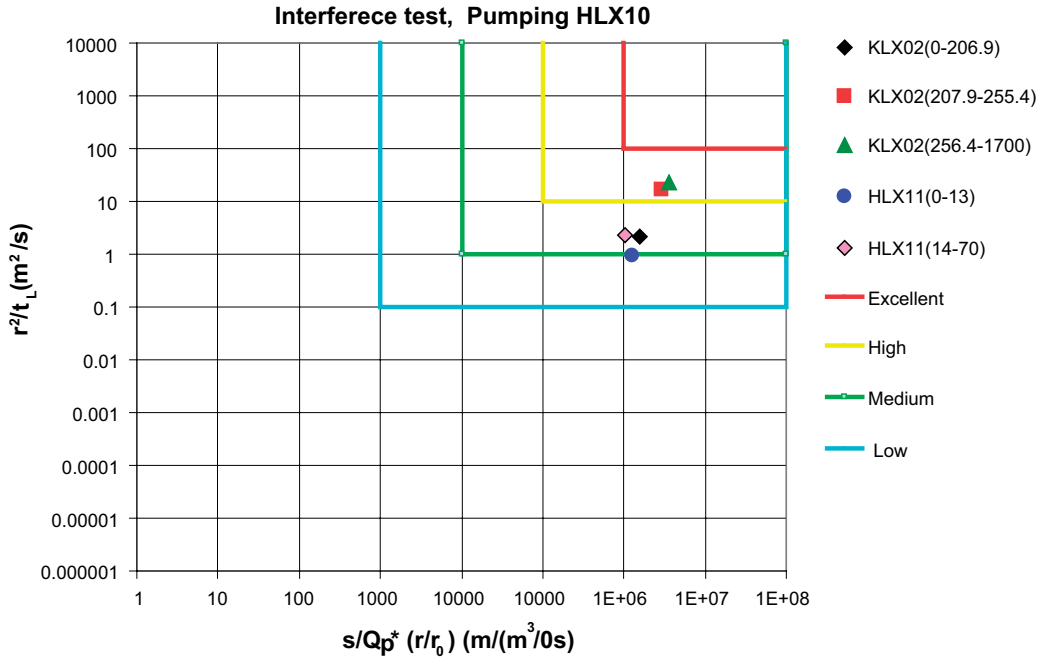

Figure 5-5. *Response classification for interference tests. Pumping well: HLX10. The rectangles represents judgements of the responses: within Red: Excellent, within Yellow (outside red rect.): High, within Green (outside yellow rect.): Medium, within Blue (outside green rect.): Low, No response is plotted as s = 0.01 m and t_L = 1E8 s. s/Q_p: drawdown at the end of the pumping phase divided with the final pumping rate. r: The distance, r, between different borehole sections has been calculated as the spherical distance using coordinates for the mid-point for each test section or the point of application calculated from the hydraulic conductivity distribution in the observation or pump section. r_0 is set to 1. t_L: The time lag t_L is defined as the time after pumping stop when the pressure response in an observation section is greater than 0.1 m.*

The main deformation zone tested while pumping in HLX10 is suggested to intersect the upper parts of KLX02 (possibly in the more transmissive borehole section 200–400 m) but the intersection with HLX11 is considered uncertain. The zone tested probably corresponds to ZSMEW007A as modelled in the current model version L1.2. As tracers were injected in section KLX02 (207.9–255.4) the registration of the drawdown was terminated after one day, the specific drawdown should probably be a bit larger than shown in Table 5-1. The responses in KLX01 (0–206.9) may possibly be affected due to that KLX02 is cased down to 202.95 m. Possibly the responses would have been larger if no casing was present. The test seems to indicate that the conductive feature in HLX10 is well-connected to the upper part of KLX02, but less well to HLX11. Only T and S considered reliable are shown in Table 5-1.

In the Laxemar subarea there exist data from two old interference tests where KLX02 is used as the pumped borehole /Ekman 2001/. These tests show fairly clear responses in the deeper sections in KLX01 (695–855, 856–1,078 m), indicating connected conductive structures between KLX01 and KLX02. The responses may be explained partly by the existence of deformation zone ZSMEW007. However, the pumping of section 805–1,103 m in KLX02 also indicates a fairly good connection to the lower part of KLX01 (695–855, 856–1,078 m), which currently lacks a plausible structural explanation.

Pumping tests were performed in HSH04–05, HAV11–14 (on Simpevarp peninsula and Ävrö) with 1–4 observation sections /Rahm and Enachescu 2004/. These results were not available in SICADA at the time for evaluation of data for L1.2 and are therefore not included in the analysis.

Table 5-1. Univariate statistics for transmissivities coupled to deterministically defined deformation zones in RVS model version L1.2. Indexes for responses are explained in Figure 5-3.

Name of HCD, RVS ID, (Earlier name)	Pumping well	Obs. well for response	Secup (m)	Seclow (m)	Specific drawdown[1], s/Qp (s/m²)	Distance from pumping section[2], r (m)	Time lag[3], t_L (min)	Index resp., (s/Qp)* (r/r_0) (–)	Index resp., r^2/t_L (–)	Mean Log10(T) (m^2/s)	Mean Log10(S) (–)
ZSMNW025A	HSH03	HSH03	12.03	201		–	–			–4.8	
		HSH01	12.03	200	1.9E4	55	8	E	M	–4.8	–5.0
ZSMEW007A	HLX10	HLX10	0	85		–	–			–3.80	–
		KLX02	0	206.9	8.4E3	190	–5.92	E	M	–	–
		KLX02	207.9	255.4	(1.14E4)	260	–5.66	E	H	–3.92	–4.44
		KLX02	256.4	1,700	1.14E4	(310)	–3.92	E	H	–3.80	–4.42
		HLX11	0	13	1.44E4	90	–5.55	E	L	–	–
		HLX11	14	70	1.38E4	76	–6.37	E	M	–	–

[1] s/Qp: drawdown at the end of the pumping phase divided with the final pumping rate

[2] r: The distance, r, between different borehole sections has been calculated as the spherical distance using co-ordinates for the mid-point for each test section or the point-of application calculated from the hydraulic conductivity distribution in the observation or pump section.

[3] t_L: The time lag t_L is defined as the time after pumping stops until the pressure response in an observation section is greater than 0.1 m.

Some interference tests have been made but not yet reported. A few preliminary comments can though be made.

ZSMEW007: Tests indicate that at lest the upper part (down to ca 200 m depth) of the deformation zone is highly transmissive, but seem less transmissive in its central part (between KLX04 and KLX02) as tests indicate low hydraulic connectivity in the central part.

ZSMEW002: Tests show that the nearby boreholes KLX06 and HLX20 are hydraulically connected. Tests indicate a transmissivity in the range 10^{-5} to 10^{-4} m^2/s.

ZSMNW042: Interference tests indicate that the deformations zone is not fully hydraulically connected along its entire length. The transmissivity is high in the western and central parts (ca 10^{-4} m^2/s) but the eastern part seems low transmissive. The eastern part seems hydraulically connected to the central part.

ZSMNS059, north part: Interference tests confirm that the deformation zone exists and have high transmissivity, ca $2 \cdot 10^{-4}$ m^2/s (Data for this HCD was not available in SICADA, therefore not included in Table 5-2).

5.2 HCD – Mean transmissivity

Table 5-2 presents mean and standard deviation for log10(T) of the transmissivity (T) values that can be connected to each HCD (each deterministic deformation zones corresponds to a HCD), without taking any possible depth dependence in consideration. HCDs with no hydraulic test data have been assigned the geometric mean value based on all transmissivity data related to interpreted deterministic HCDs, and with an assumed geological thickness of 20 m.

It can be observed that the above mean value of T is higher than that measured at the intercepts of many of the high confidence deformation zones. It is important to observe that the confidence of existence (high, medium, low) is a judgement based on the available geological and geophysical observations that provide support of the existence of any given deformation zone. Hydrogeological observations may also contribute to confirming the existence. Furthermore, the hydraulic properties may vary over wide ranges, not nessarly transferable to judgement of confidence. Many of the low confidence zones in the local model area have shorter trace length on the surface compared to the high and medium confidence deformation zones. As described in the previous section, for the stochastic modelling of fractures and minor local deformation zones, a positive correlation between size and transmissivity is used in the attribution of material properties. If this is valid for the deterministically defined deformation zones, many of the low confidence zones would be less transmissive than the high and medium confidence deformation zones. This positive correlation between size and transmissivity remain to be tested as more data is obtained. Consequently the described assignment of the mean transmissivity of all HCD transmissivity data to non-tested HCDs of low confidence zones (possible minor local zones) may not be appropriate and justified. However, this route has been taken in the current modelling. The individual hydraulic tests associated with a certain HCD are listed in Appendix 7.

In the present model, the number of high, medium and low confidence deformation zones that have any measured T-value and the number zones that have no measured T-value is shown in Table 5-3. This table also reflects that drilling is important for the judgement of “confidence of existence”. When intercepted by drilling, hydraulic tests are generally performed that can be used for material property assignment.

Table 5-2. Univariate statistics for transmissivities associated with deterministically defined deformation zones in RVS model version Laxemar 1.2. (Confidence limits for mean Log10(T) is expressed as the deviation D from the mean in the table; for confidence level of 0.95 the mean of Log10(T) will be within value "Mean Log10(T)" ±D.

Name of HCD, RVS ID, (Earlier name)	Geological confidence, High/ Medium/Low	Geological thickness, b (m)	Sample elevation range (masl)	Sample mean elevation (masl)	Sample size	Mean Log10(T) (m^2/s)	Std Log10(T) (m^2/s)	D Conf.lim Log10(T): Mean±D, conf.level 0.95: (m^2/s)
ZSMEW002A (Mederhult zone)	High	100	–37 to –389	–194.7	5	–5.41	1.37	1.70
ZSMEW007A	High	50	–2 to –995	–178.4	8	–4.34	1.05	0.88
ZSMEW009A (EW3)	High	12	–22 to –490	–158.7	4	–4.92	0.35	0.56
ZSMEW013A (EW1A)	High	45	2 to –341.6	–116.1	5	–5.92	1.47	1.83
ZSMEW014A	Medium	20[1]	4.5	4.5	1	–5.66		
ZSMEW038A (ZSMEW038A_B)	High	10	–17 to –193	–142.7	4	–3.92	1.40	2.23
ZSMEW039A	Medium	201	–5.3	–5.3	1	–6.26		
ZSMEW900A (ZSMEW005A 7A)	High	20	–1 to –135	–68	2	–4.29	0.90	–
ZSMNE004A (ZSMEW004A)	High	100	–43.7 to –151.6	–97.64	1	–5.55		
ZSMNE005A (Äspö shear zone; EW1b)	High	250	–32 to –849	–276.5	8	–4.66	1.02	0.85
ZSMNE006A (NE1)	High	130	–31 to –821	–244.6	12	–3.66	0.57	0.36
ZSMNE012A (includes NW004A (old names EW7-NE4)	High	120	–18 to –833	–193.3	9	–4.45	1.07	0.82
ZSMNE015A	High	10	–936	–936	1	–8.41		
ZSMNE016A	High	15	–49 to –129	–69.14	2	–5.60	1.06	
ZSMNE024A	High	80	–583 to –956	–386.4	4	–6.57	2.47	3.93
ZSMNE031A	High	15	–240 to –668	–454	2	–5.94	3.03	
ZSMNE040A	High	20	–4 to –38	–21	2	–6.14	2.96	
ZSMNS017B (NNW4)	High	20	–267 to –439	–300.3	9	–4.21	1.38	1.06
ZSMNW025A	High	10	–170	–170	1	–6.94		
ZSMNW028A (ZSMEW028A)	High	10	–81	–81	1	–6.45		
ZSMNW042A	High	80	–672	–672	1	–6.37		
ZSMNW048A	Medium	20[1]	–30.3	–30.3	1	–4.52		
ZSMNW928A (Reflector N)	Medium	20[1]	–746 to –869	–807.5	2	–6.12	0.05	
ZSMNW929A (ZSMNE040A)	High	50	–832 to –895	–863.5	2	–5.90	0.27	
ZSMNW932A (ZSMNW006A)	High	10	–470 to –549	–509.5	2	–6.06	0.78	
All other HCD		20[1]				–4.92	1.48	

[1] Geological thickness assumed to be 20 m due to lack of data.

Table 5-3. Number of deformation zones (DZ) in the Laxemar 1.2 that have any measured T-value or don't have any measurement.

DZ classification	No, of DZ Total	No, of DZ With one or several T-values	No, of DZ No T-values
High confidence	32	20	12
Medium confidence	56	4	52
Low confodence	92	0	92
Total	180	24	156

5.3 HCD – Depth trends in transmissivity

In Figure 5-6 all transmissivity data for the HCDs representing each tested borehole section (one "best choice" (BC) T-value for each test section representing a HCD) are plotted. The dataset was divided into three subsets based on elevation (z) intervals; down to –300, –300 to –600 and below –600 masl and univariate statistics were computed. In Figure 5-7 the standard deviation, as well as the 95% confidence level for Log10(T) are shown. Two different functions have been fitted to the mean transmissivity values evaluated for the three elevation intervals, a power law dependence (Equation 5-1) and an exponential one (Equation 5-2):

$$T = a \cdot z^b \quad (5\text{-}1)$$

$$T = a \cdot e^{(b \cdot z)} \quad (5\text{-}2)$$

In Table 5-4 the parameters for the depth trend models of the transmissivity in HCDs are shown.

Table 5-4. Coefficients of depth trend models applied to transmissivity data in HCDs. Unit for transmissivity (T): m^2/s. Unit for elevation (z): masl. Note that the regression is equated using –z as a parameter.

Depth trend model	coefficient a	Coefficient B	Coeff. of determination, R-squared r^2
Power-law (Equation 8-9)	0.219	–1.783	0.72
Exponential (Equation 8-10)	$6.24 \cdot 10^{-5}$	–0.00519	0.89

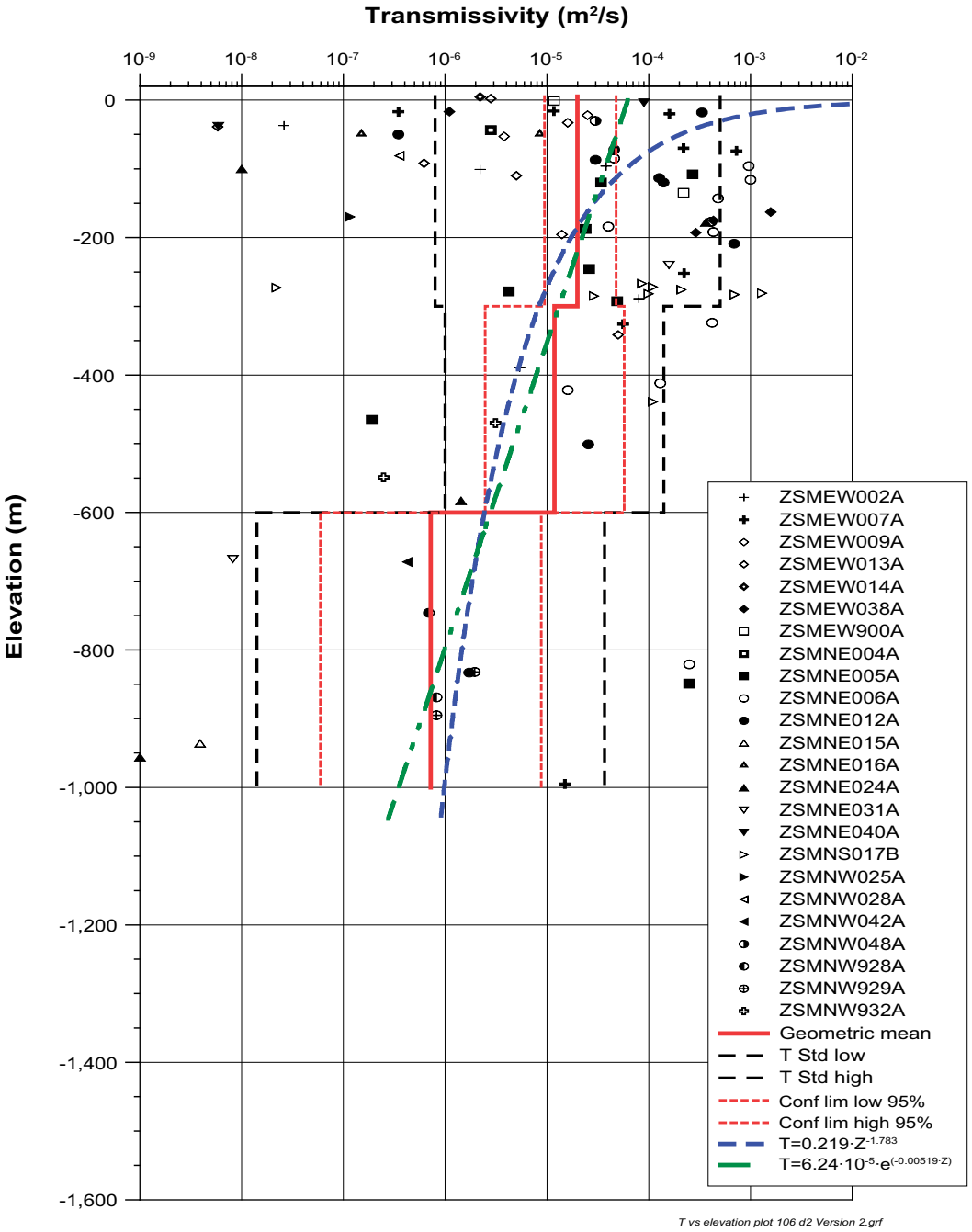

Figure 5-6. *Depth trend of the transmissivity in HCDs.*

A linear trend function was also fitted to the standard deviation of Log10(T) of the three elevation data sets, see Figure 5-7, Equation 5-3 and Table 5-5:

$$\text{Std}(\log10(T)) = a \cdot z + b \qquad (5\text{-}3)$$

As can be seen in Figure 5-6 the confidence limits for mean Log10(T) is wide for all thee depth intervals. It can be concluded that the inferred depth trend of the transmissivity is very uncertain due to sparse data for the deformation zones. The inferred depth trend of the standard deviation is of course as well uncertain.

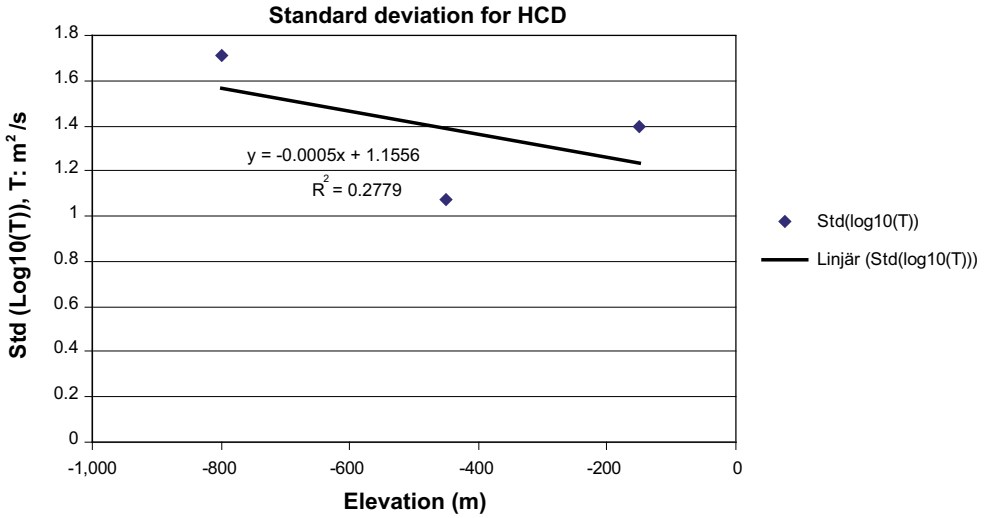

Figure 5-7. *Depth trend of the standard deviation of transmissivity in HCDs, based on the evaluated standard deviations shown in Figure 5-6 .*

Table 5-5. Coefficient for depth trend model applied the standard deviation of Log10(T) in HCDs. Unit for transmissivity (T): m²/s. Unit for elevation (z): masl. Note that the regression is equated using –z as a parameter.

Depth trend model	Coefficient a	Coefficient b	Coeff. of determination, R-squared r2
Std (log10(T))	–0.0005	1.1556	0.28

The above trend models described are possible alternatives that can be applied to the HCDs in the model version Laxemar 1.2. Using a stochastic approach and the depth trend functions to assign the transmissivity raises the question if there are any upper and lower limits of transmissivity in HCDs that should be honoured. One can probably deduce a lower limit from the reasoning given in Section 6.6 for low-conductive (matrix) rock.

The power-law function indicates very high transmissivity near the surface that is to be regarded as unrealistic. It is here proposed that the maximum transmissivity is set to 1E–3 m^2/s, which is close to the maximum value seen in Figure 5-6.

5.4 HCD – Difference in properties compared to HRD

The hydraulic conductivity (K) of each HCD transmisivity value was calculated dividing the transmissivity value with the estimated geological thickness for each deformation zone, the latter given as a mean value in Table 5-1. In Section 6.2 the depth trend for the hydraulic conductivity of the rock mass, excluding test sections intersected by deformations zones (HCDs) is shown. In Figure 5-8 the geometric mean values of K for HCDs and HRD (representing the rock mass inbetween the HCDs) are plotted. As can be seen, the mean K of the HCDs is about an order of magnitude more conductive than the mean value of the HRDs. As can be seen in the geometric mean transmissivity values differ on a confidence level of 0.95 down to elevation –600 m. Below –600 m the samples in HCD are few, so the confidence band is wide for hydraulic conductivity in HCD, thus indicating that the confidence level is less than 0.95 that the geometric means differ. In combination, the results seem rather conclusive that it is meaningful to identify and model large deformation

zones as separate domains as they have significantly higher hydraulic conductivity than the surrounding rock mass. However, the results also points out that some HCDs, as now interpreted in Laxemar 1.2, may have low transmissivity (and hydraulic conductivity). In the context of groundwater flow modelling, including or excluding such low-transmissive deformation zones is a matter of its location and hydraulic characteristics. If it may act as a hydraulic barrier, it should be included in the modelling. If it has the character of "normally fractured rock" (as can be the case for mainly ductile deformation zones) it may be justified to exclude those zones. It should be observed that in model version Laxemar 1.2 (cf Figure 5-6), none of the geologically defined deformation zones have been excluded on the basis of the above discussion.

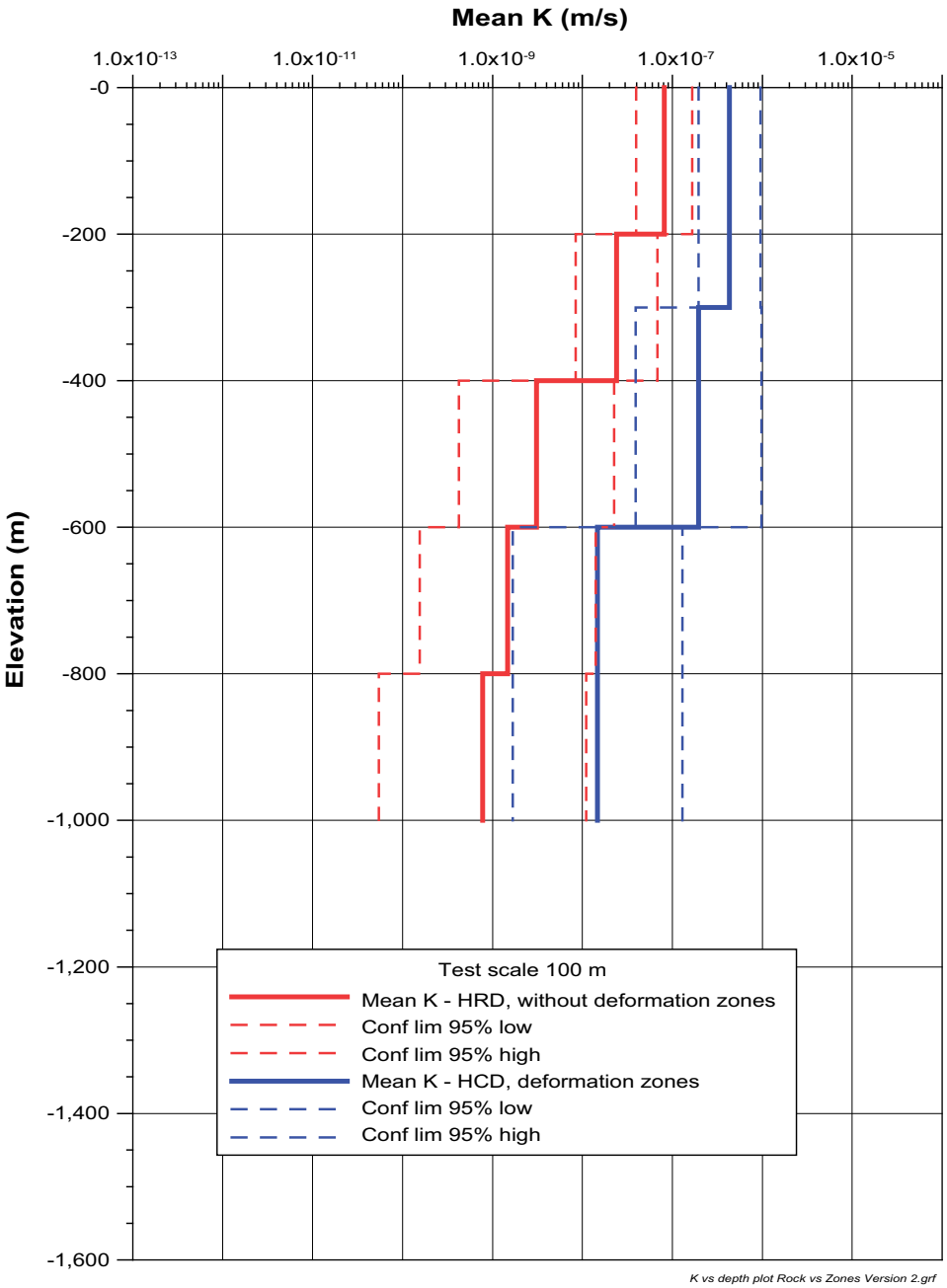

Figure 5-8. *Comparison between the depth trend of the hydraulic conductivity in HCDs (equated from on geometric mean transmissivity from Figure 5-6 and geological thickness given in Table 5-1, and the depth trend of the geometric hydraulic conductivity of HRDs (excluding data from HCDs)), as seen in Figure 6-4.*

5.5 HCD – Storage coefficient and transport aperture

Information on the storage coefficient is essential for estimating the influence radius of, and planning and interpreting, interference tests. In the regional groundwater flow modelling, the storage coefficient is of minor importance, unless the task is to test the model against interference tests.

Only one site-specific interpretation of the storage coefficient (S) has so far been made during the site investigations, but data from other investigations have been compiled. In /Rhén et al. 1997c/ the storage coefficient of deformation zones was estimated based on large-scale interference tests, and in /Rhén and Forsmark 2001/ the storage coefficient was estimated for larger and smaller deformation zones. In conjunction with the TRUE Block Scale experiment at Äspö HRL, a large number of hydraulic interference tests w made and the storage coefficient was estimated for larger and minor zones, /e.g. Andersson et al. 1998, 2000/. Data were compiled from these projects and a relation was estimated for the correlation between T and S, see Table 5-6. The variation along the regression line can be expected to be within ± one order of magnitude for a value of S calculated with the formula in Table 5-6 .

Likewise, the database for the kinematic porosity (n_e) (= mean transport aperture/hydraulic thickness of HCD; (b_T), the latter being the thickness of a HCD, to which the evaluated transmissivity for the corresponds);

$$n_e = \frac{e_T}{b_T} \qquad (5\text{-}4)$$

is also very limited. The equation given in Table 5-7 is based on the hydraulic aperture presented in /Dershowitz et al. 2003/. This equation gives similar values to those reported in /Rhén et al. 1997c/, with a = 1.428 and b = 0.523, based on a compilation of tracer tests in crystalline rock, ranging from tests of a single fracture up larger test scales with densely fractured rock and fracture zones. Kinematic porosity is considered as a calibration parameter, but Table 5-7 may be used for first estimates of the properties.

Table 5-6. Estimation of storage coefficient (S) for HCD from transmissivity (T). $S = aT^b$. T (m^2/s), S (–).

Approximate test scale (m)	Coefficient a	Coefficient b	Reference
5–100	0.0007	0.5	/Rhén et al. 1997b, Rhén and Forsmark 2001, Andersson et al. 1998, 2000/

Table 5-7. Estimation of mean transport aperture for HCD from transmissivity (T). $e_t = aT^b$. T (m^2/s), e_t(m).

Approximate test scale (m)	Coefficient a	Coefficient b	Reference
5–100	0.46	0.5	/Dershowitz et al. 2003/

5.6 HCD – Evaluation of uncertainties

The confidence in the geometry of the deformation zone model and rock domain model, hydraulic properties, boundary conditions and initial conditions to variable extent govern the overall confidence of results of the numerical groundwater flow simulations. Their identification further promotes the discussion of how and where uncertainty should be decreased, and why. In this chapter HCDs are discussed.

5.6.1 Geometry of deformation zones (HCD)

The general confidence in the existence of interpreted deterministic deformations zones generally low, as most of the members of this category of deformation zones are only based on evidence of the existence of lineaments, and no hydraulic tests are available. However, a high confidence for existence has been judged for some of the deformation zones, particularly in the local model area, cf /Wahlgren et al. 2005/. For these zones, the confidence in some of the hydraulic properties and characteristics is judged in Table 5-8.

So far only a few hydraulic interference tests have been performed, and have been able also to hydraulically confirm, as supporting evidence to the geological evidences, the existence and geometry of a given deformation zone.

The confidence in the hydraulic thickness (essentially geological thickness incorporated from /Wahlgren et al. 2005/) is very low, based on one or a few intercepts of deformation zones by boreholes. Also, the hydraulic thickness may vary along the extent of the individual deformation zone "plane". However, the thickness is judged to be of minor importance while transmissivity controls the capacity for flow in the deformation zones.

Table 5-8. Confidence in the hydraulic properties and characteristics (regional reference case) assigned to the HCDs in Laxemar 1.2. Hydraulic thickness (b) Transmissivity (T), Storage coefficient (S), Mean transport aperture (e_T).

Name of HCD, RVS ID (Earlier name)	Geological confidence, High/Medium/ Low	Geological thickness, b	T	S	e_T	Comment (intersection boreholes and other comments)
		(m)	(m^2/s)	(–)	(m)	
ZSMEW002A (Mederhult zone)	High	Low	Low-Medium	Low	Low	HAS10, HLX02, KAS03, KLX06, HLX20
ZSMEW007A	High	Low	Medium	Low	Low	KLX01, KLX02, KLX04, HLX10, HLX13, HLX14, HLX24, HLX22
ZSMEW009A (EW3)	High	Low	Low-Medium	Low	Low	HAS14, HAS21, KAS06, TASA (SA1420A,B, HA1405A,B)
ZSMEW013A (EW1A)	High	Low	Low-Medium	Low	Low	KA1755A, KAS04, HLX03, HAS18, HAS01
ZSMEW014A	Medium	Low	Low	Low	Low	HLX02
ZSMEW038A (ZSMEW038A_B)	High	Low	Medium	Low	Low	HAV05, KAS09, KBH02, TASA (SA-holes, chainage 1180)
ZSMEW039A	Medium	Low	Low	Low	Low	HLX05
ZSMEW900A (ZSMEW005A 7A)	High	Low	Low	Low	Low	HLX25, HLX14
ZSMNE004A (ZSMEW004A)	High	Low	Low	Low	Low	TASA (Sum SA0289A, SA0327A)
ZSMNE005A (Äspö shear zone; EW1b)	High	Low	Medium	Low	Low	KA1755A, KA1754A, KA1751A, KAS04, KA3590G02, KAS02, KAS12, HLX09

Name of HCD, RVS ID (Earlier name)	Geological confidence, High/Medium/ Low	Geological thickness, b	T	S	e_T	Comment (intersection boreholes and other comments)
		(m)	(m^2/s)	(–)	(m)	
ZSMNE006A (NE1)	High	Low	Medium	Low	Low	HLX18, KA1061, KA1131B, KAS07, KAS08, KAS09, KAS11, KAS14, KBH02, KAS02, KAS16, TASA (7 HA-probe-holes)
ZSMNE012A (includes NW004A (old names EW7-NE4)	High	Low	Medium	Low	Low	HAV02, HAV12, HAV13, HLX18, HMJ01, KAV01, KAV03, KAV04A, KBH02, TASA (chainage 867-Sum of pair, SA0792 more)
ZSMNE015A	High	Low	Low	Low	Low	KSH01A
ZSMNE016A	High	Low	Low	Low	Low	SA0344A, SA0344B
ZSMNE024A	High	Low	Low-Medium	Low	Low	KSH01A, KSH03A, KAV01A, KAV04A
ZSMNE031A	High	Low	Low	Low	Low	KSH01A, KSH03A
ZSMNE040A	High	Low	Low	Low	Low	HLX04, HLX01
ZSMNS017B (NNW4)	High	Low	Medium	Low	Low	HA1960A, SA1997A, SA2009A, SA2025B, SA2074B, SA2090B, SA2109B, KC0045F, KA2048B
ZSMNW025A	High	Low	Low	Low	Low	HSH01
ZSMNW028A (ZSMEW028A)	High	Low	Low	Low	Low	HAV09
ZSMNW042A	High	Low	Low	Low	Low	KLX05
ZSMNW048A	Medium	Low	Low	Low	Low	HLX07
ZSMNW928A (Reflector N)	Medium	Low	Low	Low	Low	KLX02, KLX04
ZSMNW929A (ZSMNE040A)	High	Low	Low	Low	Low	KLX02, KLX04
ZSMNW932A (ZSMNW006A)	High	Low	Low	Low	Low	KLX03, KLX05
All other HCD		Low	Low	Low	Low	–

5.6.2 Hydraulic properties of deformation zones (HCD)

The confidence in the transmissivity assigned to a particular deformation zone (HCD) is medium to low due to zero, one or a few borehole intercepts of individual deformation zones, see Table 5-8. Having 2–3 hydraulic test results in different boreholes in a deformation zone, the confidence is set to low to medium. Having 4 up to ca 10 hydraulic test results, the confidence is set to medium. The transmissivity can be expected to vary along the "plane" of the deformation zones, and since most zones are larger than 1 km one can expect that there will always be great difficulties to obtain a high confidence in the properties and heterogeneity by drilling and borehole testing. Several observations of a deformation zone transmissvity have been judged as low to medium, despite four or more borehole intercepts. The reason for this is that the borehole intercepts have to be examined in more detail, or that the observations are fairly local compared with the entire extent of the deformation zone.

The observations indicate that there may be a depth dependence of the transmissivity in deformation zones. The data are few and the depth dependency must be considered uncertain.

The confidence in the storage coefficient is low, and will be lower than the confidence in transmissivity, due to difficulties in making proper tests. However, it is judged that this is of minor importance, as it controls the transient responses on time scales of days-months when pumping, and during drawdown caused by tunnelling, which is deemed being of minor importance to long-term safety. The variation of the storage coefficient is less than that of transmissivity, making it easier to analyse using sensitivity studies. However, the storage coefficient is important when the size of hydraulic features is to be assessed from hydraulic tests, and the size is an essential component when studying the transmissivity models suggested for the hydraulic DFN. The storage coefficient is also important when judging results from interference tests.

The confidence in the mean transport aperture (giving the flow porosity when used jointly with the hydraulic thickness) is low, and probably will be rather low for individual deformation zones. However, some new data will be collected and probably the confidence in transport aperture assigned will be increased during the continued site investigations. Still, the confidence will probably be low-medium, demanding sensitivity studies to investigate the implications of uncertainty in this property. The importance for Safety Assessment is also considered low.

The defined deformation zones (with high to low confidence) create a well-connected system, partly because of the geometrical definition (assumed to intersect or stop mutually or to be continuous over the plane) and partly because of the assigned hydraulic properties (assumed to be constant over the plane and to have a rather high transmissivity). The spatial distribution of properties within HCDs is difficult to assess (generally very few samples).

6 Hydraulic rock domains (HRD)

This section explores assignment of hydraulic properties representative for the rock mass (HRD) between the deterministically defined deformation zones. To some extent the entire data set representing both the HCD and the rock mass in between the HCD is also explored, but mainly presented in Appendix 2.

Properties for the HRDs presented in this section are based on statistical analysis of borehole data. The report covers data of interest for HydroDFN (Discrete Fracture Network) modelling, but does not include HydroDFN modelling. The HydroDFN modelling results can be found in /SKB 2006, Hartley et al. 2006, Follin et al. 2006/.

The hydraulic tests performed at a 100 m test scale as presented in this section have the largest coverage in terms of area/volume and that data for different test scales do not entirely represent the same boreholes or depth. Test scales 20 m (actually 10, 20 and 30 m with 20 m dominating) and 5 m (actually 2, 3 and 5 m) show similar trends as test scale 100 m, but do not cover the area as well as at the test scale of 100 m. E.g. tests in borehole lengths 0–100 m are missing for the 20 m test sections and very few tests are available for the 5 m tests sections, but for the 100 m test sections the data set representing borehole length 0–100 m are rather large. This is the main reason why 100 m test sections are used for the evaluation of depth trends. Observe that data for the depth trends are plotted for elevation intervals, but it is almost equal to depth intervals due to the low topographic relief. How the hydraulic tests are distributed in the boreholes is shown in /Rhén et al. 2006ab/.

6.1 General tendency of difference between areas

As a starting point for the analysis, data for the entire Simpevarp area was explored, not just the Laxemar subarea. Scrutiny of hydraulic data from the individual boreholes revealed that there seemed to be differences between the defined subareas Simpevarp and Laxemar, but also differences between subregions within the Simpevarp subarea. The Simpevarp subarea was consequently further subdivided as Ävrö seems to differ, being more permeable, compared with the Simpevarp peninsula.

100 m scale: As can be seen in Figure 6-1, the general tendency is that Simpevarp peninsula has the lowest hydraulic conductivity followed by the Laxemar subarea with Äspö and Ävrö as the most conductive units. It should however be remembered that the observations cover depth ca 0–1,000 m, with a slight dominance of observations in the depth interval 0–200 m. As will be seen in the next section, there is probably a depth dependence such the representative hydraulic conductivity at repository depth is less than that indicated by Figure 6-1.

20 m scale: The median hydraulic conductivities are lower than those at the 100 m scale. The general tendency is that the Laxemar subarea shows the lowest hydraulic conductivity followed by the Simpevarp peninsula and then Äspö and Ävrö as the most conductive units, see Figure 6-2 and Figure 6-3.

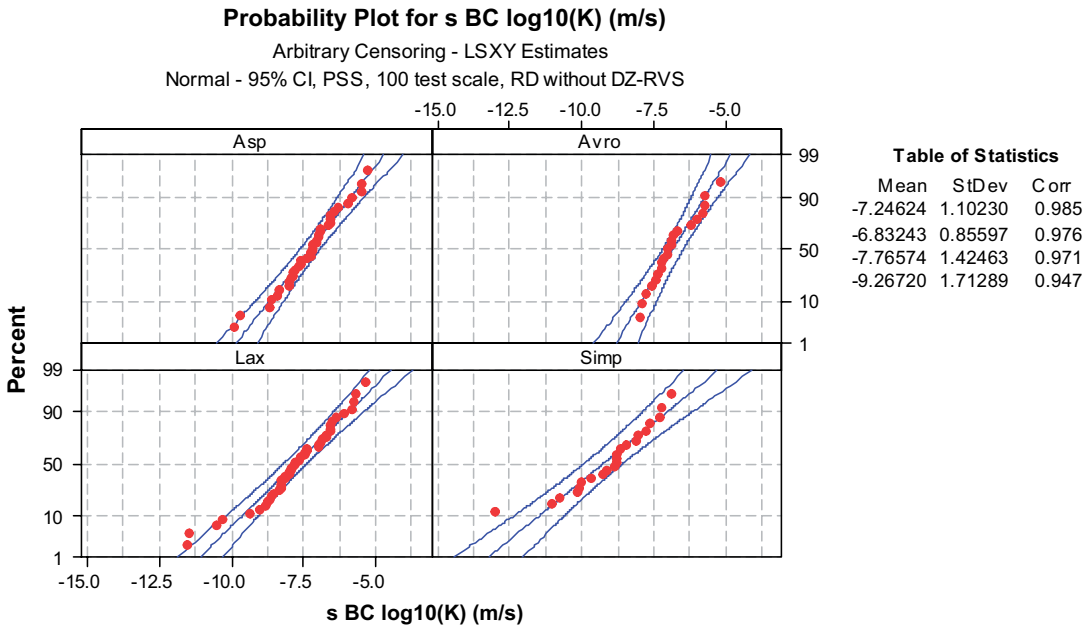

Figure 6-1. *Hydraulic conductivity distribution of the rock mass by geographical area. Test scale 100 m. Data from the Laxemar subarea, Simpevarp peninsula, Äspö, Ävrö-Hålö-Mjälen. Data representing deterministically defined deformation zones in RVS model version L1.2 are excluded. (Tabulated results follow read upper left to right corner followed by lower left to right corner.)*

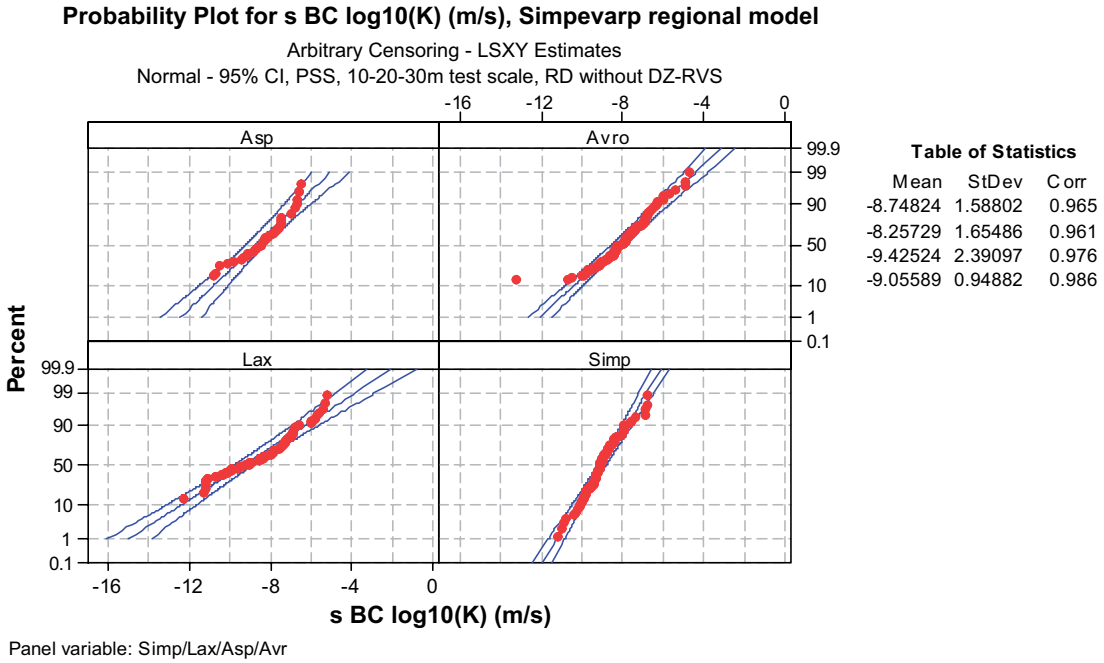

Figure 6-2. *Hydraulic conductivity distribution of the rock mass by geographical area. Test scale 10–20–30 m. Data from the Laxemar subarea, Simpevarp peninsula, Äspö, Ävrö-Hålö-Mjälen. Data representing deterministically defined deformation zones in RVS model version L1.2 are excluded. (Tabulated results follow read upper left to right corner followed by lower left to right corner.)*

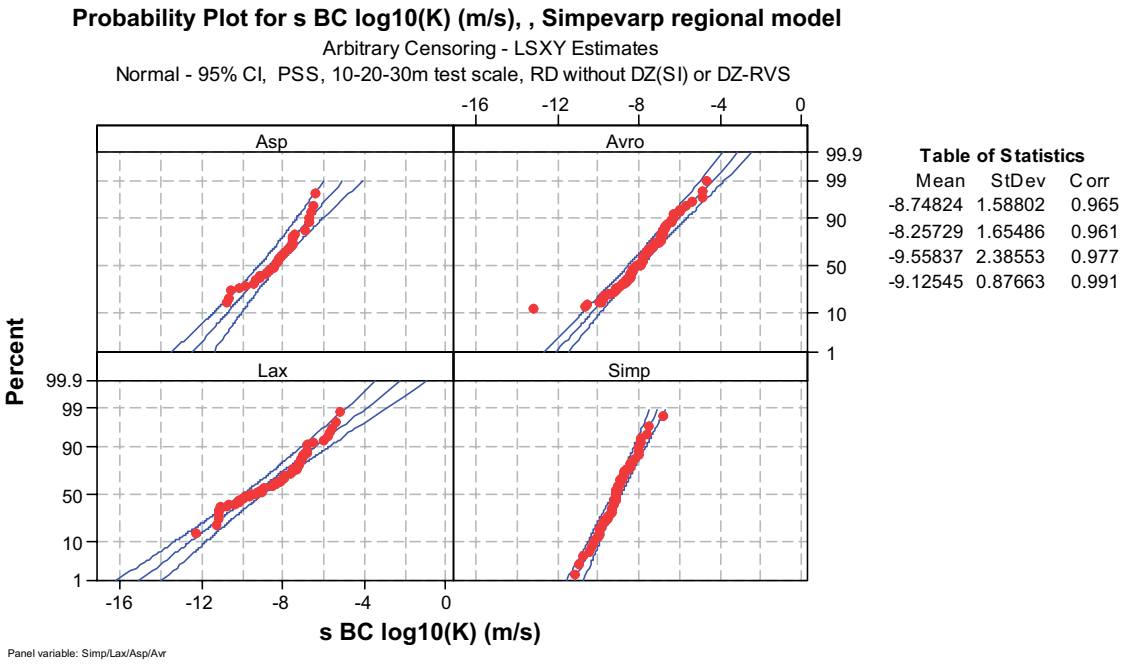

Figure 6-3. *Hydraulic conductivity distribution of the rock mass by geographical area. Test scale 10–20–30 m. Data from the Laxemar subarea, Simpevarp peninsula, Äspö, Ävrö-Hålö-Mjälen. Data representing deterministically defined deformation zones in RVS model version L1.2 and deformation zones identified in the Geological single-hole interpretation are excluded. (Tabulated results follow read upper left to right corner followed by lower left to right corner.)*

6.2 Depth trends

Figure 6-4 to Figure 6-10 plot the HRD data (pure rock mass, with sections representing deformation zones excluded) at a test scale of 100 m, for a) the entire data set (Simpevarp peninsula, Laxemar subarea, Äspö, and Mjälen) with statistics given for the entire data set and for b) Laxemar subarea, c) Simpevarp peninsula, d) Äspö island and e) Ävrö island, respectively. The data sets were subdivided in subsets based on 200 m elevation intervals and the corresponding univariate statistics were computed. The data set was divided in sets based on elevation (z) levels grouped into 200 m sections and univariate statistics was computed see Appendix 2. In Figure 6-4, Figure 6-7 to Figure 6-10 the standard deviations as well as the 95% confidence level for Log10 (K) are shown for the entire data set (Some of the confidence intervals for the mean Log10(K) in the figures and Tables in Appendix 2 are extremely wide due to very few samples.). Two depth trend functions, a power law and an exponential model, cf Equations 6-1 and 6-2, respectively, were also fitted to the mean values of the three elevation-stratified datasets, cf Table 6-1.

$$K = a \cdot z^{b} \qquad (6\text{-}1)$$

$$K = a \cdot e^{(b \cdot z)} \qquad (6\text{-}2)$$

The fitting of these depth trend models was not considered reasonable for the Äspö and Ävrö data, but for data from Laxemar subarea and Simpevarp peninsula. A few remarks can be made in relation to the results from the different areas. The 100 m results do not indicate any depth-dependence in the 0–500 m interval of the Äspö HRL data, cf Figure 6-9.

In the data from the Laxemar subarea, see Figure 6-7, and the Simpevarp peninsula, see Figure 6-8, there seem to be a slight decrease in hydraulic conductivity with depth. There are hardly any data at depth from the Ävrö Island, but the few existing data indicate a depth trend such that values below 100 m are lower than that above 100 m, cf Figure 6-10. One should also observe that there are rather few observations in the elevation intervals 100–200 and 200–300 m in the Laxemar subarea, and some of the data may be directly or indirectly affected by the existence of fracture zones (minor deformation zones, not considered in the RVS model). The increase in hydraulic conductivity from ground surface down to 300–400 m depth in both KLX02 and KLX04 may also possibly be related to the fact that the rock above, and bounded by ZSMEW007A and ZSMEW002A above ZSMEW007A, is subject to stress release that may have caused widening of fractures, and hence resulting in an increase in hydraulic conductivity. In other boreholes the decrease of the hydraulic conductivity seems to commence at 100–300 m depth.

Looking at test scale 20 m results (see Appendix 3), hardly any depth trend at Äspö depth 0–800 m is seen. At Ävrö, there is a depth trend above elevation –500 m, but below –500 m it increases. However, possibly a part in KAV04A should probably belong to a Deformation zone. The Laxemar data show a weakly decreasing trend down to –300 m, then a "jump", as for 100 m tests, then decreasing again. Data from –700 to –800 m are uncertain due to few data. Data for Simpevarp peninsula is weakly decreasing by depth, and show a bit different behaviour from –100 to –300 m and –300 m and downwards, compared to 100 m scale. The 100 m scale seems to indicate a larger difference between median for 0–300 m compared to below –300 m than for 20 m scale. The reason is that the KSH03A is included test scale 100 m for elevation in 0 to –100 m and –200 to –300 m, due to the definition of RVS zones and there are no 20 m tests in KSH03A (There are few tests in 100 m test scale at each depth interval!). Thus, the depth dependency on Simpevarp peninsula is probably more conductive 0–100 m and a weakly depth dependent below –100 m.

A linear trend function was also fitted to the standard deviation of Log10(K) of the elevation data-sets shown in Figure 6-4, see Equation 6-3, Figure 6-5 and Table 6-2.

Looking at the entire data set, see Figure 6-4, the confidence limits indicate that there is probably a depth trend. For the Laxemar subarea, see Figure 6-7, the depth trend must be considered uncertain, as the number of observations is rather few at depth. The trend of an increasing standard deviation with depth should be considered as uncertain.

$$\mathrm{Std}(\log10(K)) = a \cdot z + b \qquad (6\text{-}3)$$

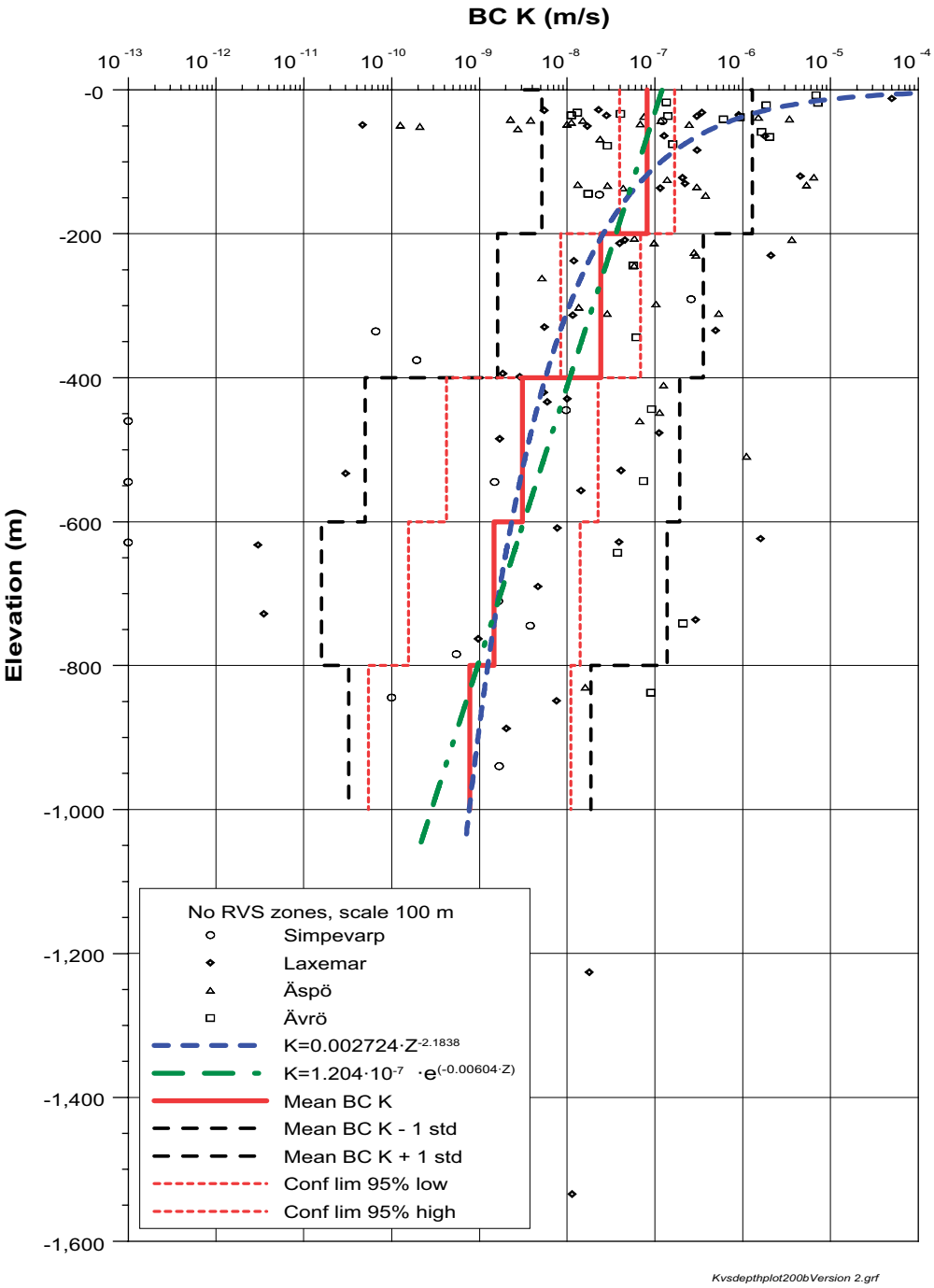

Figure 6-4. *Depth trend of the hydraulic conductivity in HRDs. Test scale 100 m. Data from all areas (Laxemar subarea, Simpevarp peninsula, Äspö, Ävrö-Hålö-Mjälen) indicated. Depth trends and statistics given for a combined data set made up of data from the entire regional area. Data representing deterministically interpreted deformation zones in RVS model version Laxemar 1.2 are excluded. BC = Best choice value.*

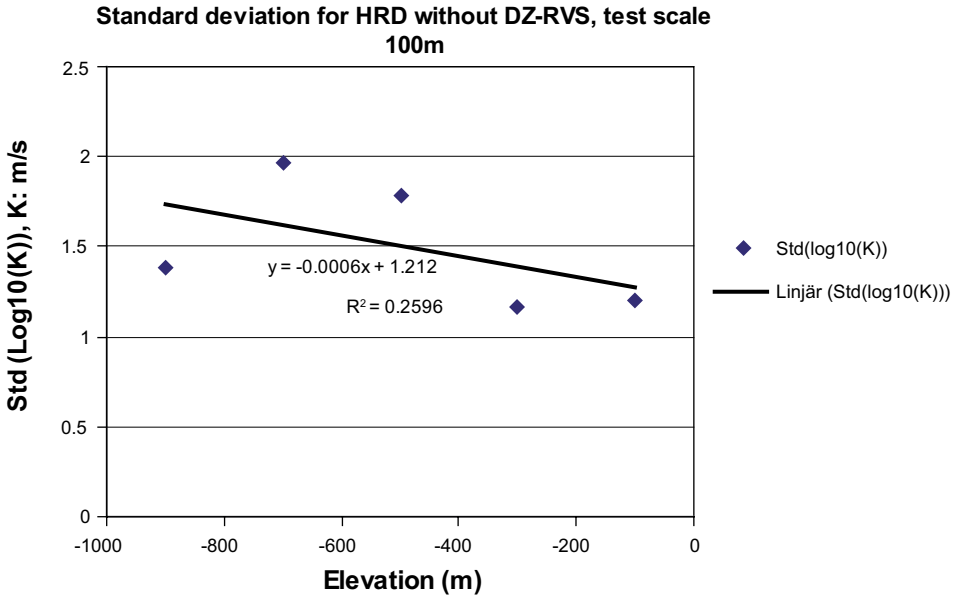

Figure 6-5. *Depth trend of the standard deviation of transmissivity in HRDs, based on the evaluated standard deviations shown in Figure 6-4.*

Table 6-1. Coefficients of depth trend models applied to hydraulic conductivity in HRDs. Test scale 100 m. Unit for hydraulic conductivity (K): m/s. Unit for elevation (z): masl. Note that the regression is equated using –z as a parameter.

Area	Depth trend model	coefficient a	coefficient b	Coeff. of determination, R-squared r^2
Regional model	Power-law (Equation 8-9)	0.002724	–2.1838	0.94
	Exponential (Equation 8-10)	$1.204 \cdot 10^{-7}$	–0.00604	0.96
Laxemar subarea	Power-law (Equation 8-9)	0.00146	–2.0633	0.99
	Exponential (Equation 8-10)	$1.0471 \cdot 10^{-7}$	–0.00557	0.95
Simpevarp peninsula	Power-law (Equation 8-9)	0.006332	–2.852	0.71
	Exponential (Equation 8-10)	$9.495 \cdot 10^{-9}$	–0.00726	0.61

Table 6-2. Coefficient for depth trend model applied the standard deviation of Log10(K) in HRDs. Test scale 100 m. Unit for hydraulic conductivity (K): m/s. Unit for elevation (z): masl. The regression is based on –z.

Area	Depth trend model	coefficient a	coefficient b	Coeff. of determination, R-squared r^2
Regional model	Std (log10(K))	–0.0006	1.212	0.26

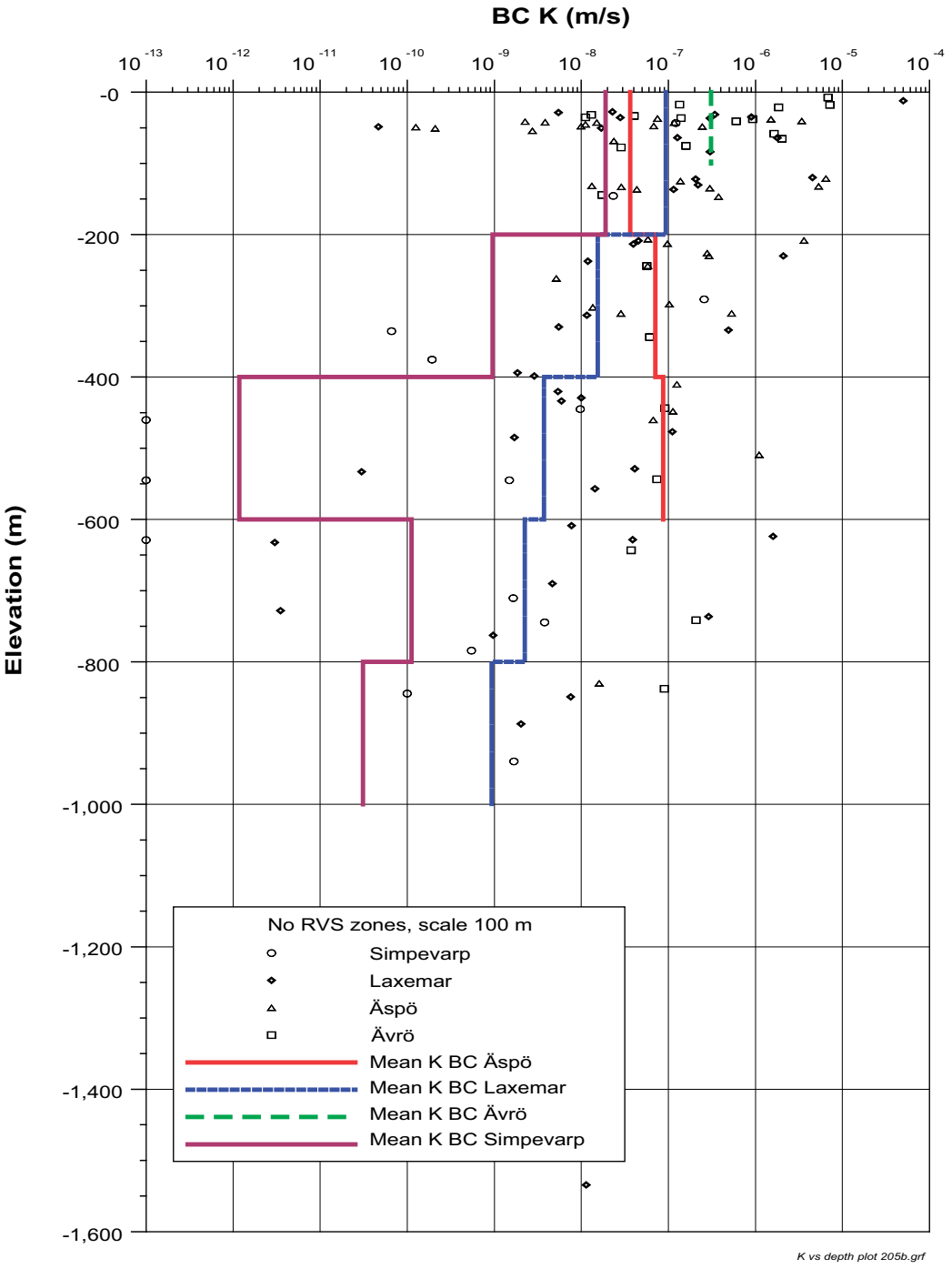

Figure 6-6. *Depth trend of the hydraulic conductivity in HRDs. Test scale 100 m. Data from all areas (Laxemar subarea, Simpevarp peninsula, Äspö, Ävrö-Hålö-Mjälen) indicated. Depth trends for mean Log10(K) shown for the sub-areas. Data representing deterministically interpreted deformation zones in RVS model version Laxemar 1.2 are excluded. BC = Best choice value.*

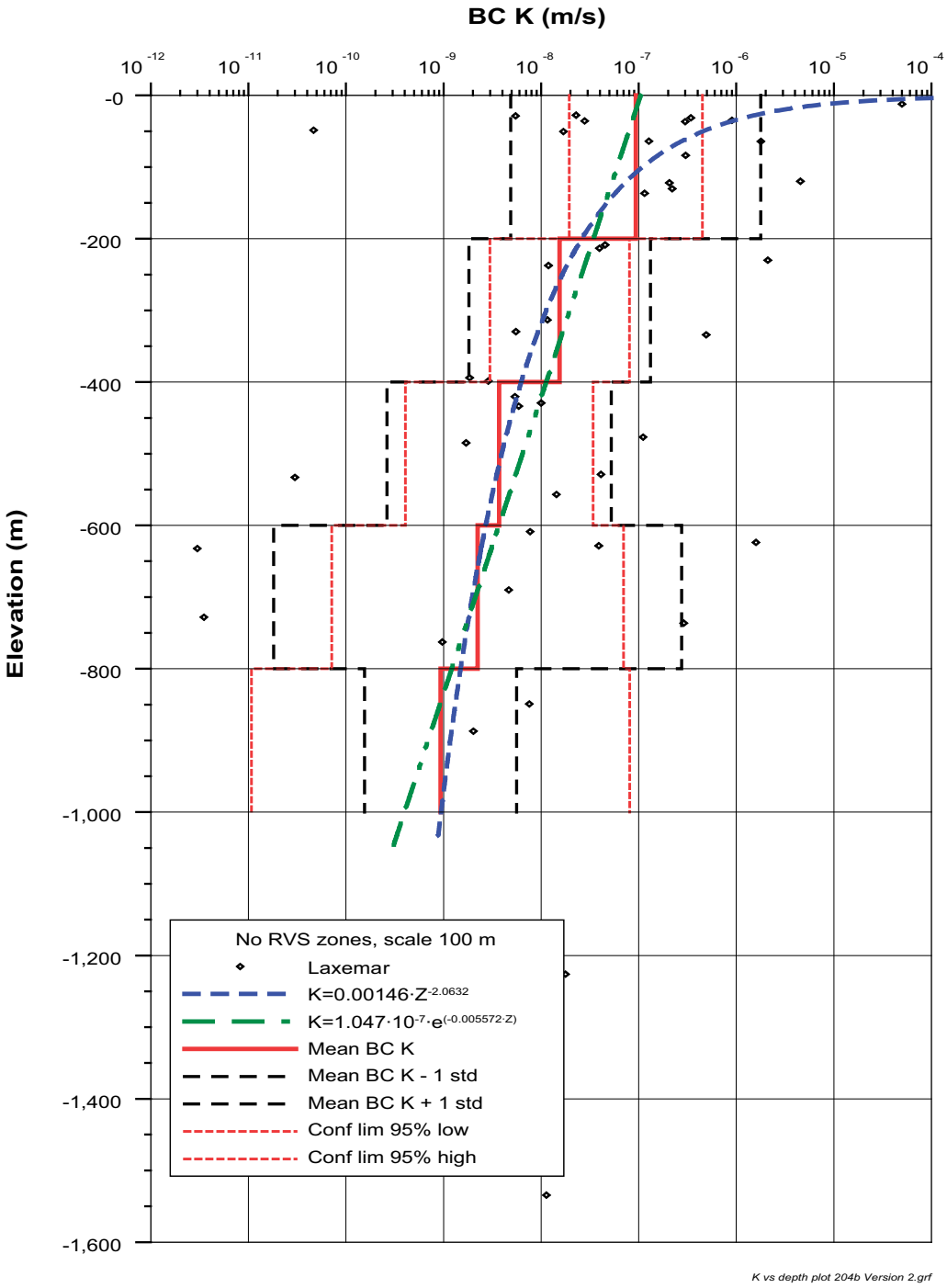

Figure 6-7. *Depth trend of the hydraulic conductivity in HRDs. Test scale 100 m. Data, statistics and depth trends based on data from the Laxemar subarea alone. Data representing deterministically interpreted deformation zones in RVS model version Laxemar 1.2 are excluded. Based onBoreholes HLX01–09, –32, KLX01–KLX06 (In KLX05 and KLX06, only data from WLP measurements are included). BC = Best choice value. (Confidence interval extremely wide in some cases due to very few sample and should just be seen as indicators of great uncertainty.)*

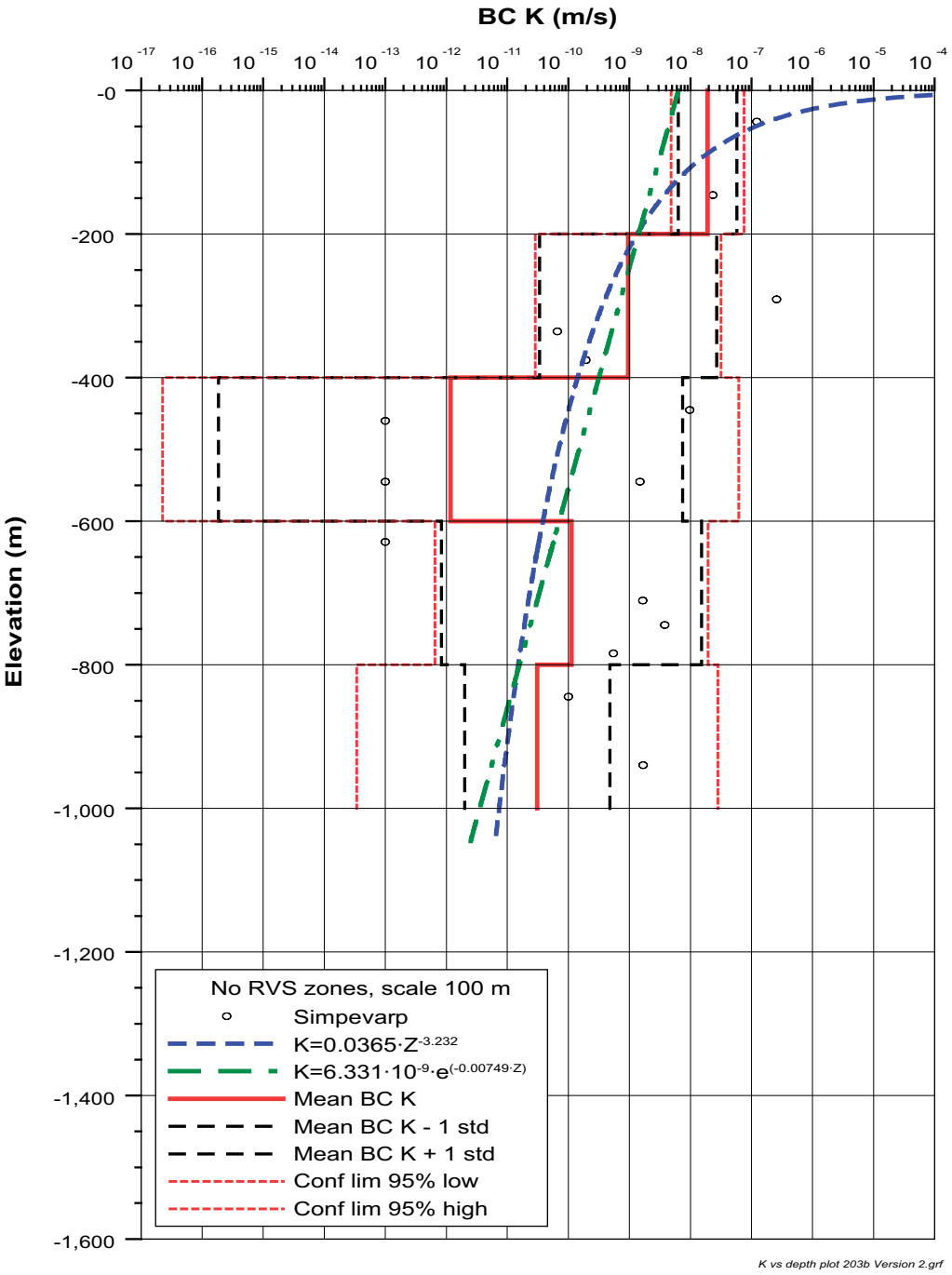

Figure 6-8. *Depth trend of the hydraulic conductivity in HRDs. Test scale 100 m. Data, statistics and depth trends based on data from the Simpevarp peninsula alone. Depth trends and statistics given for a combined data set made up of data from the entire regional area. Data representing deterministically interpreted deformation zones in RVS model version Laxemar 1.2 are excluded. BC = Best choice value.*

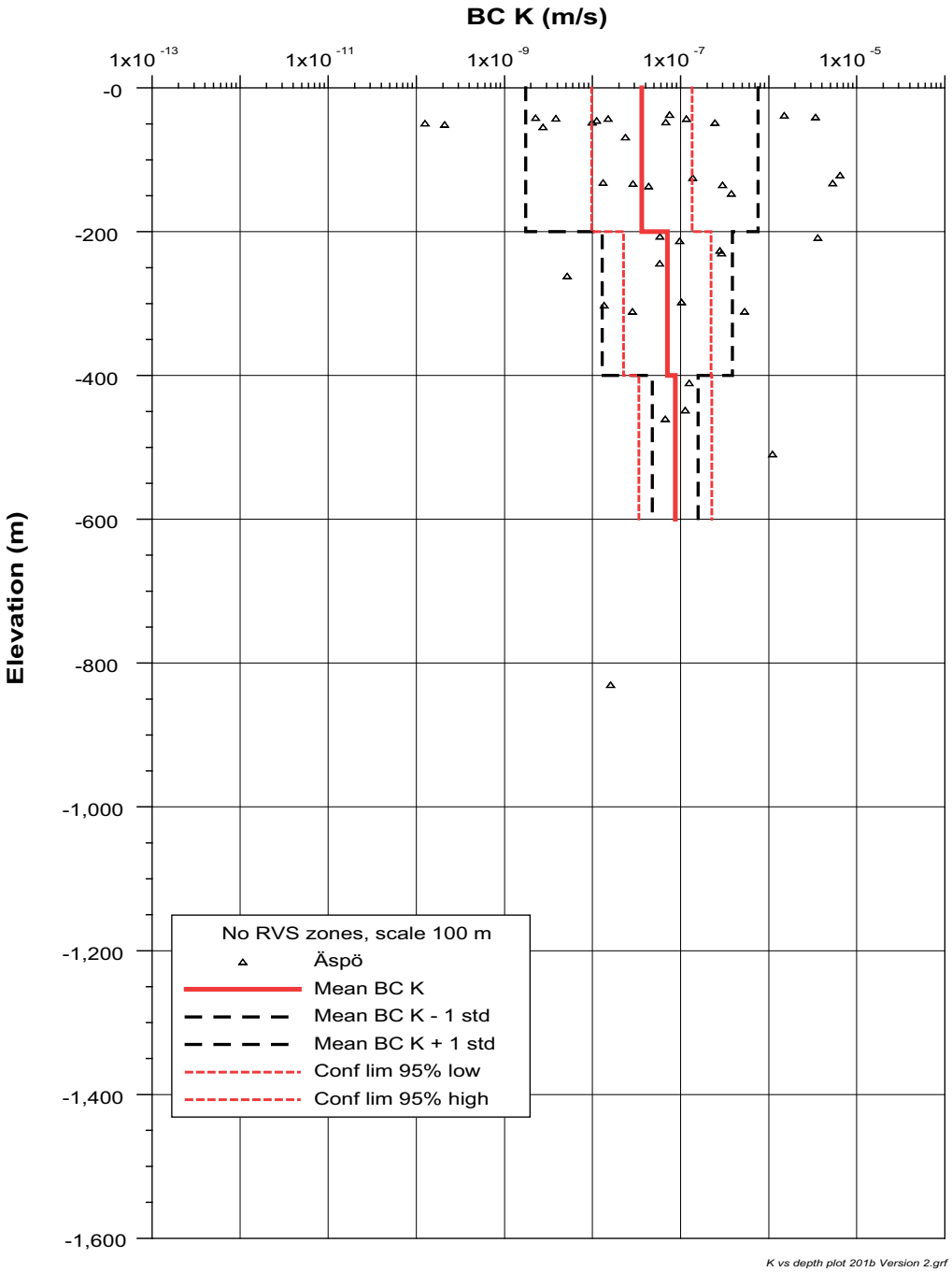

Figure 6-9. *Depth trend of the hydraulic conductivity in HRDs. Test scale 100 m. Data, statistics and depth trends based on data from the Äspö area alone. Depth trends and statistics given for a combined data set made up of data from the entire regional area. Data representing deterministically interpreted deformation zones in RVS model version Laxemar 1.2 are excluded. BC = Best choice value.*

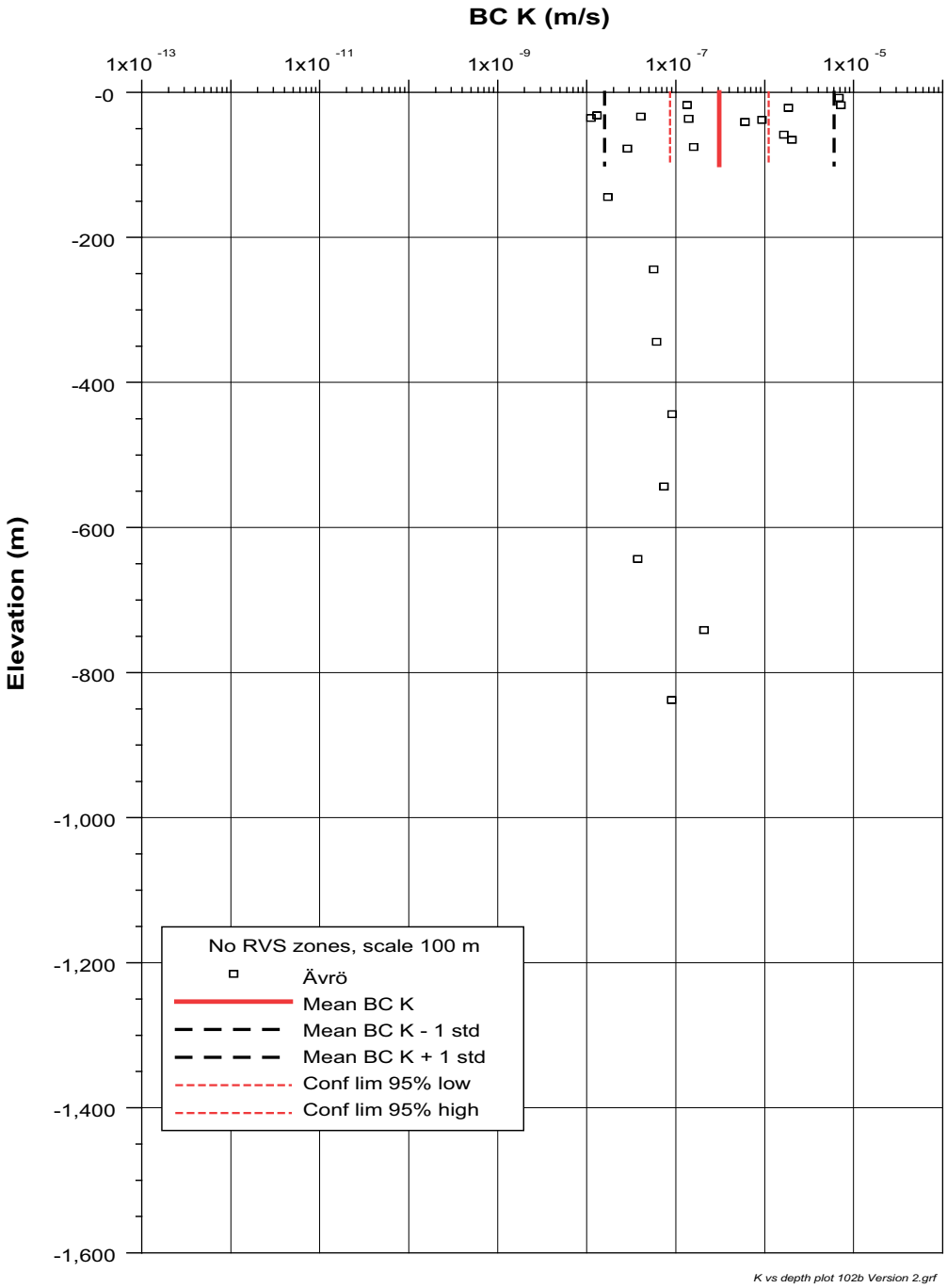

Figure 6-10. *Depth trend of the hydraulic conductivity in HRDs. Test scale 100 m. Data, statistics and depth trends based on data from the Äspö, Ävrö-Hålö-Mjälen area alone. Depth trends and statistics given for a combined data set made up of data from the entire regional area. Data representing deterministically interpreted deformation zones in RVS model version Laxemar 1.2 are excluded. BC = Best choice value.*

6.3 Hydraulic properties of rock types

Rock types are mapped in outcrop and in boreholes and are an essential base for dividing the rock mass into geological rock domains with different properties relevant to the different types of modelling performed for the SDM Laxemar 1.2. Figure 6-11 shows the bedrock map indicating the distribution of rock types.

The information on rock types in boreholes is grouped into to classes: “Rock Type” in the SICADA data base for boreholes includes individual mapped objects longer than 1 m in the core. If the mapped length of an individual object is less than 1 m it is classified as a “Rock Occurrence”. The analysis of the hydraulic properties focus on both “Rock Type” and “Rock Occurrence” as defined above.

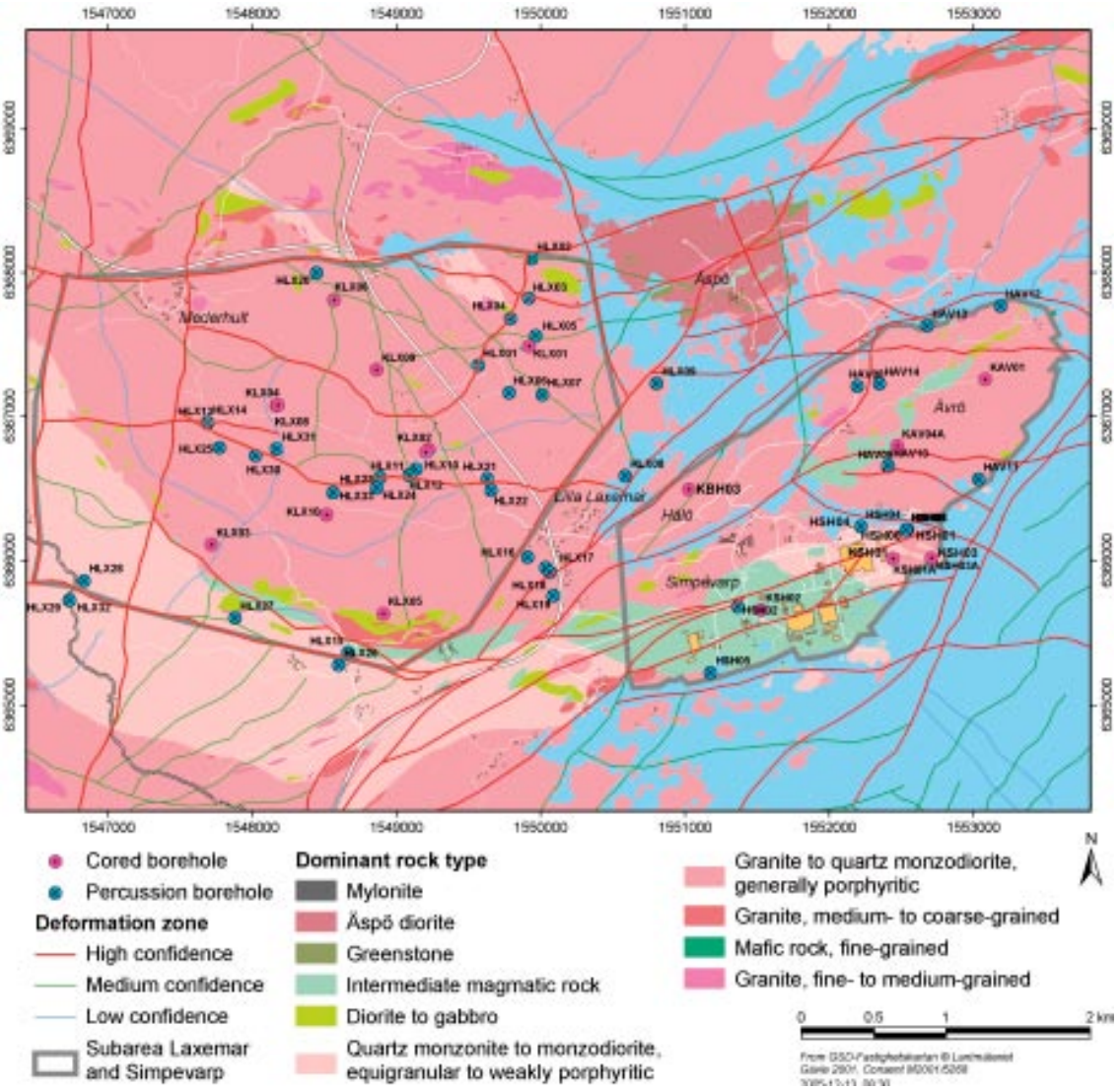

Figure 6-11. *Surface map of the interpreted distribution of identified rock types within the Simpevarp regional model. Deformation zones interpreted in model version L1.2 is also included in the figure. (KLX07–10 and some of the percussion holes were not available for L1.2 modelling.) Based on data from /Wahlgren et al. 2005/.*

6.3.1 Based on regular test sections (mean hydraulic conductivity)

To determine if rock types have different hydraulic properties, it is necessary to use short test sections. The data set with the highest degree of spatial distribution, extensive both in terms of number of tests and tests of similar type is the PFL-s tests at 5 and 3 m test scale. The dominant "Rock Type" (some test sections may include two or more rock types) has been used to label the individual test sections.

Table 6-3 and Figure 6-12 shows the statistics of the hydraulic conductivity for the Simpevarp area related to "Rock type" and the simplified rock type names used for the site investigations at Oskarshamn. Figure 6-13 shows the similar results, but just for Laxemar subarea. Table 6-4 shows the SICADA codes and corresponding rock type names.

There is a clear difference in mean hydraulic conductivity between rock types. As seen in Table 6-3 the Granite and Fine-grained granite (rock type codes 501058, 511058) are the most permeable. Ävrö granite (rock code 501044) has a lower hydraulic conductivity and the lowest hydraulic conductivity is found in the more basic rock types (rock type codes 501030, 501033, 501036, 505102). On the confidence level 0.95 these three groups have different geometric mean values, see Table 6-3.

As noted above, fine-grained granite mapped as "Rock Type" in SICADA represents core pieces > 1 m in the core. However, rock types shorter than 1 m in the core are mapped as "Rock Occurrence". In parts of the core, there may be a large number of veins and smaller dykes intersecting the core, and a large number of them are fine-grained granites. The influence of the fine-grained granite has been studied by identifying all test sections with fine-grained granite mapped either as "Rock Type" or " Rock Occurrence".

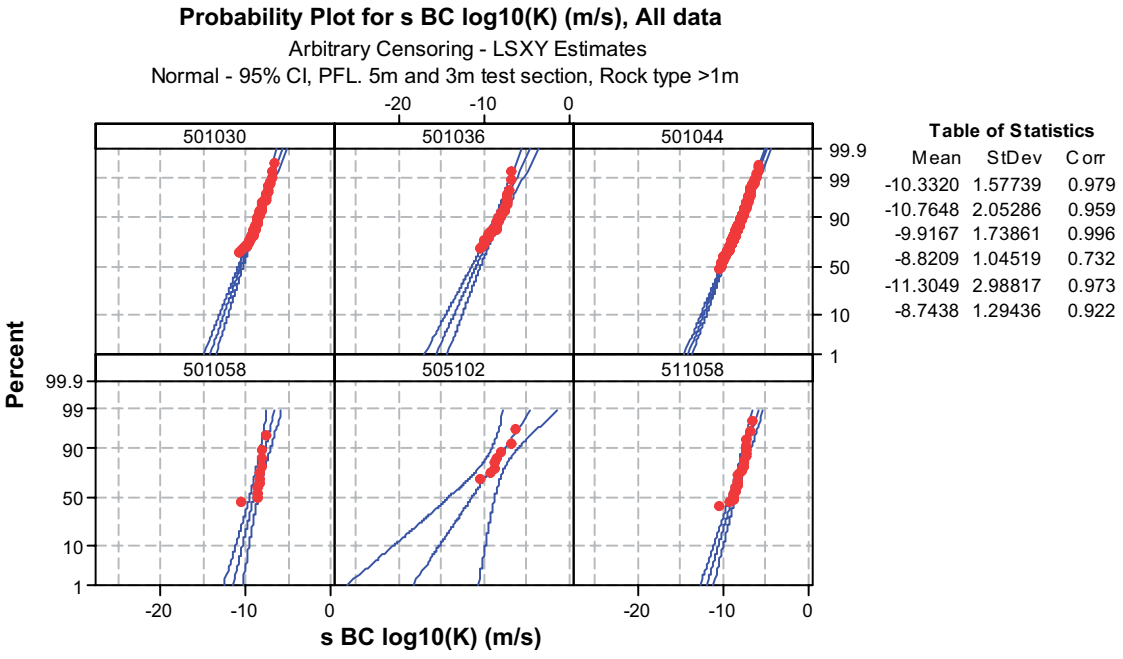

Panel variable: Rock type (1). CODE

Figure 6-12. *Hydraulic conductivity of different rock types based on PFL-s measurements. Test scale 5 m. Data separated on rock types. Data from the Simpevarp area.*

Table 6-3. Hydraulic conductivity of different rock types based on PFL-s measurements. Test scale 5 m. Data from KAV01, KAV04A, KSH01, KSH02A, KLX02, KLX03 and KLX04. Data divided according to the SICADA code "Rock type". Deformation zones in the geological single-hole interpretation and the deterministic deformation zones defined in RVS for version Laxemar 1.2 have not been excluded in the statistics presented. (Excluding the deformation zones would decrease the mean values, but the analysis have not yet been made). (Confidence limits for mean Log10(K) is expressed as the deviation D from mean in the table; for confidence level of 0.95 the mean of Log10(K) will be within value "Mean Log10(K)" ±D.)

Rock code	Rock type	Sample size	Mean Log10(K) (m/s)	Std Log10(K) (m/s)	D Conf.lim Log10(T): Mean±D, conf. level 0.95: (m/s)	Comments
All	All rock types	1,426	–10.01	1.72	0.09	
501033	Diorite/gabbro	5	–	–	–	Only one measurement above measlimit. Possibly similar to 501030 and 501036
501030	Fine-grained dioritoid	327	–10.33	1.58	0.17	
505102	Fine-grained diorite-gabbro	28	–11.30	2.99	1.16	
501036	Quartz monzodiorite	167	–10.76	2.05	0.31	
501044	Ävrö granite	827	–9.92	1.74	0.12	
501058	Granite	20	–8.82	1.74	0.81	
511058	Fine-grained granite	50	–8.74	1.29	0.37	
501061	Pegmatite	2	–	–	–	Only one measurement above measlimit: K = 1.1E–9 m/s

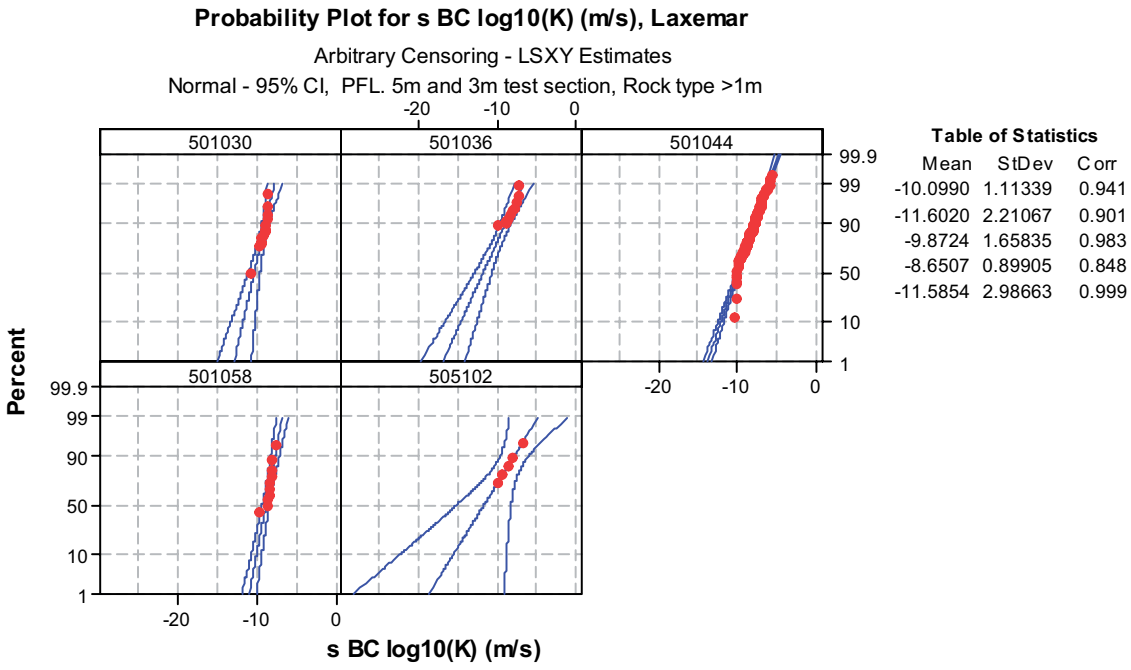

Panel variable: Rock type (1). CODE

Figure 6-13. *Hydraulic conductivity of different rock types based on PFL-s measurements. Test scale 5 m. Data separated on rock types. Data from Laxemar area.*

Table 6-4. Rock type names and their code in SICADA.

Name_code	Name
1056	Granodiorite
1058	Granite
1061	Pegmatite
1062	Aplite
3072	Basalt
5102	Mafic igneous rock, unspecified
5105	Hybrid rock
6005	Breccia
501030	Fine-grained dioritoid (Metavolcanite, volcanite)
501033	Diorite to gabbro
501036	Quartz monzonite to monzodiorite, equigranular to weakly porphyritic
501044	Granite to quartz monzodiorite, generally porphyritic
501058	Granite, medium- to coarse-grained
501061	Pegmatite
505102	Mafic rock, fine-grained

Figure 6-14 shows the statistics for all sections that entirely or partly have the rock type code ID 511058 (= Granite, fine- to medium-grained). Table 6-5 shows that the presence of Fine-grained granite veins does not seem to have a larger impact comparing to the main rock type in Table 6-5; Ävrö granite (501044). Fine grained granite can be expected to be more conductive than the dominating rock type if appearing in thicker dykes (thicker than 1 m).

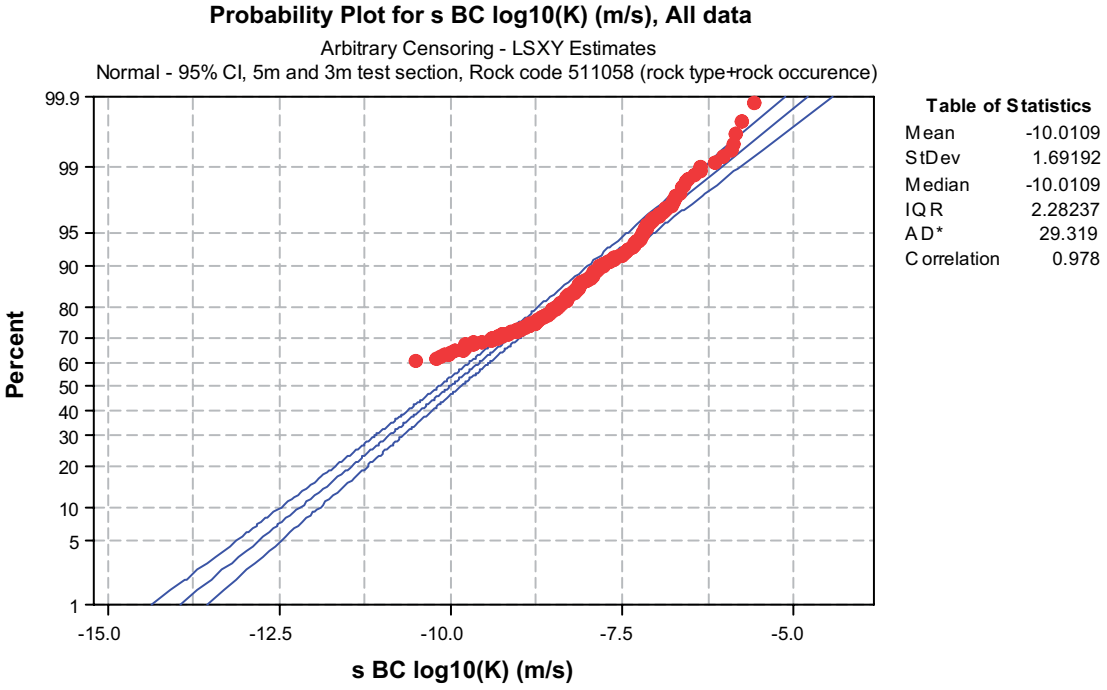

Figure 6-14. *Hydraulic conductivity of test sections which have "Rock Type" or "Rock occurrence" with code ID 511058 (= Granite, fine- to medium-grained) based on PFL-s measurements. Test scale 3 and 5 m. Data from the Simpevarp area.*

Table 6-5. Hydraulic conductivity of different rock types based on PFL-s measurements. Test scale 5 m. Data from KAV01, KAV04A, KSH01, KSH02A, KLX02, KLX03 and KLX04. Data based on the SICADA code "Rock type" or "Rock occurrence" that have the rock code ID 511058 (= Granite, fine- to medium-grained). Deformation zones in the geological single-hole interpretation and the deterministic deformation zones defined in RVS for version L1.2 are included.

Rock code	Rock type	Hydraulic conductivity K, (m/s) Geometric mean	Std Log10 K	Number of observations	Comments
511058 (Rock type)	Granite, fine- to medium-grained	$1.8 \cdot 10^{-9}$	1.29	50	
511058 (Rock type or Rock occurrence)	Granite, fine- to medium-grained	$9.8 \cdot 10^{-11}$	1.69	823	

The result is that the presence of fine-grained granite veins does not seem to have a substantial impact on the hydraulic conductivity compared with the variation between different rock types as seen in Table 6-3. Fine-grained granite can, however, be expected to be more conductive than the dominant rock type when appearing in the form of thick dikes (thicker than 1 m).

6.4 Hydraulic properties of domains

Geological domains in 3D are defined in /Wahlgren et al. 2005/ and are shown in Figure 6-15 to Figure 6-18. Each test section with hydraulic data has been classified according to the interpreted dominant geological rock domain, to explore if there is a difference in hydraulic properties between the geologically defined rock domains. However, rock domain M , which is a complex domain (see /Wahlgren et al. 2005/) was at an early stage of the modelling further divided into one domain dominated by Ävrö granite M(A) and one dominated by quartz monzodiorite M(D). This information was used to test if there is any hydraulic difference within the geological M domain.

6.4.1 Analysis of hydraulic properties based on geological domains

Hydraulic tests with short test sections are the most suitable for the analysis of whether rock domains have different hydraulic properties, as there will not be many test sections that straddle a boundary between two geological rock domains. The PFL-s tests at 3 and 5 m test scale cover several boreholes and geographical areas and are considered the most suitable data set for this analysis. Figure 6-19, Figure 6-20, Table 6-6 and Table 6-7 present the associated statistics for these measurements. On the confidence level 0.95 the rock domains have different geometric mean hydraulic conductivity when comparing groupings based on geological rock domains with similar K; (A and BA) ; (B , C and M(A)); (D and M(D)), see Table 6-6 and Table 6-7.

Hydraulic conductivities of different rock domains based on PSS measurements were also examined for the 100 m and "20 m" (10–20–30 m) test scales which also cover many boreholes and depth ranges, example of probability distributions is shown in Figure 6-21 and Appendix 4. For these tests the dominant rock domain within a test section was used for the classification of test sections. PSS measurements with test scale 5 m were not examined, as these tests cover only a minor part of the rock mass. The statistics give similar values. However, not all rock domains according to Table 6-6 are represented in the analysis.

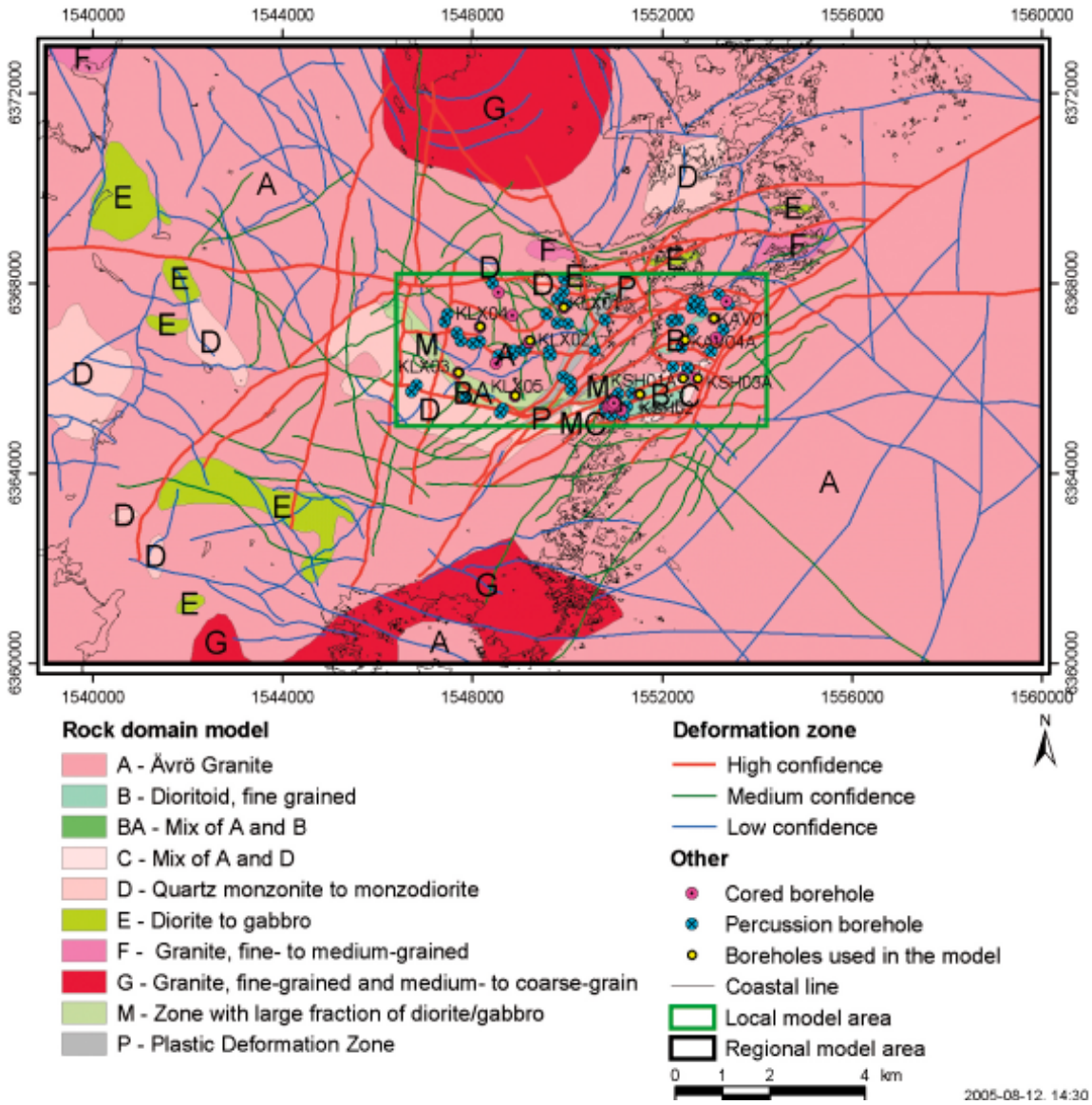

Figure 6-15. *Geological domains in the regional model. Based on data from /Wahlgren et al. 2005/.*

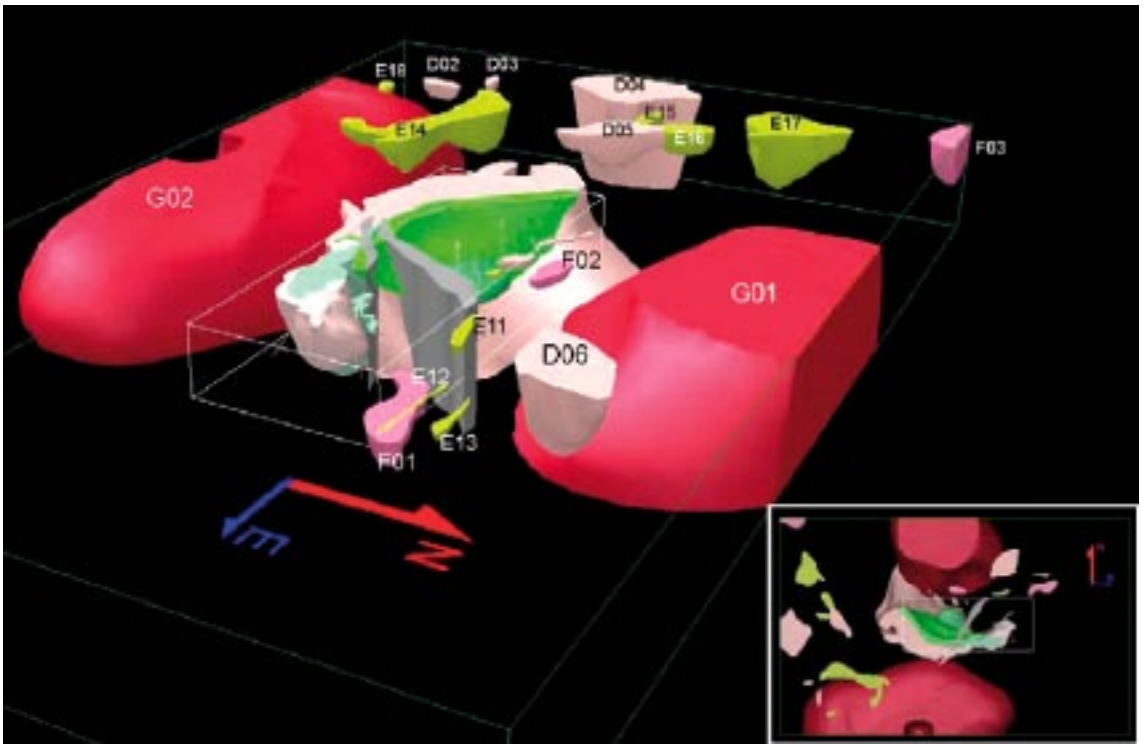

Figure 6-16. *Geological domains in the regional model- 3D representation. Regional rock domain model with the local scale model domain inserted. In the regional model volume, modifications are mainly restricted to the rock domains RSMG01 (Götemar granite) and RSMG02 (Uthammar granite). The Ävrö granite (RSMA01) is transparent. View from the northeast. /Wahlgren et al. 2005/.*

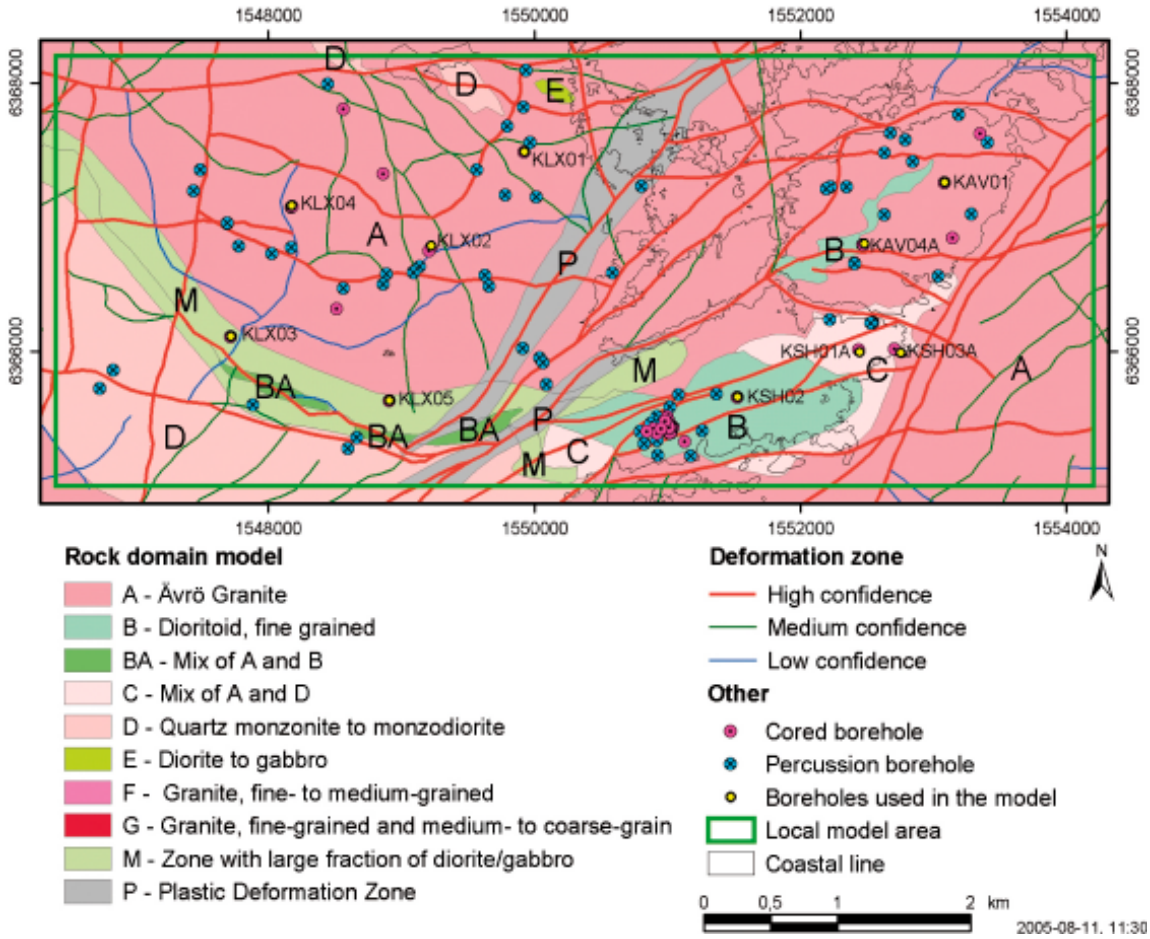

Figure 6-17. *Geological domains in the local model. Based on data from /Wahlgren et al. 2005/.*

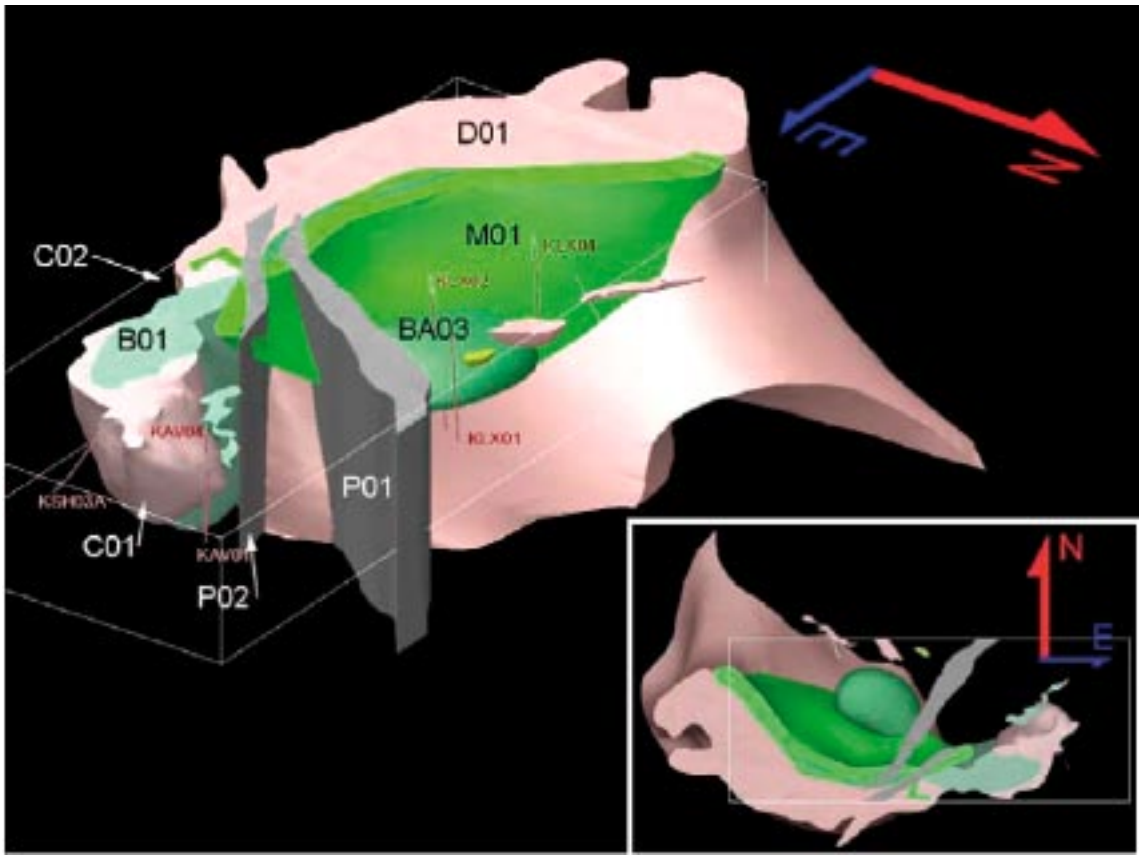

Figure 6-18. *Geological domains in the local model-3D representation. Close up of the rock domains in the local scale model volume. Note the northward extension at depth of the RSMD01 and RSMM01 domains. The RSMA01 domain is transparent. View from the northeast. /Wahlgren et al. 2005/.*

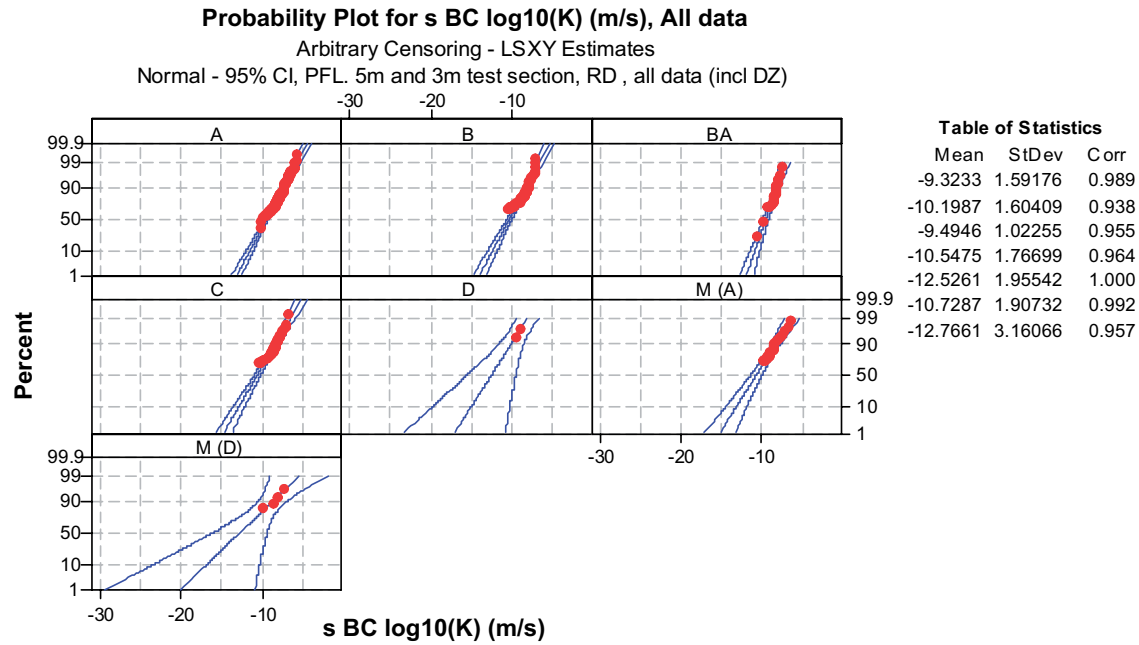

Figure 6-19. *Statistics of hydraulic conductivity of different rock domains based on PFL-s measurements, cf Table 6-6. Test scale 3 and 5 m. Data from the entire Simpevarp regional area. Based on data from KAV01, KAV04A, KSH01A, KSH02, KLX02–04. Tabulated results follow plotted results top left to right followed by lower left to right.*

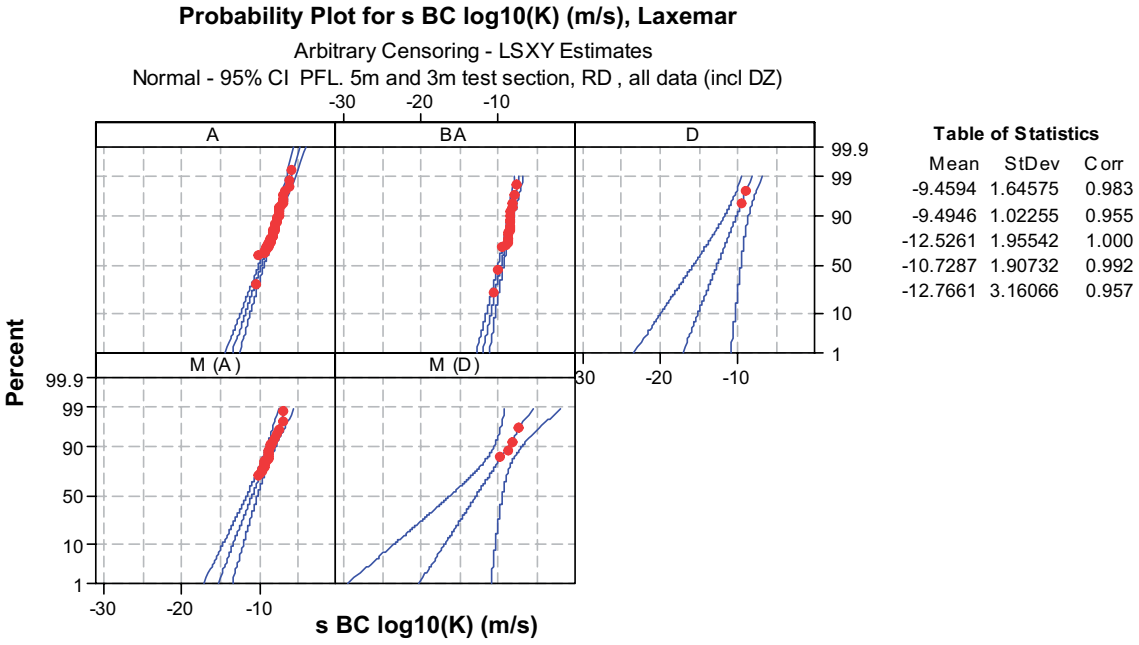

Figure 6-20. *Statistics of hydraulic conductivity of different rock domains based on PFL-s measurements, cf Table 6-7. Test scale 3 and 5 m. Data from the Laxemar subarea. Based on data from KLX02–04. Tabulated results follow plotted results top left to right followed by lower left to right.*

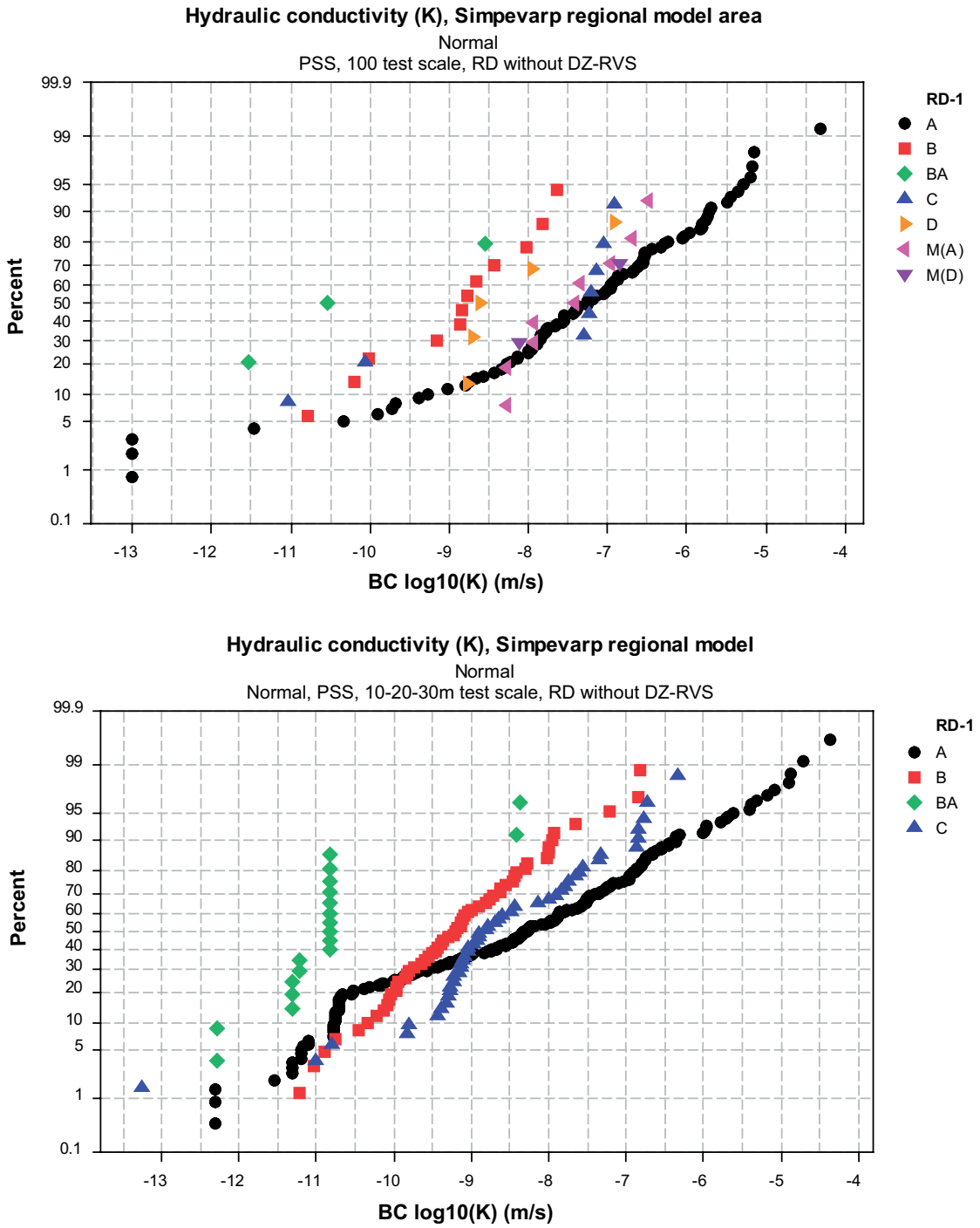

Figure 6-21. *Hydraulic conductivity of different rock domains based on PSS measurements. Data from the entire area. Top: Test scale 100 m. Bottom: Test scale 10–20–30 m.*

Table 6-6. Hydraulic conductivity of different rock domains based on PFL-s measurements. Test scale 3 and 5 m. Data from Simpevarp regional area. Deformation zones in the geological single-hole interpretation and the deterministic deformation zones defined in RVS for version Laxemar 1.2 are not excluded. Based on data from KAV01, KAV04A, KSH01A, KSH02, KLX02–04 (Confidence limits for mean Log10(K) is expressed as the deviation D from mean in the table; for confidence level of 0.95 the mean of Log10(K) will be within value "Mean Log10(K)" ±D.)

Rock domain	Sample size	Mean Log10(K) (m/s)	Std Log10(K) (m/s)	D Conf.lim Log10(T): Mean±D, conf. level 0.95: (m/s)	Comments
All	1,426	–10.01	1.69	0.09	
A	666	–9.32	1.59	0.12	
B	245	–10.20	1.60	0.20	
BA	140	–9.49	1.02	0.17	
C	197	–10.55	1.77	0.25	
D	39	–12.53	1.96	0.64	Only 2 measurement above measlimit
M(A)	104	–10.73	1.91	0.37	
M(D)	35	–12.77	3.16	1.09	Only 4 measurement above measlimit

Table 6-7. Hydraulic conductivity of different rock domains based on PFL-s measurements. Test scale 3 and 5 m. Data from Laxemar subarea. Deformation zones in the geological single-hole interpretation and the deterministic deformation zones defined in RVS for version Laxemar 1.2 are not excluded. Based on data from KLX02–04 (Confidence limits for mean Log10(K) is expressed as the deviation D from mean in the table; for confidence level of 0.95 the mean of Log10(K) will be within value "Mean Log10(K)" ±D.)

Rock domain	Sample size	Mean Log10(K) (m/s)	Std Log10(K) (m/s)	D Conf.lim Log10(T): Mean±D, conf. level 0.95: (m/s)	Comments
All	753	–9.92	1.63	0.12	
A	435	–9.45	1.65	0.16	
BA	140	–9.49	1.02	0.17	
D	39	–12.53	1.96	0.64	Only 2 measurement above measlimit
M(A)	104	–10.73	1.91	0.37	
M(D)	35	–12.77	3.16	1.09	Only 4 measurement above measlimit

Based on the probability plots for the different test methods and test scale, the rock domains can be ranked:

PSS 100 m scale

Most conductive: A, M(A)

"Middle " conductive: C, D (D small sample for "RD without DZ-RVS")

Least conductive: B, BA (BA was a very small sample!)

PSS 10–20–30 m scale

Most conductive: A

"Middle " conductive: C

Least conductive: B, BA (BA was a small sample!)

PFL 3, 5 m scale

Most conductive: (A+BA)

"Middle " conductive: (B+C)

Least conductive: (M(A)+M(D)+ D+E) (D and M(D) were small samples)

Götemar and Uthammar granites

The Götemar and Uthammar granites are not represented above, but there are data available for the Götemar granite. These data have been analysed, see Appendix 5. The Götemar granite appears to be the most conductive domain in the regional area. The data from the Götemar Granite is difficult to interpret as these measurements are old and less is known about the boreholes. However comparing the 20 m measurements in the Götemar granite with the statistics of 10–20–30 m PSS (for "all data") shows that the geometric mean of the hydraulic conductivity is more than a magnitude larger than for rock domain A. The sample in test scale 2 and 3 m in the Götemar granite is larger, and two boreholes indicate a geometric mean of the hydraulic conductivity is more than a magnitude larger than for rock domain A- PFL (5 m scale). One borehole, KKR03, is rather similar to rock domain A- PFL (5 m scale). Uthammar granite is of similar origin as Götemar granite and can probably be assumed to have similar properties.

General conclusions.

The main tendency is similar for the different hydraulic tests (that partly represents different borehole sections), but the 5 m test results should possibly be considered more relevant for showing difference between RDs.

6.4.2 Suggested hydraulic rock domains (HRD)

Based on PFL (5 m scale) measurements, the fine-grained granite bodies (SICADA rock type code 511058) are an order of magnitude more conductive than the dominant rock type in the regional modelling area (SICADA code 501044, Ävrö granite), which is the main rock type in the geological Rock domain A. Possibly the fine-grained granite bodies modelled in the RVS can be assumed to be as conductive as the smaller fine-grained granites intersecting the boreholes.

Hydraulic properties of geological Rock domain A differs between the Laxemar subarea and the Äspö and Ävrö areas; the Laxemar area appearing to be less permeable. A reason for this may be that the rock mass east of the Äspö shear zone, including the southern part of Äspö and Ävrö as well as the Simevarp peninsula, see the rhombohedral area indicated in Figure 6-22, may be part of a large-scale shear belt, cf /Wahlgren et al. 2005/, that can explain the observed difference in hydraulic properties. The geological Rock domain A is therefore suggested to be divided into two HRDs as defined below.

The following hydraulic rock domains (HRDs) are proposed, based on grouping of geological rock domains as defined in /Wahlgren et al. 2005/ (letters given within parantheses indicate the underlying geological rock domains):

HRD(F,G) (G01, (Götemar granite), G02 (Uthammar granites) The most conductive domain. Assume 10* HRD(A) properties.

(F) (Granite, Fine- to medium-grained). One of the most conductive rock types. Assume 10* HRD(A) properties. The bodies are small and may probably be neglected in the regional model, but have been implemented.

HRD(A) (A+BA), Part of rock domain A outside rhombohedral area shown in Figure 6-22.) It is motivated due to the higher hydraulic conductivity in domain A in boreholes on Ävrö and southern Äspö compared to the Laxemar subarea.

HRD(A2) (A), Part of rock domain A within rhombohedral area shown in Figure 6-22). See comment on HRD (A) above.

HRD(B,C) (B+C). Low conductive domain.

HRD(D,E,M) (M(A)+M(D)+ D+E). The least conductive domain. Data corresponding to rock domains D and M(D) constitute small samples. M(A) is included in HRD(D, M) as it has a low hydraulic conductivity and is fairly small in size and is part of the M domain. There are no hydraulic data for rock domain E (diorite to gabbro), but as it is a basic rock type, the hydraulic conductivity is probably small according to the text above.

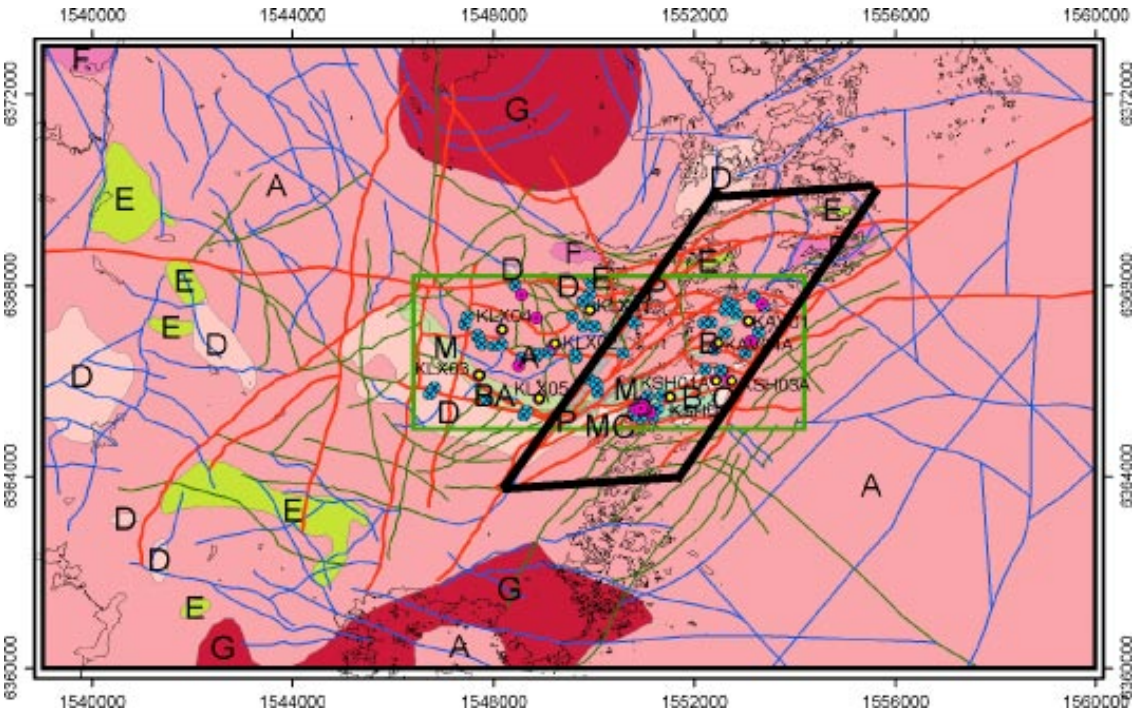

Figure 6-22. *Rock domain model for Laxemar model version 1.2. The rhombohedral area indicates the area of HRD(A2), interpreted more strongly affected by low-grade ductile shear zones than the corresponding HRD(A) in the Laxemar subarea, see /Wahlgren et al. 2005/.*

6.5 Hydraulic properties of fractures

In /Rhén et al 2006ab/ the PFL-f flow anomalies were evaluated for the different boreholes. A few observations can be highlighted. For details see /Rhén et al. 2006ab/.

It should be stressed that the statistics in Section 6.5 is based on transmissivity values above a measurement limit. There are geological features (some of fractures mapped as open and crush zones) that most likely have transmissivities below this limit.

6.5.1 Frequency of mapped fractures and PFL-f flow anomalies

The mapped frequencies of fractures; total, open total, partly open, sealed are cross-plotted against the PFL-f frequency in Figure 6-23 and Figure 6-24. The number of fractures in crush zones was estimated as the borehole length of the crush zone in metres multiplied by 40 fractures/m (Standard procedure in the SICADA database for obtaining a rough estimate of the total fracture frequency including mapped fractures and crush zones. A core is mapped as “crush” if individual fractures cannot be mapped. Generally rock pieces in the core in a crush zone may be in the cm scale, as also found when mapping crush zones in tunnels. It is therefore reasonable to designate a frequency of 40 fractures/m in crush zones as a rough estimate.)

As indicated in Figure 6-24 there seems to be approximately a linear correlation between the frequencies of open fractures and the flow anomalies, except for KAV04B, which is the only borehole where data have been collected in the uppermost 100 m of the bedrock. All

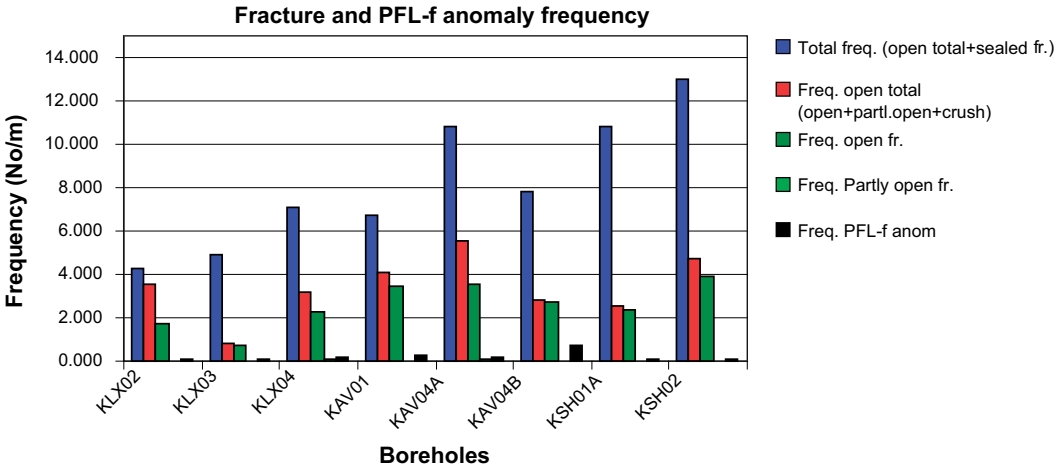

Figure 6-23. *Frequency of fractures (open fractures, Partly open fractures, open total fractures (open+partly open+estimated No of open fractures in crush) and Total No of fracture (open total+sealed) and PFL-f anomalies. All fractures mapped as "Certain", "Probable" and "Possible" are included in each fracture category.*

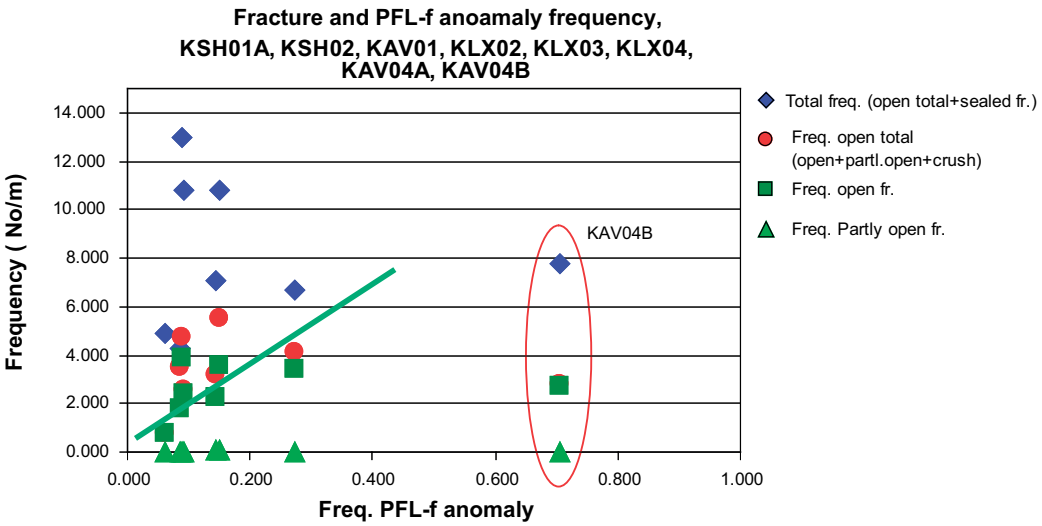

Figure 6-24. *Cross plot of Frequency of fractures (open fractures, partly open fractures, open total fractures (open+partly open+estimated number of open fractures in crush) and total number of fractures (open total+sealed) versus the frequency of PFL-f anomalies. All fractures mapped as "Certain", "Probable" and "Possible" are included in each fracture category (borehole sections interpreted as deformation zones are included.*

other data start at approximately 100 m depth below surface. The reason for this difference may be that near the surface there is a lower effective rock stress that affects the open fractures.

Figure 6-25 indicates that one can expect 0.02–0.1 flow anomalies per mapped open fracture above a transmissivity about 1E–9 m^2/s (the approximate measurement limit for PFL-f) for rock between 100 to 1,000 m depth.

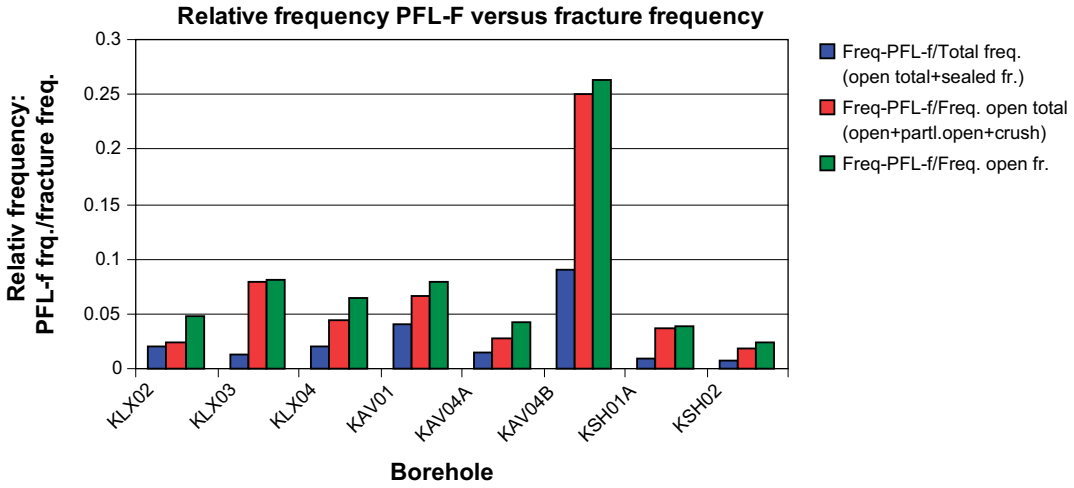

Figure 6-25. *Relative frequency of PFL-f flow anomalies in relation to fractures (open fractures, open total fractures (open+partly open+estimated No of open fractures in crush) and Total No of fracture (open total+sealed) and PFL-f anomalies. All fractures mapped as "Certain", "Probable" and "Possible" are included in each fracture category.*

6.5.2 Transmissivity of PFL-f flow anomalies

In Table 6-8 and Table 6-9 statistics for PFL-f anomalies, excluding deformation zones (both deterministically modelled and the deformation zones in the geological single-hole interpretation), are shown for three elevation intervals. Transmissivity distributions and frequency of PFL-f anomalies are shown. As can be seen the transmissivity distributions are fairly similar. The major difference is in the frequency of conductive fractures (P_{10PFL}). The transmissivity distributions are shown in Figure 6-26.

In /Rhén et al. 2006ab/ similar tables are shown, but also for "all data", including the deformation zones. The transmissivity distributions for "all data" are similar to the ones in Table 6-8 and Table 6-9.

Table 6-8. Univariate statistics of hydraulic tests performed in cored boreholes in the Simpevarp subarea based on a lognormal distribution. Method employed: PFL-f. Sample size always refer to No. of anomalies. Data based on elevation reasonable for repository depth. (Confidence limits for mean Log10(T) is expressed as the deviation D from mean in the table; for confidence level of 0.95 the mean will be within value "Mean Log10(T)" ±D. Sample type "No DZ" means that PFL-f anomalies in deformation zones from geological single hole interpretation and deterministically defined deformation zones for Laxemar model 1.2 in RVS are excluded.

Borehole	Test type	Upper elevation limit (m)	Lower elevation limit (m)	Bh length (m)	Sample type (m)	Sample size	P10PFL PFL-f anom. (m–1)	Lower meas. limit[1] Log10 T (m^2/s)	Mean Log10(T) (m^2/s)	Std Log10(T) (m^2/s)	D Conf.lim Log10(T): Mean±D, conf.level 0.95: (m^2/s)
KSH01A	PFL-f	–95	–300	139	No DZ	34	0.24	(–9.1)–(–9.0)	–8.25	0.86	0.30
	PFL-f	–300	–700	266	No DZ	6	0.023	(–9.1)–(–9.0)	–9.14	0.26	0.27
	PFL-f	–700	–957	270	No DZ	1	0.004	(–9.1)–(–9.0)	–	–	–
KSH02	PFL-f	–75	–300	155	No DZ	14	0.090	(–9.1)–(–8.7)	–7.02	0.76	0.44
	PFL-f	–300	–700	353	No DZ	50	0.14	(–9.1)–(–8.7)	–7.93	0.63	0.18
	PFL-f	–700	–989	282	No DZ	8	0.028	(–9.1)–(–8.7)	–7.06	0.57	0.48
KAV01	PFL-f	–57	–300	258	No DZ	106	0.41	(–9.6)–(–8.1)	–7.94	0.89	0.17
	PFL-f	–300	–700	185	No DZ	11	0.060	(–9.6)–(–8.1)	–8.52	0.70	0.47
	PFL-f	–700	–717	0	No DZ	0		(–9.6)–(–8.1)	–	–	–
KAV04A	PFL-f	–89	–300	211	No DZ	43	0.20	(–9.6)–(–9.0)	–7.59	0.66	0.20
	PFL-f	–300	–700	391	No DZ	52	0.13	(–9.6)–(–9.0)	–7.66	0.57	0.16
	PFL-f	–700	–982	160	No DZ	31	0.19		–7.25	0.78	0.29
KAV04B	PFL-f	–10	–85	76	No DZ	54	0.71	(–9.6)–(–9.0)	–7.21	1.04	0.28

Table 6-9. Univariate statistics of hydraulic tests performed in cored boreholes in the Laxemar subarea based on a lognormal distribution. Method employed: PFL-f. Sample size always refer to No. of anomalies. Data based on elevation reasonable for repository depth. (Confidence limits for mean Log10(T) is expressed as the deviation D from mean in the table; for confidence level of 0.95 the mean will be within value "Mean Log10(T)" ±D. Sample type "No DZ" means that PFL-f anomalies in deformation zones from geological single hole interpretation and deterministically defined deformation zones for Laxemar model 1.2 in RVS are excluded.

Borehole	Test type	Upper elevation limit (m)	Lower elevation limit (m)	Bh length (m)	Sample type (m)	Sample size	P10PFL PFL-f anom. (m^{-1})	Lower meas. limit[1] Log10 T (m^2/s)	Mean Log10(T) (m^2/s)	Std Log10(T) (m^2/s)	D Conf.lim Log10(T): Mean±D, conf.level 0.95: (m^2/s)
KLX02	PFL-f	–186	–300	104	No DZ	32	0.31	(–10)–(–8.3)	–7.23	0.95	0.34
	PFL-f	–300	–700	402	No DZ	21	0.052	(–10)–(–8.3)	–7.93	0.75	0.34
	PFL-f	–700	–1,372	488	No DZ	21	0.043	(–10)–(–8.3)	–7.77	0.89	0.41
KLX03	PFL-f	–79	–300	229	No DZ	25	0.11	(–9.8)–(–8.2)[1]	–7.81	1.05	0.43
	PFL-f	–300	–700	392	No DZ	15	0.038	(–9.8)–(–8.2)[1]	–7.87	0.70	0.39
	PFL-f	–700	–944	178	No DZ	3	0.017	(–9.8)–(–8.2)[1]	–7.44	0.94	2.3
KLX04	PFL-f	–75	–300	215	No DZ	44	0.20	(–9.6)–(–8.7)	–7.01	0.85	0.26
	PFL-f	–300	–700	393	No DZ	51	0.13	(–9.6)–(–8.7)	–7.34	0.77	0.22
	PFL-f	–700	–957	158	No DZ	1	0.0063	(–9.6)–(–8.7)	–	–	–

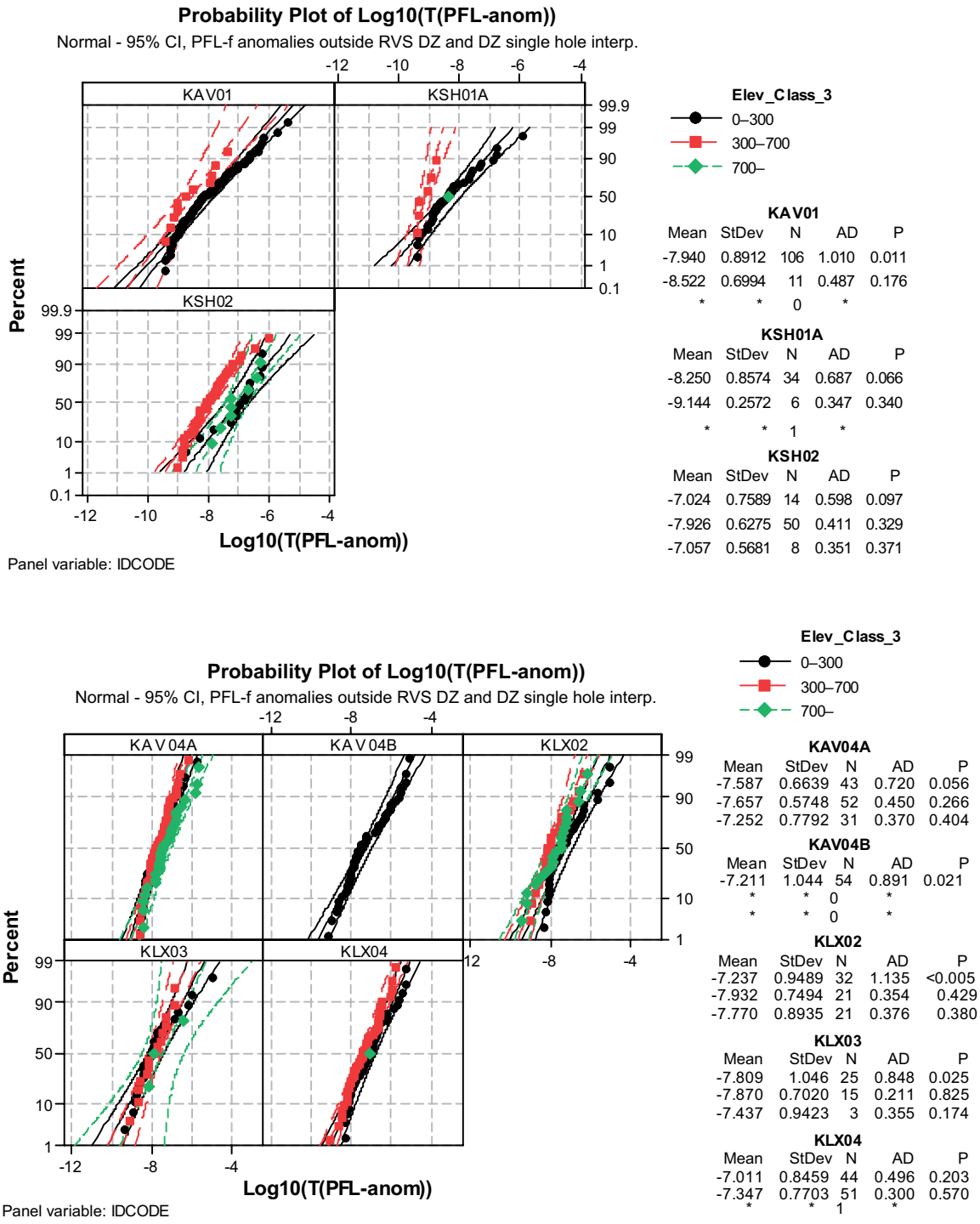

Figure 6-26. *Statistics of PFL-f anomaly transmissivities. Data from the entire Simpevarp regional area. PFL-f anomalies in deformation zones from geological single hole interpretation and deterministically defined deformation zones for Laxemar model 1.2 in RVS are excluded.*

6.5.3 Transmisivity distributions for flow anomalies and fractures

One flow anomaly may represent several fractures, due to the resolution of the PFL-f measurements (ca 0.1–0.2 m) and the number of open fracture in the PFL-f measurement interval. In the correlations studies of Posiva Flow Logg anomalies to core mapped features /Forssman et al. 2005ab/ some PFL-f anomalies are connected to several possible open fractures, and it is said that one or all of them may be contributing to the PFL-f anomaly. A borehole section mapped as crush in the core also represents part of the rock that is likely to represent several fractures. Below an attempt is made to see what the transmissivity distribution of fractures can be, if we assume that the all possible open fractures connected to a PFL-f anomaly actually are flowing, and that all fractures assumed to represent the crush zone all are flowing. These assumptions are if of course uncertain, but gives some idea of a lower limits for the transmissivity distributions. Below it is explained in more detail.

In Figure 6-27 and Figure 6-28 the statistics for all flow anomalies, only flow anomalies coupled to mapped single fractures and flow anomalies coupled to mapped crush zones. The transmissivity distributions for single fractures has also been estimated, based on the following assumptions: If a flow anomaly have been connected to X fractures (as possible object that are flowing, one or all of X) the transmissivity was estimated as T-PFL-anomaly/X. If the flow anomaly was connected to a crush zone, the number of fractures was estimated as the borehole length of the crush zone in m multiplied with 40 fr./m. (This is the general way of estimating the fracture frequency in crush zones in SICADA.) However, the maximum No. of fractures coupled to a flow anomaly was set to 10, based on that generally flow anomaly is detected with some 2 dm. It is thus unrealistic to assign 40 fractures for a 1 m crush zone with just one flow anomaly. These estimates of the fracture transmissivity are of course uncertain, but can be seen as some lower limit for the transmissivity distribution. The following should be recognized:

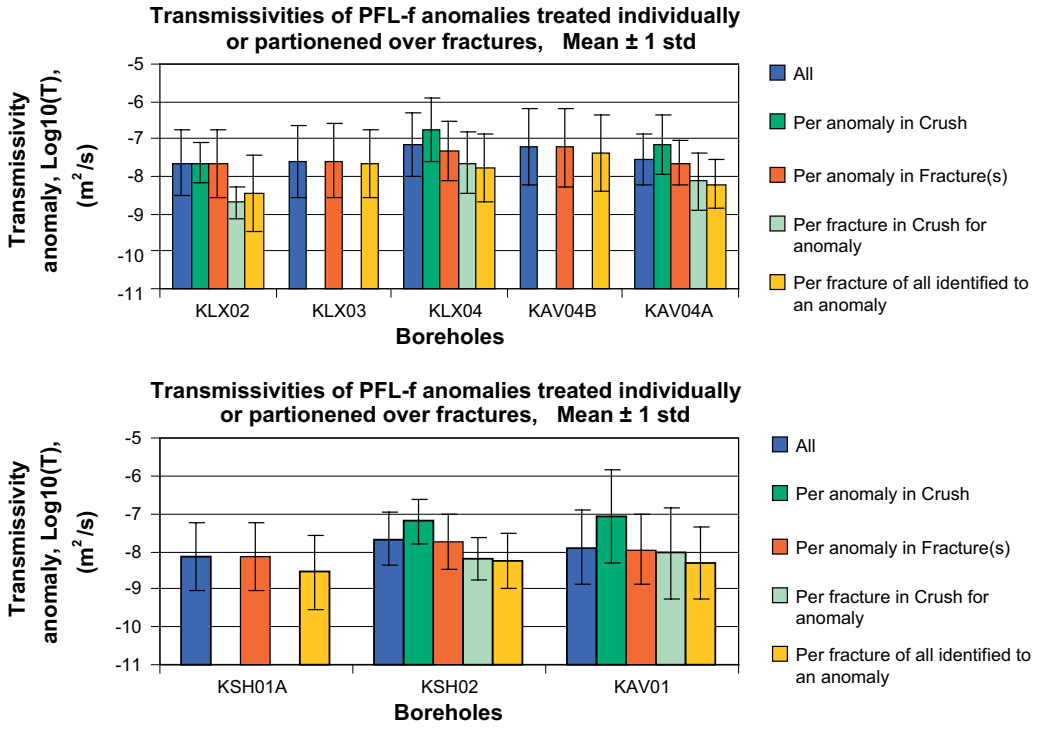

Figure 6-27. *Transmissivity distribution of PFL-f flow anomalies and fractures. Plotted categories: All flow anomalies, All flow anomalies found in crush zones, all flow anomalies related to fractures not in crush zone, fracture transmissivity for flow anomalies found in crush zones, fracture transmissivity for flow anomalies related to fractures not in crush zone.*

Transmissivity distributions of the flow anomalies are fairly similar between the boreholes; however the flow anomalies in crush have a tendency to have a higher geometric mean than fractures outside crush zones. KLX02 is an exception, but data from that borehole is not of the same standard as the ones tested during SI.

Transmissivities associated with fractures ("Per fracture…" in Figure 6-27 and Figure 6-28):

- Mean: As the maximum number of possible fractures from the PFL-f interpretation is used, the estimated mean should probably be smaller than the true mean for the fractures. The true mean for the fractures can be as for the flow anomalies or smaller, but not smaller than "per fracture..." value.
- Standard deviation: As the flow transmissivity is just divided with the number of possible fractures, the standard deviation is probably underestimated to some extent.

Transmissivities associated with crush ("Per fracture…" in Figure 6-27 and Figure 6-28):

- Mean: As the maximum number of possible fractures is based on a rough generalization the estimated mean may possibly be larger or smaller than the true mean for the fractures, but still give a tendency in the right direction. The true mean for the fractures should probably be lower than for the flow anomalies as we can expect that the crush consists of several fractures.
- Standard deviation: As the flow transmissivity is just divided with the number of possible fractures, the standard deviation is probably underestimated to some extent.

From the PFL data one can estimate the specific capacity (Q/s) for each flow anomaly, and in principle Q/s = T. Calculated T/(Q/s) = 1 to 0.98 for all boreholes but KLX02, which have rather large variation. The old data for KLX02 is however much more uncertain than the new measurements. For details of tabulated statistics, see /Rhén et al. 2006ab/.

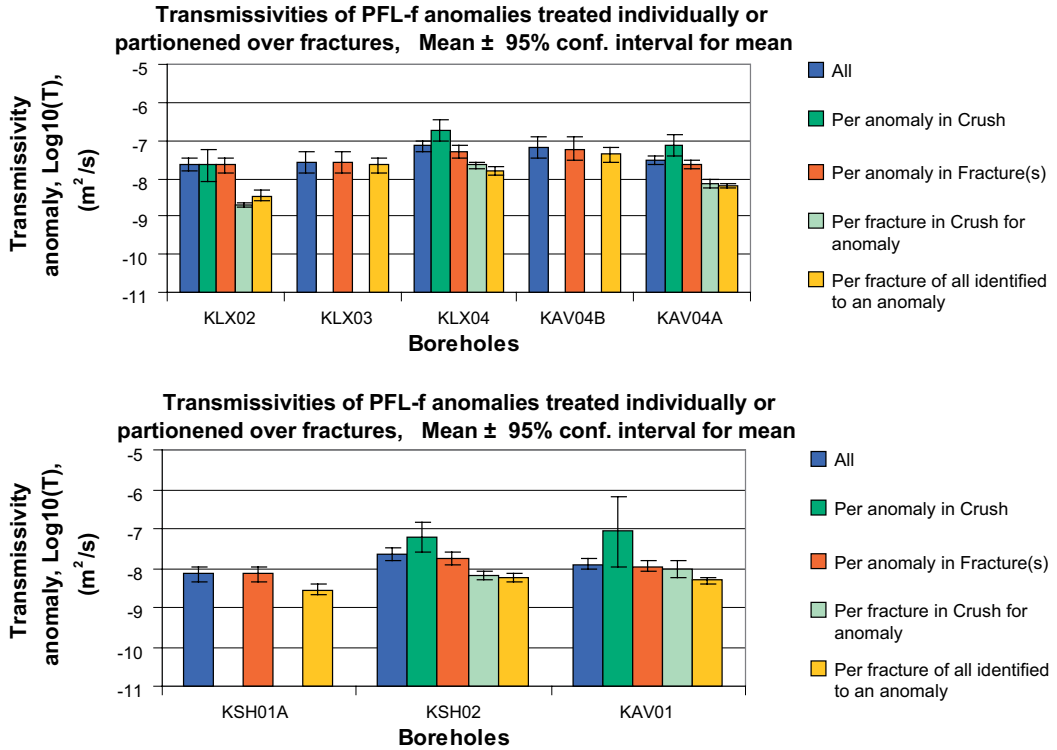

Figure 6-28. *Transmissivity distribution of PFL-f flow anomalies and fractures. Plotted categories: All flow anomalies, all flow anomalies found in crush zones, all flow anomalies related to fractures not in crush zone, fracture transmissivity for flow anomalies found in crush zones, fracture transmissivity for flow anomalies related to fractures not in crush zone.*

6.5.1 Transmissivity of crush zones

One or several flow anomalies have been observed in some, but not all, mapped crush zones. If several flow anomalies are observed in a borehole section mapped as crush, these transmissivities are summed up to represent the transmissivity of the crush zone. Figure 6-29 and Figure 6-30 shows the statistics for the transmissivity for crush zones, based on data were transmissivities were possible to measure for the crush zones.

In two of the boreholes (KSH01A and KAV01) the geometric mean transmissivity is ca 10 times greater for crush zones (as individual features) than for individual flow anomalies outside the mapped crush zone, with a bit less difference noted for KLX04 and KSH02, and no difference in KLX02. However, the uncertainty is high for the mean value estimated for each borehole considering the confidence limits for the mean. The confidence interval for the mean of the KLX02 data is relatively small, but should still be considered highly uncertain while the data quality is lower than for the new boreholes, as mentioned earlier in this section.

The frequency of crush zones with one or more PFL-f anomalies in relation to all mapped crush zones (Number of crush zones with PFL-anomaly/Number of all crush zones) is 0.23–0.43 for all boreholes (KLX02, KLX03, KLX04, KAV04A, KSH02A, KAV01) except two which have frequencies 0 and 1 (KSH01A, KAV04B respectively) /Rhén et al. 2006ab/. The total number of crush zones varies significantly between the boreholes, from 3 to 78, excluding the short borehole KAV04B. Thus, about 1/3 of the crush zones are conductive and about 2/3 are non-conductive, or rather below the measurement limit for PFL-f. For details see /Rhén et al. 2006ab/.

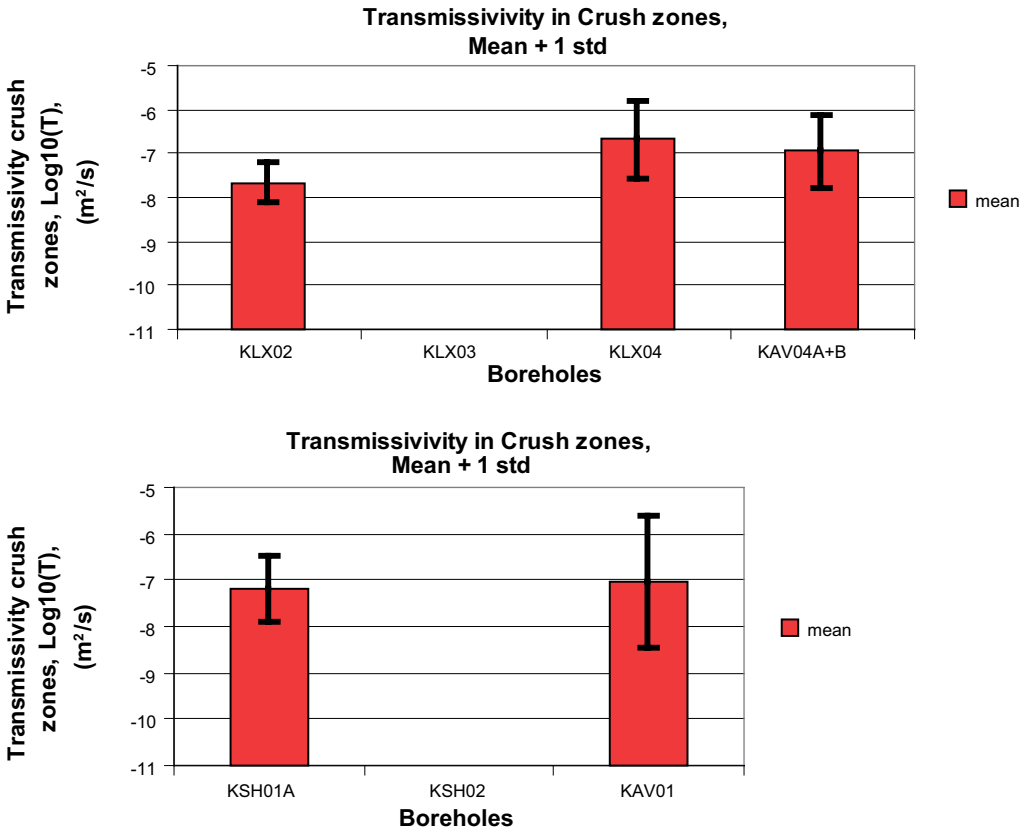

Figure 6-29. *Transmissivity distribution for crush zones based on the sum of PFL-f flow anomalies for each crush zone.*

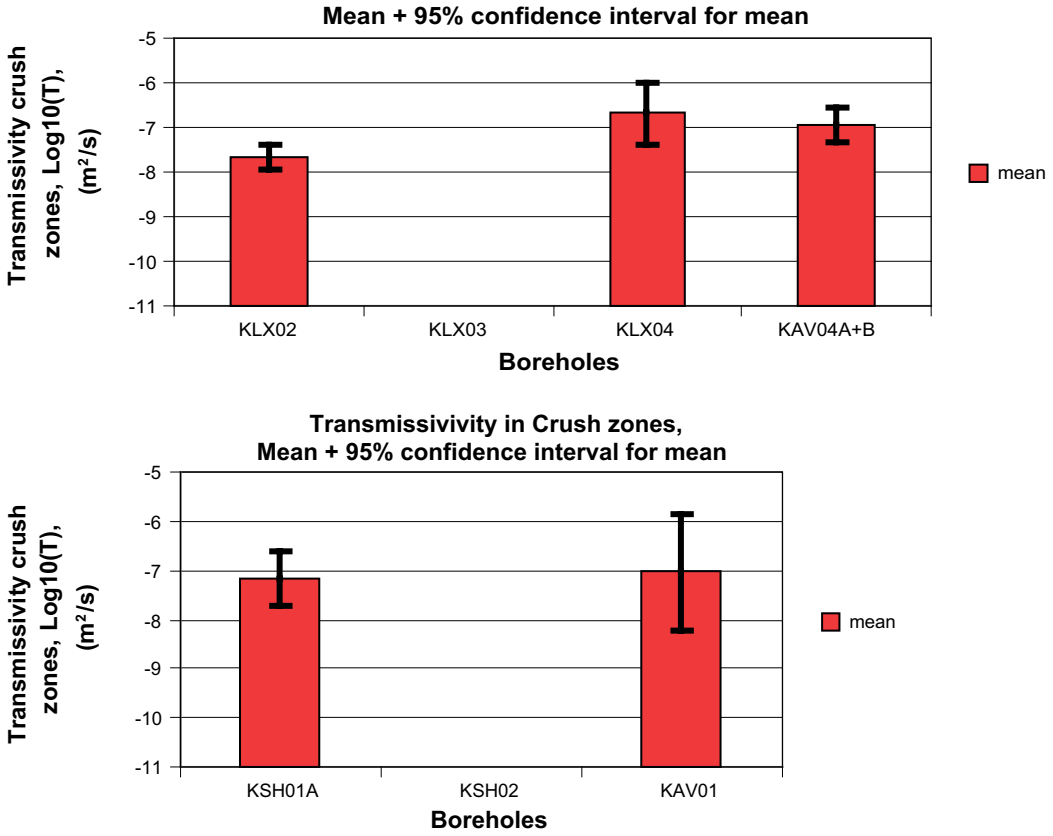

Figure 6-30. *Transmissivity distribution for crush zones based on the sum of PFL-f flow anomalies for each crush zone.*

6.6 Modelling parameters

Modelling parameters for the rock between the HCD is expected to be based on HydroDFN for the regional modelling, so the data in Chapter 6 not expected to be directly implemented in the regional groundwater flow models, but rather guide the assessment of proper HydroDFN models. However, the trend functions given in Section 6.2 should be commented.

The depth trend models in Section 6.2 can be applied to the HRDs in model version L1.2. Using a stochastic approach and the depth trend functions to assign the hydraulic conductivity raises the question if there is any upper and lower limit of hydraulic conductivity that should be applied. Data from the SKB investigations but also other projects /Juhlin et al. 1998, Smellie 2004/ suggests that the permeability (k) at great depth (6–8 km) is 1E–18 to 1E–20 m^2, which corresponds to a hydraulic conductivity of about 1E–11 to 1E–13 m/s. It is here suggested that for test scale 100 m a minimum hydraulic conductivity of 1E–12 m/s is used.

The power-law function indicates very high values near surface that become unrealistic. It is here suggested that for test scale 100 m the maximum hydraulic conductivity is set to 1E–5 m/s, based on Figure 6-4.

6.7 Evaluation of uncertainties

The confidence in the geometry of the deformation zone model and rock domain model, hydraulic properties, boundary conditions and initial conditions to variable extent govern the overall confidence of results of the numerical groundwater flow simulations. Their identification further promotes the discussion of how and where uncertainty should be decreased, and why. In this chapter HRDs are discussed.

6.7.1 Geometry of rock domains

Rock domains (HRD)

Hydraulic tests cannot directly give information of rock domain geometry, but the hydraulic tests performed in rock domain volumes, interpreted with support from geological and geophysical data, can be used to assess if there are significant differences in hydraulic properties between the geologically defined rock domains, that should give rise to changes in the geometries of hydraulic rock domain geometries.

It was found that several of the rock domains had different hydraulic properties, thus indicating that rock domain geometry should be employed when devising hydraulic rock domains, subsequently used in flow models. The uncertainty in the geometries of interpreted geological rock domains is discussed in /Wahlgren et al. 2005/.

6.7.2 Hydraulic properties of rock domains

Rock domains (HRD)

The hydraulic borehole data indicate that there may be a depth dependence in the hydraulic conductivity of the HRDs between the deterministically described deformation zones (HCDs). The data set test scale 100 m is rather large and seems to support that there is a depth dependency with some statistical significance. However, it may mainly be a difference between near-surface rock (0–200 m) and the rock below.

The hydraulic properties are different for the different rock domains, but for some rock domains, the statistics were based on data from one single borehole. As there is really no spatial distribution of the borehole information, the models must be considered as uncertain.

7 In situ pressure measured with WLP

During drilling of core holes, hydraulic tests are made generally for every drilled 100 m section with the SKB developed Wire Line Probe (WLP), see /Rhén et al. 2006a/. One part of the hydraulic test program has been absolute pressure measurements of the formation pressure in the test section. As these tests are the first to be done in the borehole, the tests should give estimates of the undisturbed formation pressure.

The methodology is as follows. The wireline probe is placed in position at the drill bit. The packer is inflated and the pressure build-up in the test section is recorded for a period of at least eight hours, typically this is done overnight. The measuring range for the pressure gauge is 0–20 MPa (± 0.05% FSD).

In Figure 7-1 the so far measured borehole sections are shown. As can be seen the pressure is nearly hydrostatic. No greater difference can be seen that could indicate compartmentalisation or features giving confined conditions that generate different hydraulic regimes. The fracture system seems to be hydraulically connected on the scale tested.

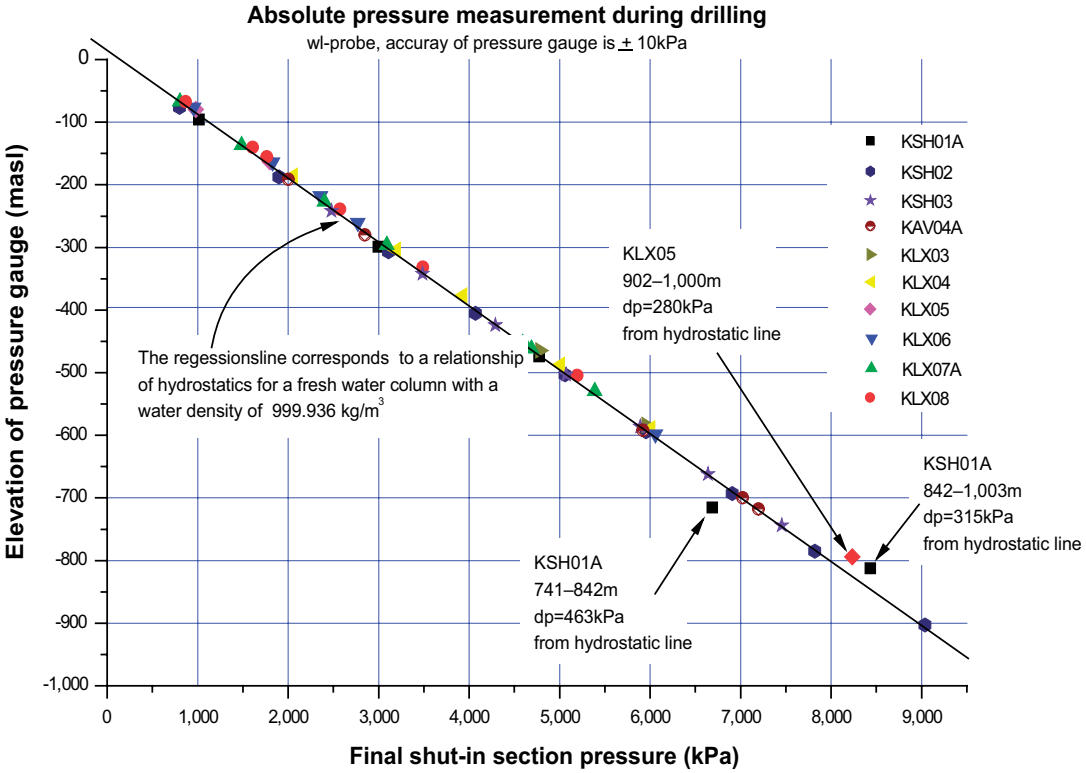

Figure 7-1. *Absolute pressure measurement with WLP of the undisturbed formation pressure.*

8 Overburden – Hydraulic properties of the hydraulic soil domains (HSD)

The investigation performed in the overburden and resulting models are reported in /Werner et al. 2005, Nyman 2005/. In this section only a few results from these reports are highlighted.

The surface map of the quaternary deposits is shown in Figure 8-1 and the conceptual model of the overburden is shown in Figure 8-2. Generally a thin cover of till (Z3) is found on the entire rock surface, except for some areas where the rock is outcropping /Nyman 2005/. In the valley the till is generally overlain by clay deposits (Z2). In some areas peat (M1) is on top of the clay layer. In a few places glacial deposits (M2) are found and e.g. the nuclear power plants artificial fill (M3) covers limited areas. The uppermost part of the overburden (Z1) can be considered to be affected by surface processes, such as roots, biological activity and frost. This leads to a higher permeability and porosity compared to deeper layers of the overburden.

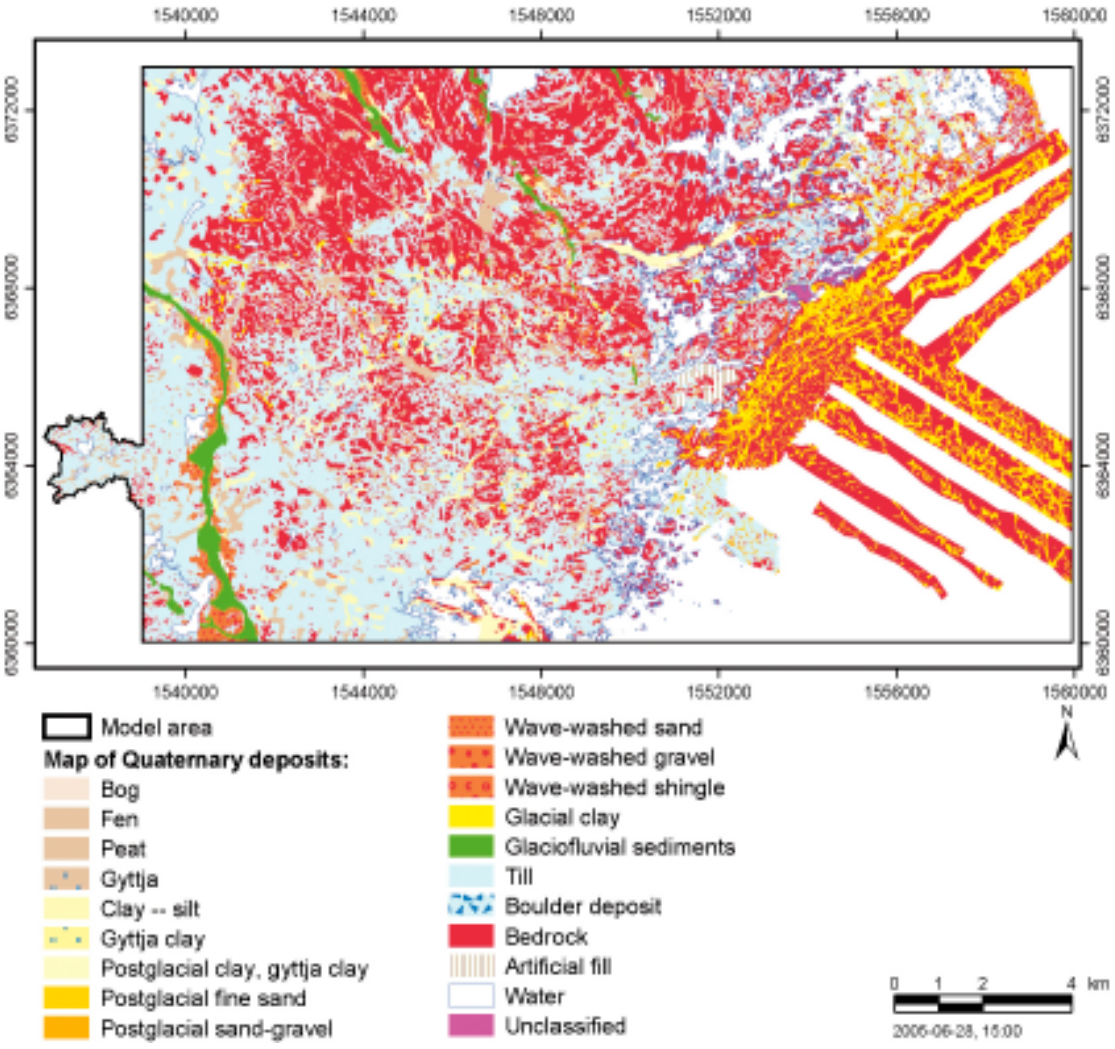

Figure 8-1. *Map showing the distribution of the Quaternary deposits in the Simpevarp area /Nyman 2005/.*

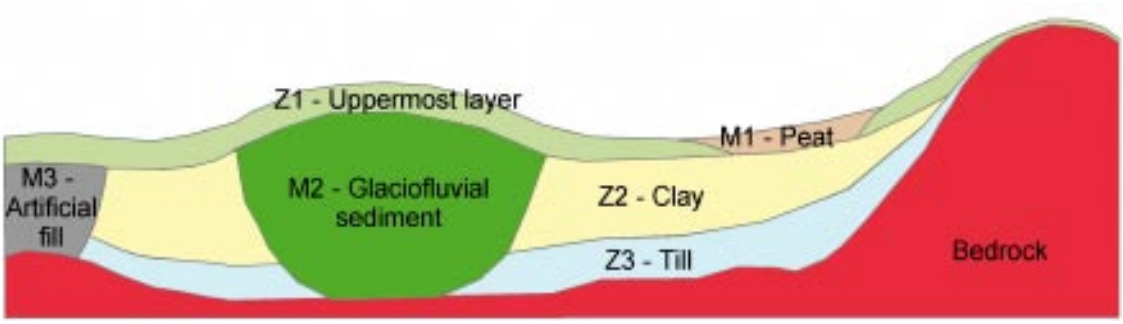

Figure 8-2. *Conceptual model of the overburden /Nyman 2005/.*

The hydraulic properties of the Hydraulic Soil Domains (HSD) Z1–3 and M1–3 are described in /Werner et al. 2005/. The properties for the HSDs are summarized in Table 8-1.

It should be observed that the K-values in Table 8-1 generally are higher than in the bedrock. This means that e.g. the clay layers will not significantly reduce the infiltration or have a large effect on the deep hydrogeology.

Table 8-1. HSD properties based on /Werner et al. 2005/. Hydraulic conductivity (K), Horizontal hydraulic conductivity (K_H), Vertical hydraulic conductivity (K_V).

HSD	Description	KH (m/s)	KH/KV (–)	Specific yield, S_y (–)	Specific storage coefficient, S_s (1/m)
HSD (Z1-1)	Surface process affected layer, Clay	1E–6	1	0.03	6E–3
HSD (Z1-2)	Surface process affected layer, Till	4E–5	1	0.15	1E–3
HSD (Z1-3)	Surface process affected layer, Artificial fill	4E–5	1	0.15	1E–3
HSD (Z2)	Clay layer	1E–8	1	0.03	6E–3
HSD (Z3)	Till layer	4E–5	1	0.05	1E–3
HSD (M1)	Peat layer	1.5E–6	1	0.24	5E–2
HSD (M2)	Glaciofluvial sediment layer	1E–4	1	0.25	2.5E–2
HSD (M3)	Artificial fill layer	4E–5	1	0.05	1E–3

8.1 Evaluation of uncertainties

The confidence in the geometry of the deformation zone model and rock domain model, hydraulic properties, boundary conditions and initial conditions to variable extent govern the overall confidence of results of the numerical groundwater flow simulations. Their identification further promotes the discussion of how and where uncertainty should be decreased, and why. In this chapter HSDs are briefly discussed.

8.1.1 Overburden – HSD

The model suggested has low-medium confidence as the geological description of the overburden is simplified in Laxemar 1.2, although with considerable improvements from SDM Simpevarp 1.2. The model uncertainty is more described in /Lindborg (ed) 2006/.

9 Estimation of water table level

The upper boundary of a groundwater flow model generally has either head boundary conditions or flux boundary conditions. In principal it is more correct to apply a flux boundary condition, having rain as the main source for recharging groundwater, than a head boundary condition. However, numerically the head boundary condition is more efficient and in several cases it may be a sufficiently good approximation. In a case having a low conductive bed rock and relatively high precipitation, as in most part of Sweden, one can expect that the water table follows the topography rather well and that the topography may be used as a head boundary.

The numerous small streams, small lakes and peat lands in the Simpevarp regional model confirms that the discharge areas are well spread over the area, and also indicating a lower possible level for the water table. This level could be an alternative representation of the head boundary condition compared to the topography.

In Figure 9-1 the topography is shown and in Figure 9-2 all points representing streams, lakes, peat lands and sea level as elevation 0 as well as the interpolated surface between in all these points. This elevation model of the water table is called Water table–base.

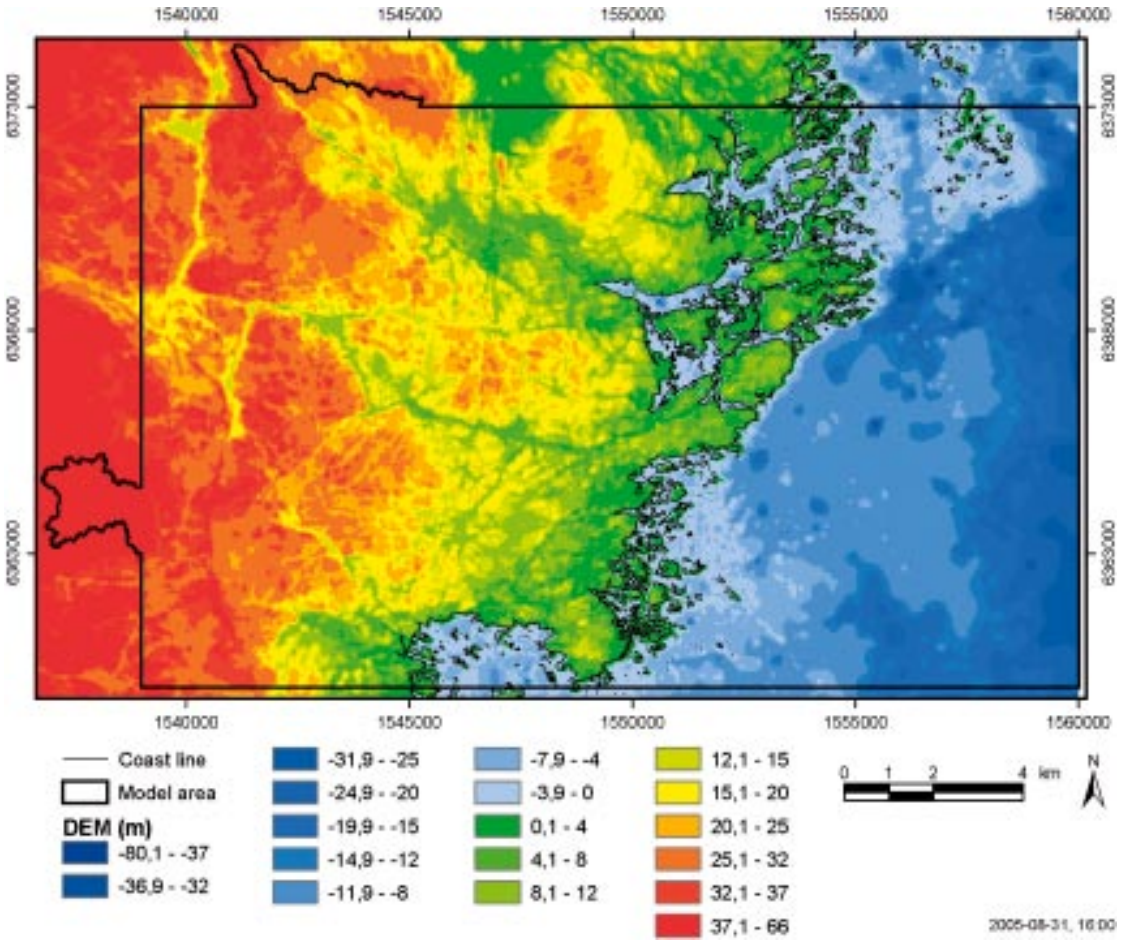

Figure 9-1. *Topography in the Simpevarp area. The black line shows the regional model area and parts of drainage areas of catchments in the regional area that extends a bit outside the regional model area.*

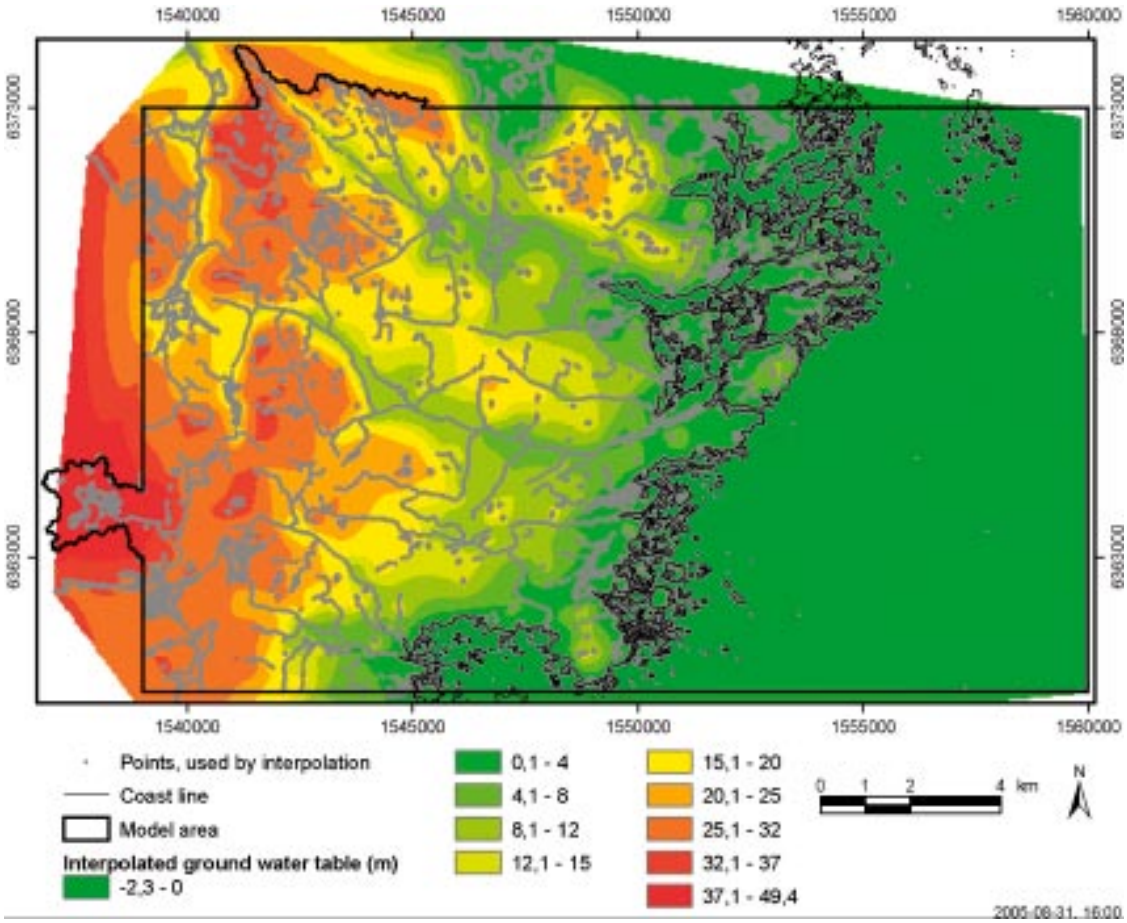

Figure 9-2. *Estimated level of the water table (Water table-base) based on levels of discharge points. Discharge points used for the interpolation shown in grey. The black line shows the regional model area and parts of drainage areas of catchments in the regional area that extends a bit outside the regional model area.*

The evaluation of groundwater levels on Äspö indicated that the water table roughly could be approximated with 0.3·level of topography /Rhén et al. 1997c/.

By taking the difference between the topography and Water table-base one gets an estimate of the maximum depth to the water table, see Figure 9-3. By multiplying this difference with a value between 0 and 1 and add to the Water table-base, one can create possible water table maps that are between the topography and the Water table–base. In Figure 9-4 and Figure 9-5 two alternatives of possible water tables are shown for coefficients 0.3 and 0.6 (Water table –0.3 and Water table –0.6).

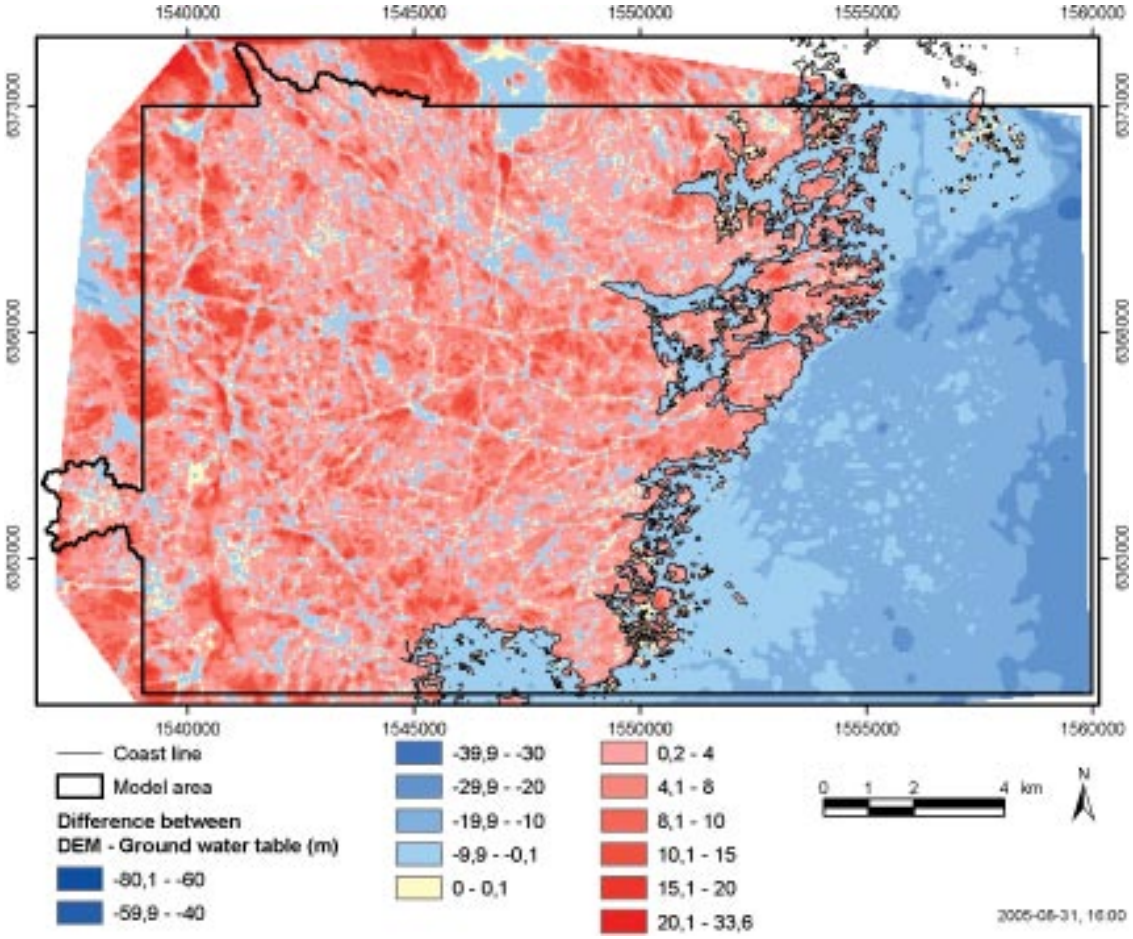

Figure 9-3. *The difference between the topography and Water table-base case. The black line shows the regional model area and parts of drainage areas of catchments in the regional area that extends a bit outside the regional model area.*

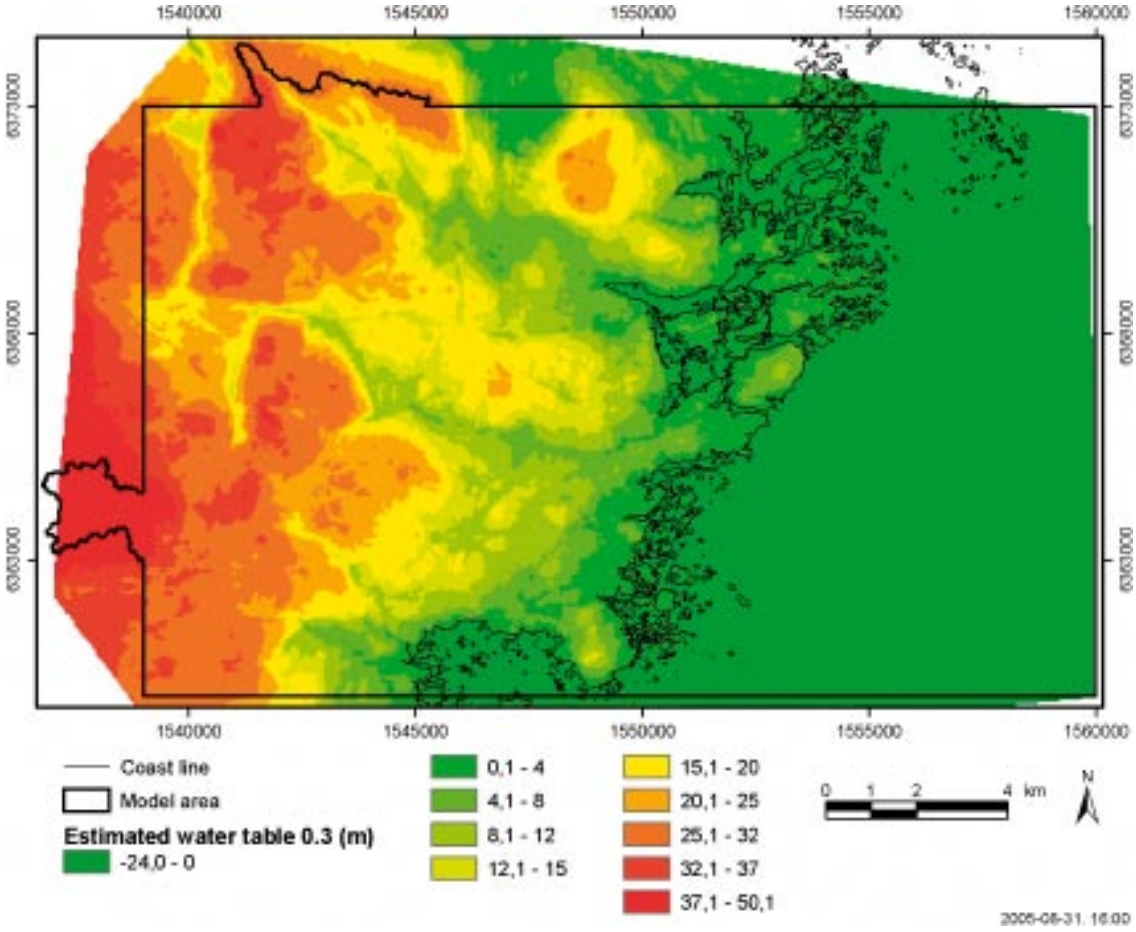

Figure 9-4. *The Water table–0.3 case. The black line shows the regional model area and parts of drainage areas of catchments in the regional area that extends a bit outside the regional model area.*

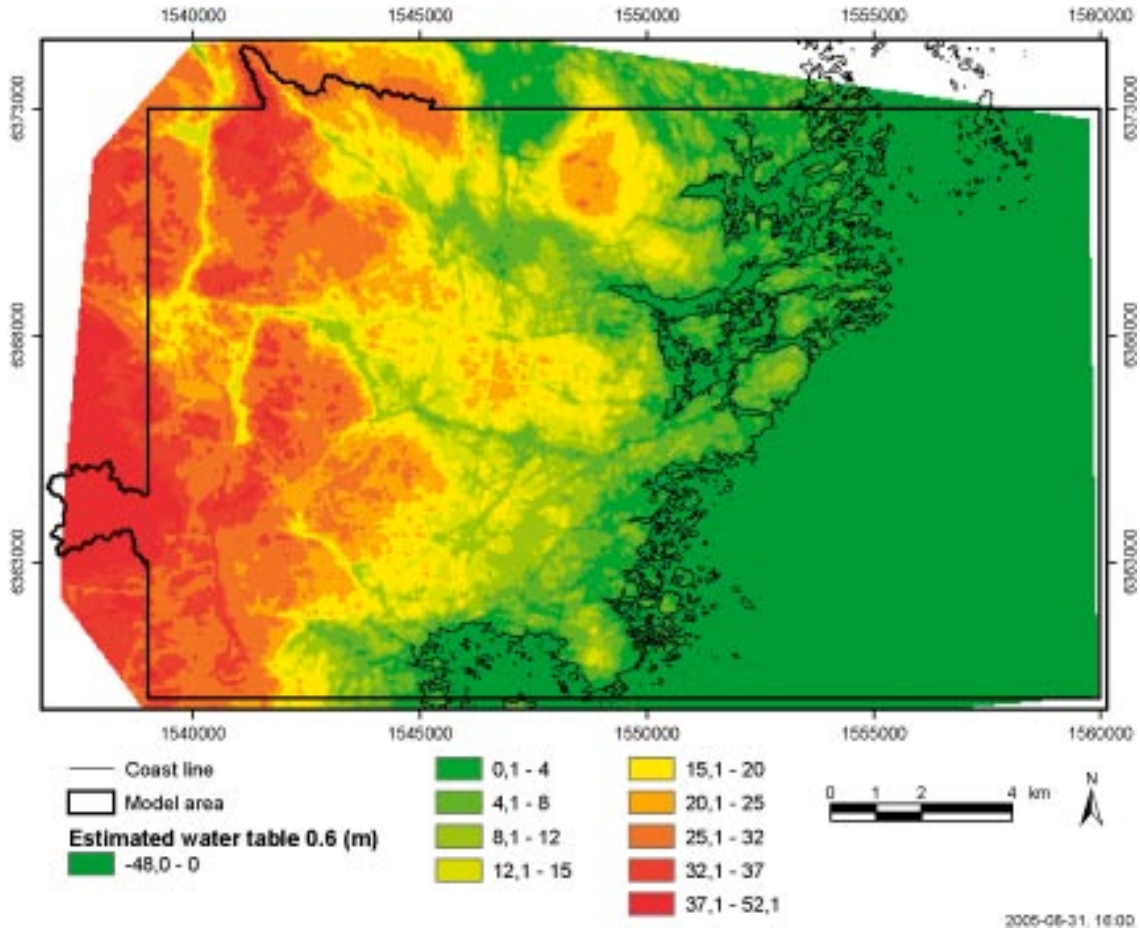

Figure 9-5. *The Water table–0.6 case. The black line shows the regional model area and parts of drainage areas of catchments in the regional area that extends a bit outside the regional model area.*

10 References

Andersson P, Ludvigson J-E, Wass E, 1998. Äspö Hard Rock Laboratory, True Block Scale Project, Preliminary characterisation. Combined interference tests and tracer tests, SKB IPR-01-44, Svensk Kärnbränslehantering AB.

Andersson P, Ludvigson J-E, Wass E, Holmqvist M, 2000. Äspö Hard Rock Laboratory, True Block Scale Project, Tracer test stage. Interference tests, dilutiontests and tracer tests, SKB IPR-00-28, Svensk Kärnbränslehantering AB.

Brace W F, 1980. Permeability of Crystalline and Argillaceous Rocks. Int. J. Rock. Mech. & Geomech. Abstr. Vol. 17, pp. 241–251.

Dershowitz W, Winberg A, Hermanson J, Byegård J, Tullborg E-L, Andersson P, Mazurek M, 2003. Äspö Hard Rock Laboratory. Äspö Task Force on modelling of groundwater flow and transport of solutes – Task 6C – A semi-synthetic model of block scale conductive structures at the Äspö HRL. SKB IPR-03-13. Svensk Kärnbränslehantering AB.

Ekman L, 2001. Project deep drilling KLX02 – Phase 2, Methods, scope of activities and results. Summary report SKB TR-01-11. Svensk Kärnbränslehantering AB

Follin S, Stigsson M, Svensson U, 2006. Hydrogeological DFN modelling using structural and hydraulic data from KLX04, Preliminary site description, Laxemar subarea – version 1.2 . SKB R-06-24, Svensk Kärnbränslehantering AB.

Forssman I, Zetterlund M, Forsmark T, Rhén I, 2005a. Oskarshamn site investigation. Correlation of Posiva Flow Log anomalies to core mapped features in KSH01A, KSH02A and KAV01. SKB P-05-65, Svensk Kärnbränslehantering AB.

Forssman I, Zetterlund M, Forsmark T, Rhén I, 2005b. Oskarshamn site investigation. Correlation of Posiva Flow Log anomalies to core mapped features in KLX02, KLX03, KLX04, KAV04A and KAV04b. SKB P-05-241, Svensk Kärnbränslehantering AB.

Jensen J L, Lake L W, Corbett P W M, Goggin D J, 2000. Statistics for petroleum engineers and geoscientists, Handbook of Petroleum Exploration and Production, 2, Second ed, Elsevier, Amsterdam.

Gustafsson E, Ludvigson J-E, 2005. Oskarshamn site investigation. Combined interference test and tracer test between KLX02 och HLX10. SKB P-05-20. Svensk Kärnbränslehantering AB.

Hartley L, Hunter F, Jackson P, McCarthy R, Gylling B, Marsic N, 2006. Regional hydrogeological simulations – Numerical modelling using ConnectFlow. Preliminary site description, Laxemar subarea – version 1.2. SKB R-06-23, Svensk Kärnbränslehantering AB.

Juhlin C, Wallroth T, Smellie J, Eliasson T, Ljunggren C, Leijon B, Beswick J, 1998. The very deep hole concept – Geoscientific appraisal of conditions at great depth, SKB TR98-05, Svensk Kärnbränslehantering AB.

Lindborg T (ed), 2006. Description of surface systems, Preliminary site description Laxemar subarea – version 1.2. SKB R-06-11, Svensk Kärnbränslehantering AB.

Ludvigson J-E, Levén J, Jönsson S, 2003. Oskarshamn site investigation. Hydraulic tests and flow logging in borehole HSH03. SKB P-03-56. Svensk Kärnbränslehantering AB.

Nyman H, 2005. Depth and stratigraphy of Quaternary deposits. Preliminary site description Laxemar subarea – version 1.2. SKB R-05-54. Svensk Kärnnbränslehantering AB.

Rahm N, Enachescu C, 2004. Oskarshamn site investigation. Hydraulic testing of percussion drilled lineament boreholes on Ävrö and Simpevarp, 2004. SKB P-04-287. Svensk Kärnbränslehantering AB.

Rhén I, Bäckblom G, Gustafson G, Stanfors R, Wikberg P, 1997a. Äspö HRL – Geoscientific evaluation 1997/2. Results from pre-investigations and detailed characterization. Summary Report SKB TR-97-03. Svensk Kärnbränslehantering AB.

Rhén I, Gustafson G, Wikberg P, 1997b. Äspö HRL – Geoscientific evaluation 1997/4. Results from pre-investigations and detailed site characterization. Comparisons of predictions and observations. Hydrogeology, groundwater chemistry and transport of solutes. SKB TR-97-05. Svensk Kärnbränslehantering AB.

Rhén I, Gustafson G, Wikberg P, 1997c. Äspö HRL – Geoscientific evaluation 1997/5. Models based on site characterization 1986–1995. SKB TR-97-06. Svensk Kärnbränslehantering AB.

Rhén I, Forsmark T, 2001. Äspö Hard Rock Laboratory, Prototype repository, Hydrogeology, Summary report of investigations before the operation phase. SKB IPR-01-65, Svensk Kärnbränslehantering AB.

Rhén I, Follin S, Hermanson J, 2003. Hydrological Site Descriptive Model – a strategy for its development during site investigations. SKB R-03-08. Svensk Kärnbränslehantering AB.

Rhén I, Forsmark T, Forssman I, Zetterlund M, 2006a. Hydrogeological single-hole interpretation of KSH01A, KSH02, KSH03A, KAV01, KLX02 and HSH01–03, Simpevarp subarea – version 1.2, SKB R-06-20, Svensk Kärnbränslehantering AB.

Rhén I, Forsmark T, Forssman I, Zetterlund M, 2006b. Hydrogeological single-hole interpretation of KLX02, KLX03, KLX04, KAV04A and B, HAV09–10 and 9 HLXxx boreholes, Laxemar subarea – version 1.2, SKB R-06-21, Svensk Kärnbränslehantering AB.

Smellie J, 2004. Recent geoscientific information relating to deep crustal studies, SKB R-04-09, Svensk Kärnbränslehantering AB.

SKB, 2006. Preliminary site description. Laxemar subarea – version 1.2. SKB R-06-10. Svensk Kärnbränslehantering AB.

Wahlgren C-H, Hermanson J, Curtis P, Forssberg O, Triumf C-A, Drake H, Tullborg E-L, 2005. Geological description of rock domains and deformation zones in the Simpevarp and Laxemar subareas. Preliminary site description, Laxemar subarea, version 1.2. SKB P-05-69, Svensk Kärnbränslehantering AB.

Werner K, Bosson E, Berglund S, 2005. Description of climate, surface hydrology, and near-surface hydrogeology. Preliminary site description Laxemar subarea – version 1.2. SKB R-05-61, Svensk Kärnbränslehantering AB.

Appendix 1

Depth trends of transmissivity in large deformation zones

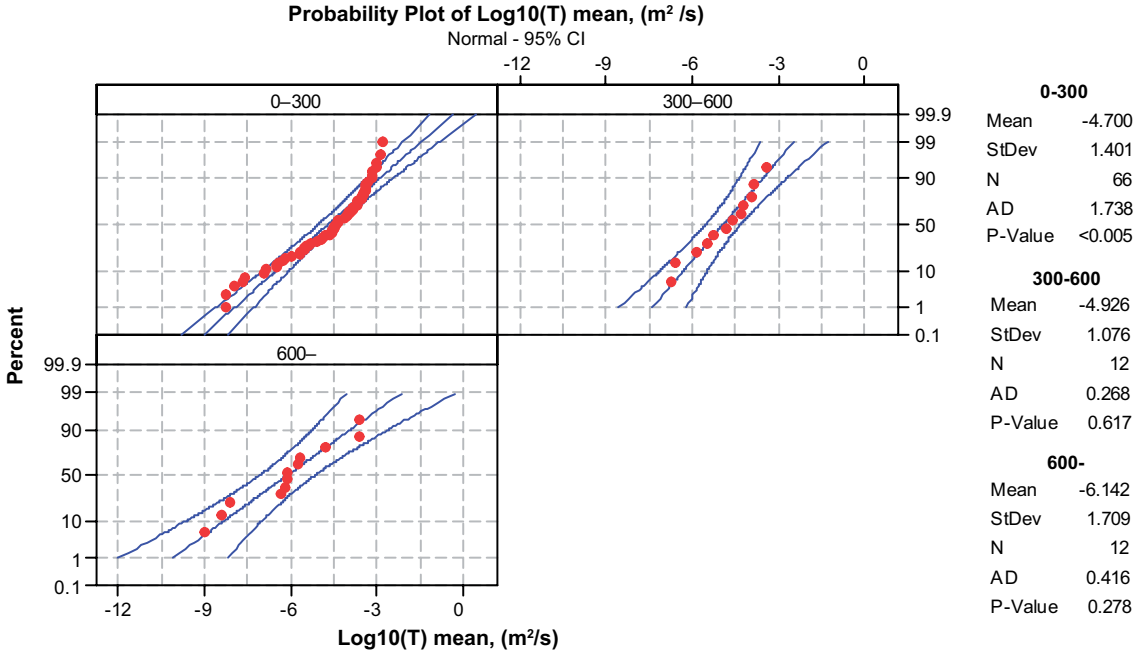

Panel variable: Elevation class 2

Figure A1-1. *Univariate statistics of the transmissivity in HCDs for elevation intervals: 0 to –300, –300 to –600 and deeper than –600 m. Data from all areas (Laxemar, Simpevarp peninsula, Äspö, Ävrö-Hålö-Mjälen based on deterministically defined deformation zones in RVS model version L1.2.*

Table A1-1. Univariate statistics of the transmissivity in HCDs for elevation intervals: 0 to –300, –300 to –600 and deeper than –600 m. Data from all areas (Laxemar, Simpevarp peninsula, Äspö, Ävrö-Hålö-Mjälen based on deterministically defined deformation zones in RVS model version L1.2. (ch: core drilled holes, ph: percussion drilled holes)

Area	Data type	Test type	Elevation Upper limit (m)	Elevation Lower limit (m)	Test scale (m)	Sample size, all	Sample size, lower meas lim	Lower meas. limit[1] Log10 T (m^2/s)	T Log10(T) (m^2/s)	Mean Log10 T (m^2/s)	Std Log10 T (m^2/s)	Conf.lim Log10(T) Mean±D, conf. level 0.95: D (m^2/s)
All	DZ	PSS, HTHB, Airlift	0	–300	3–100	66	0	(ph≈ –8 to –6) (ch≈ –9)		–4.70	1.40	0.34
All	DZ	PSS, HTHB, Airlift	–300	–600	3–100	12	0	(ph≈ –8 to –6) (ch≈ –9)		–4.93	1.08	0.69
All	DZ	PSS, HTHB, Airlift	–600	–1,000	3–100	12	0	(ph≈ –8 to –6) (ch≈ –9)		–6.14	1.71	1.09

Appendix 2

Depth trends of hydraulic conductivity in rock mass, test scale 100 m

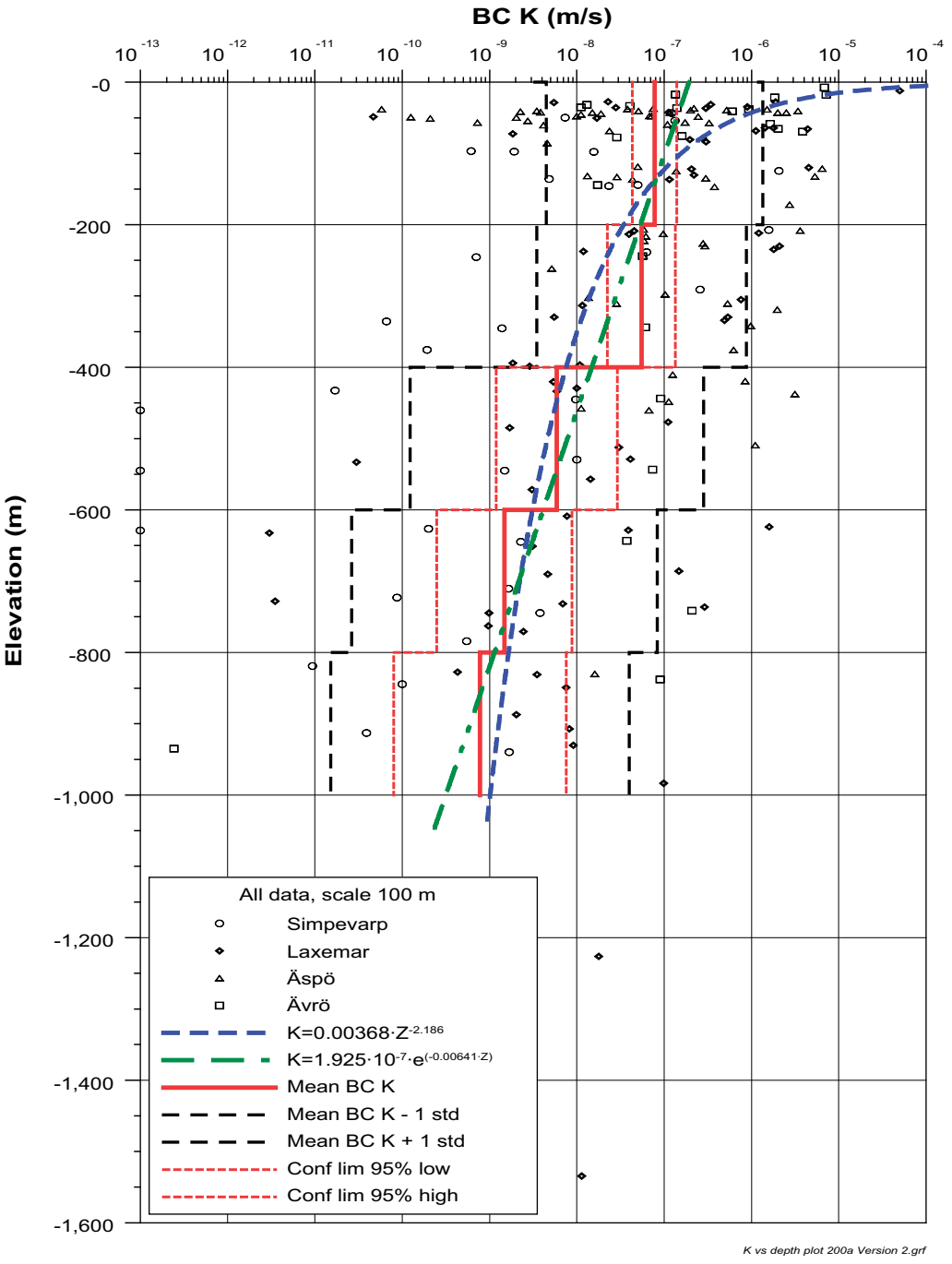

Figure A2-1. *Depth trend of the hydraulic conductivity in HRDs. Test scale 100 m. Data from all areas (Laxemar, Simpevarp peninsula, Äspö, Ävrö-Hålö-Mjälen. Data representing all data* ***including*** *deterministically defined deformation zones in RVS model version L1.2. Statistics for elevation interval 200 m.*

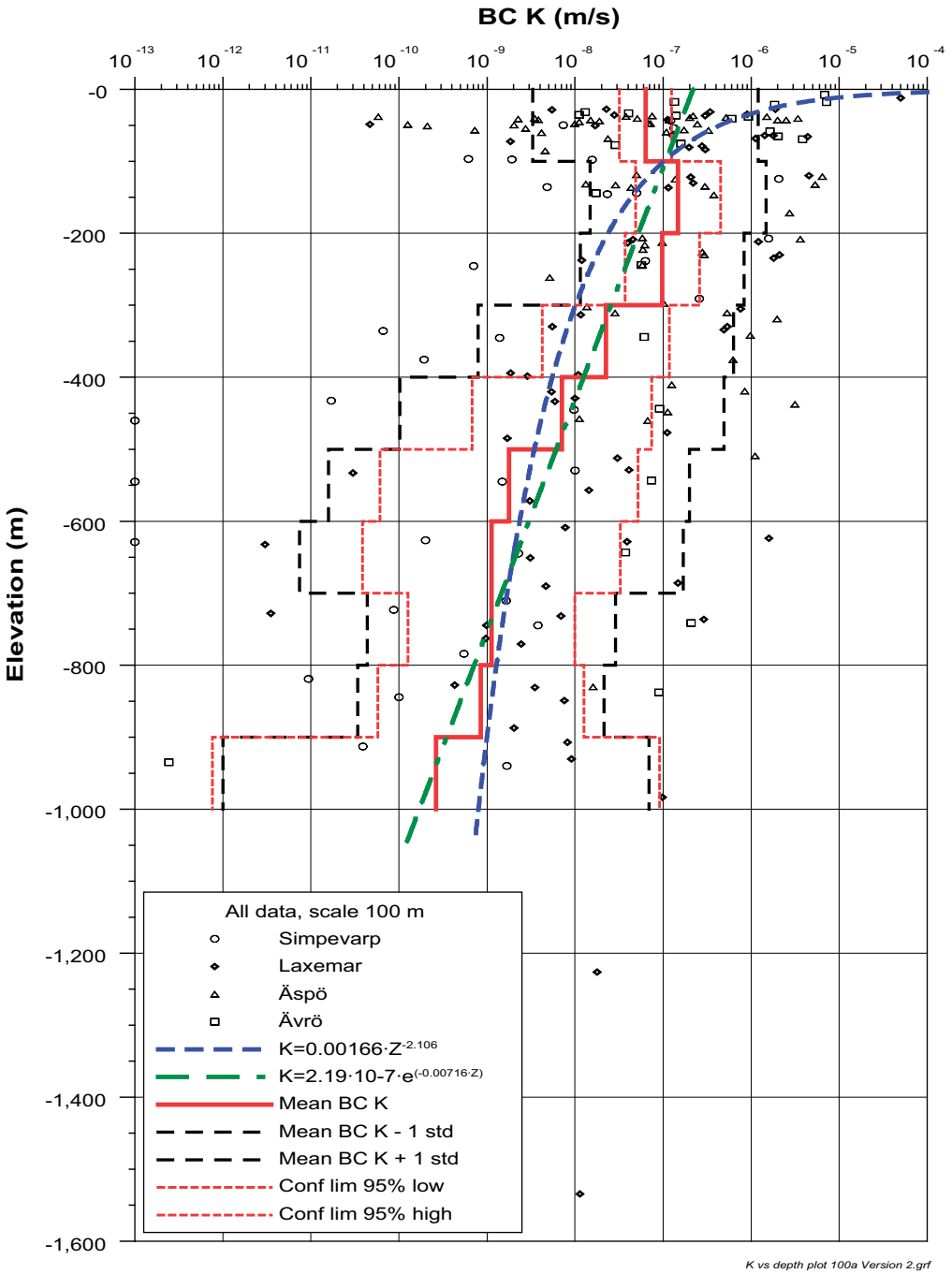

Figure A2-2. *Depth trend of the hydraulic conductivity in HRDs. Test scale 100 m. Data from all areas (Laxemar, Simpevarp peninsula, Äspö, Ävrö-Hålö-Mjälen. Data representing all data* ***including*** *deterministically defined deformation zones in RVS model version L1.2. Statistics for elevation interval 100 m.*

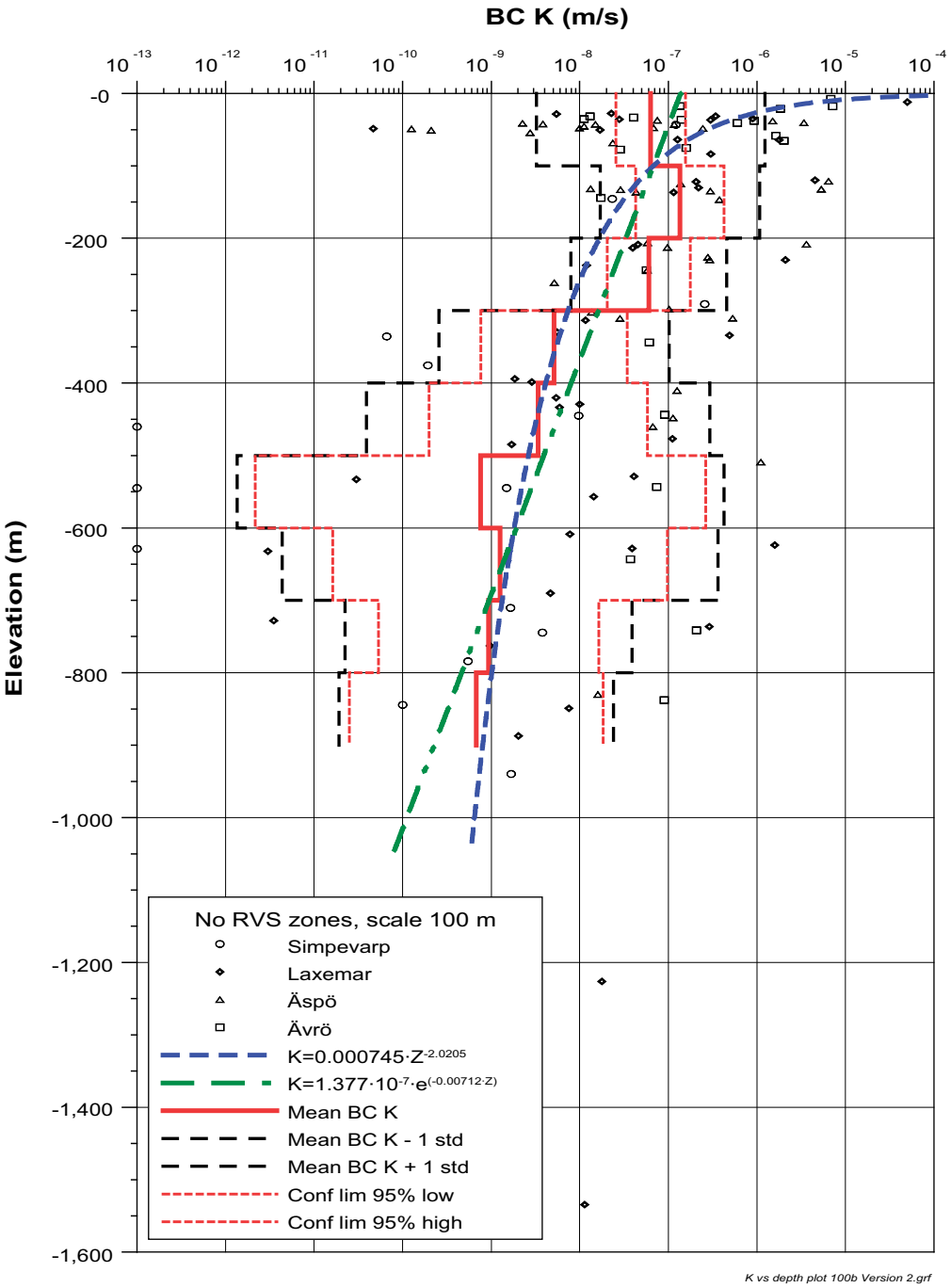

Figure A2-3. *Depth trend of the hydraulic conductivity in HRDs. Test scale 100 m. Data from all areas (Laxemar, Simpevarp peninsula, Äspö, Ävrö-Hålö-Mjälen. Data representing all data* ***excluding*** *deterministically defined deformation zones in RVS model version L1.2. Statistics for elevation interval 100 m.*

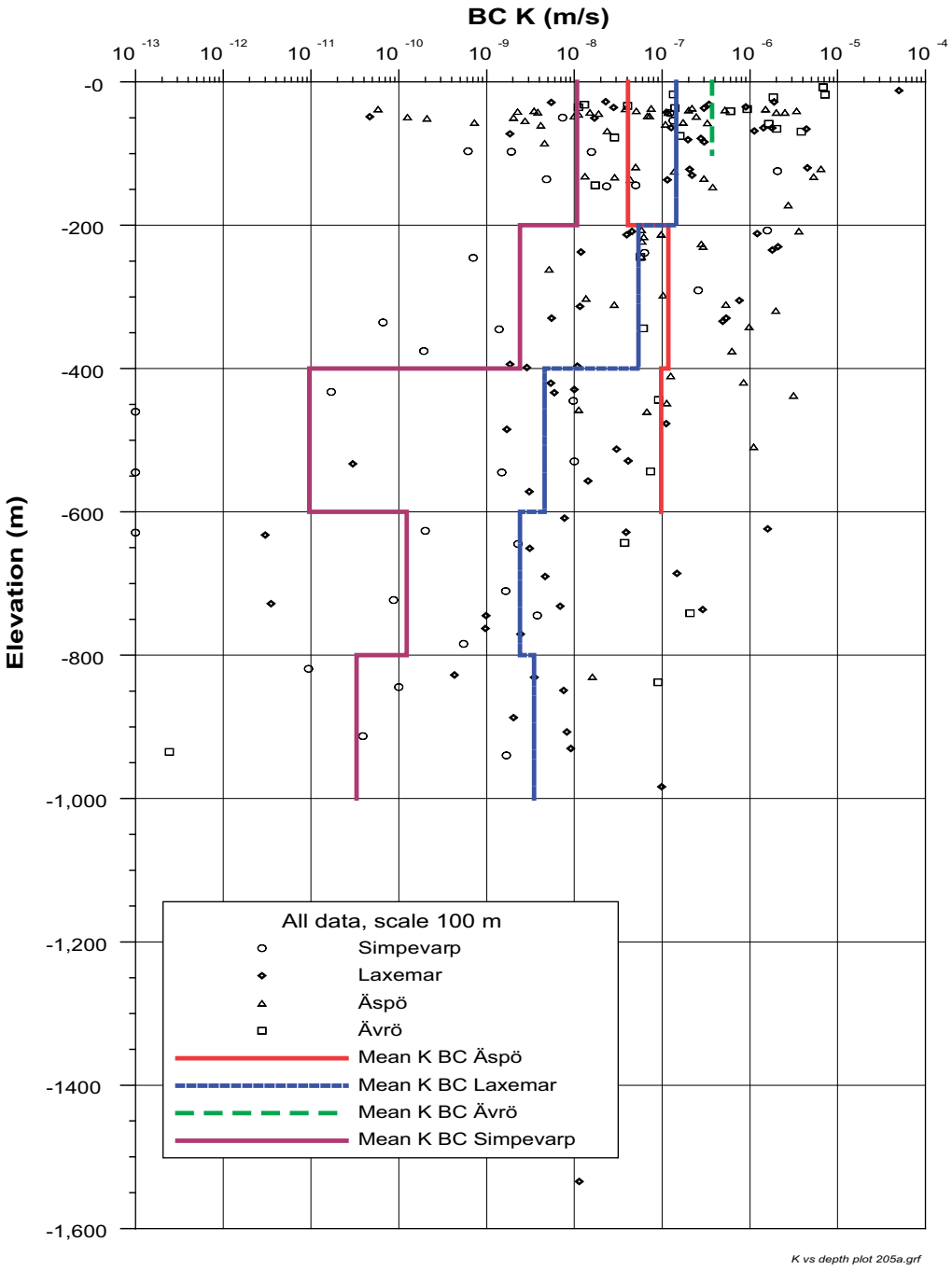

Figure A2-4. *Depth trend of the hydraulic conductivity in HRDs. Test scale 100 m. Data from all areas (Laxemar, Simpevarp peninsula, Äspö, Ävrö-Hålö-Mjälen. Depth trends for mean Log10(K) shown for the sub-areas. Data representing all data* ***including*** *deterministically defined deformation zones in RVS model version L1.2. Statistics for elevation interval 200 m.*

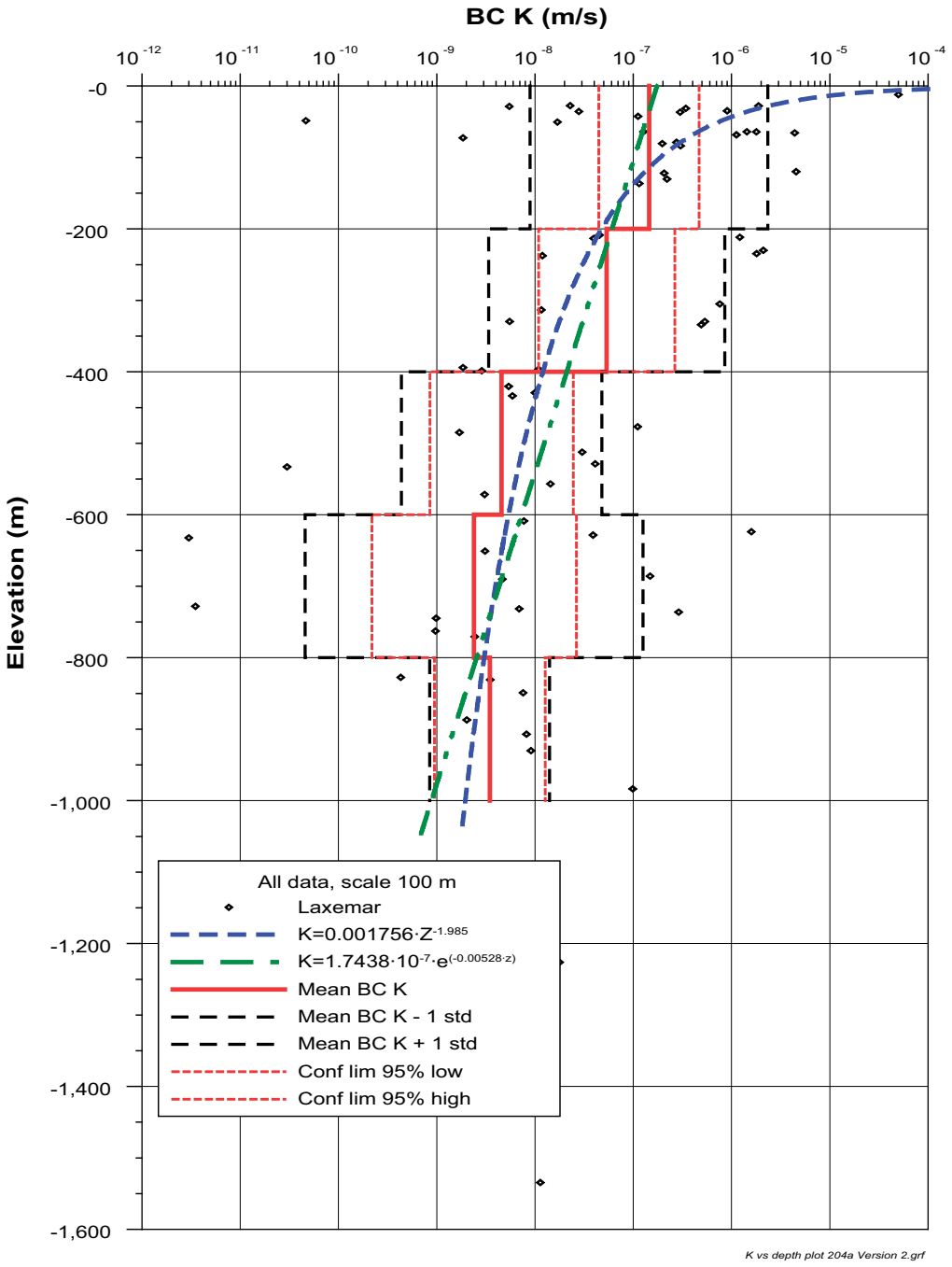

Figure A2-5. *Depth trend of the hydraulic conductivity in HRDs. Test scale 100 m. Data from Laxemar area. Data representing all data* ***including*** *deterministically defined deformation zones in RVS model version L1.2. Statistics for elevation interval 200 m.*

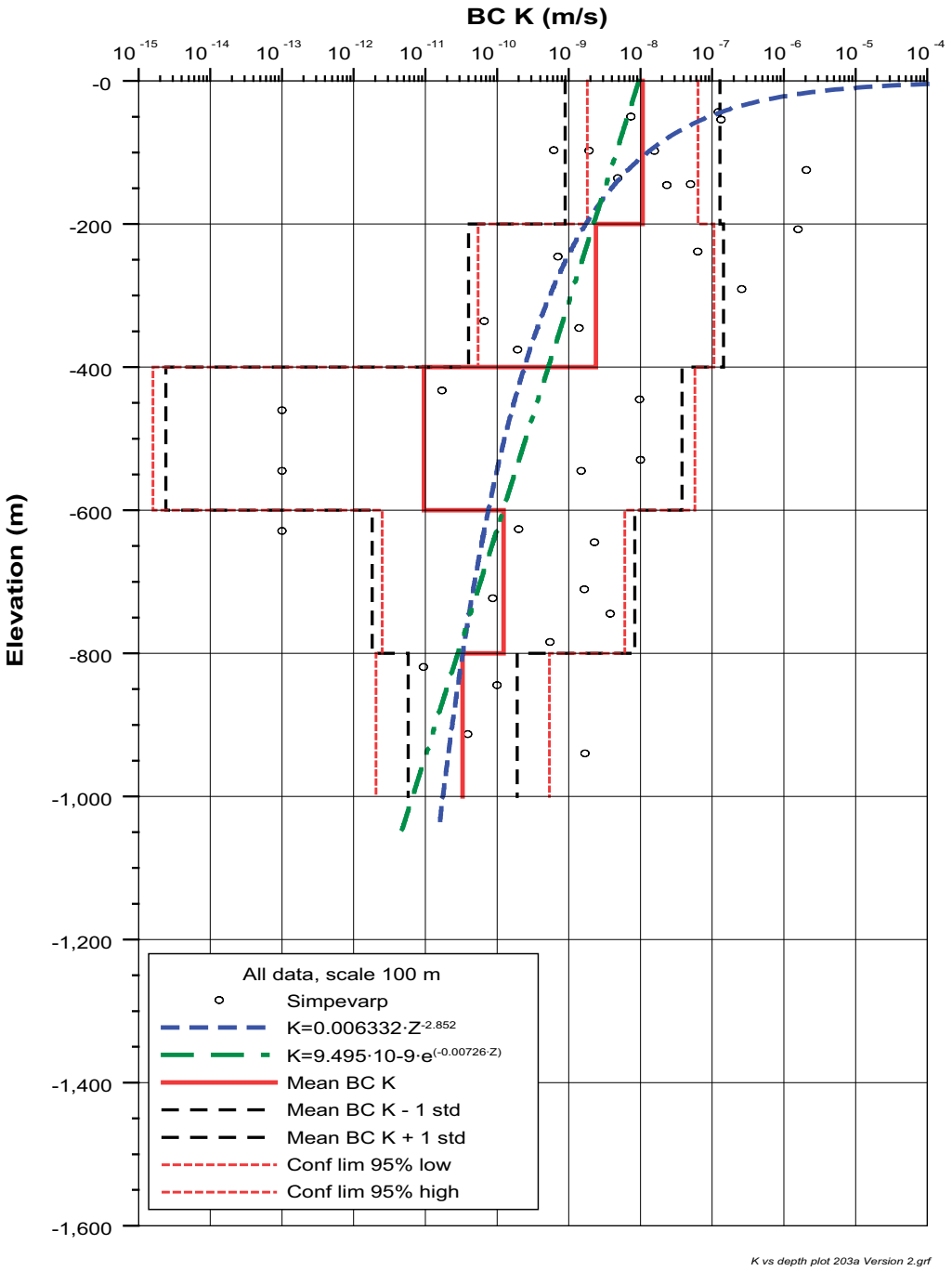

Figure A2-6. *Depth trend of the hydraulic conductivity in HRDs. Test scale 100 m. Data from Simpevarp peninsula. Data representing all data* ***including*** *deterministically defined deformation zones in RVS model version L1.2. (Confidence interval extremely wide in some cases due to very few sample and should just be seen as indicators of great uncertainty.) Statistics for elevation interval 200 m.*

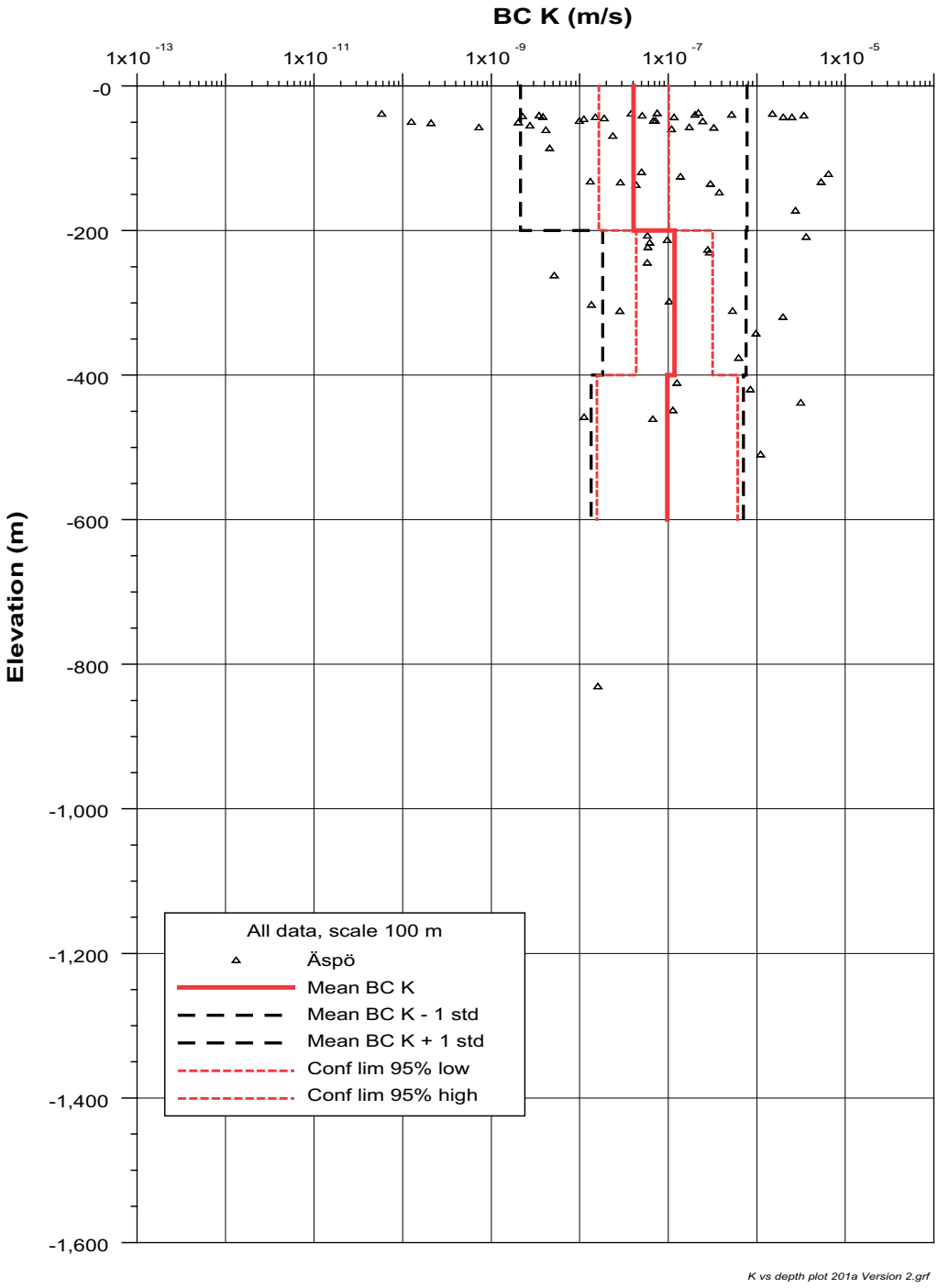

Figure A2-7. *Depth trend of the hydraulic conductivity in HRDs. Test scale 100 m. Data from Äspö area. Data representing all data* ***including*** *deterministically defined deformation zones in RVS model version L1.2. Statistics for elevation interval 200 m.*

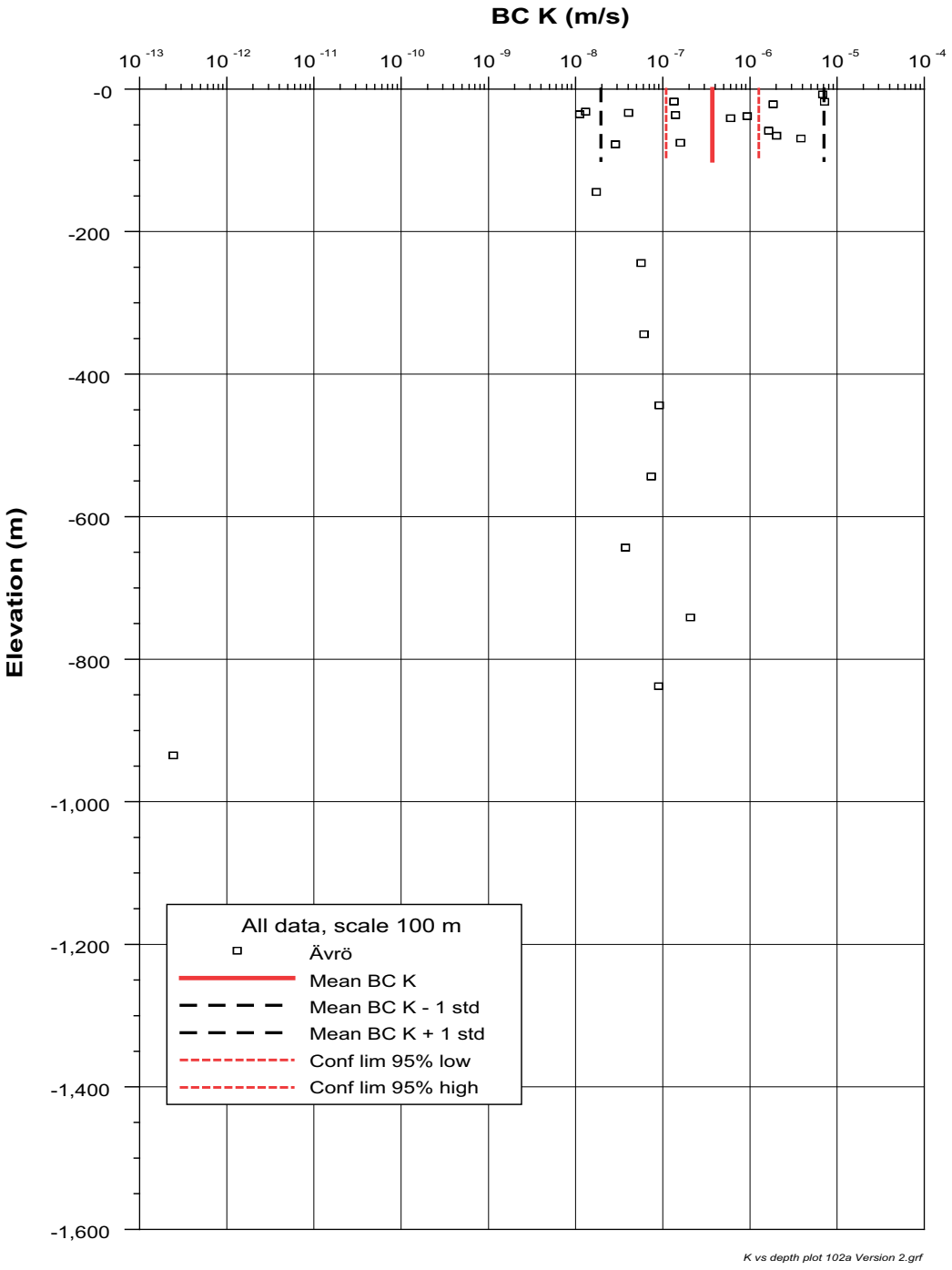

Figure A2-8. *Depth trend of the hydraulic conductivity in HRDs. Test scale 100 m. Data from Ävrö-Hålö-Mjälen area. Data representing all data* ***including*** *deterministically defined deformation zones in RVS model version L1.2. Statistics for elevation interval 100 m.*

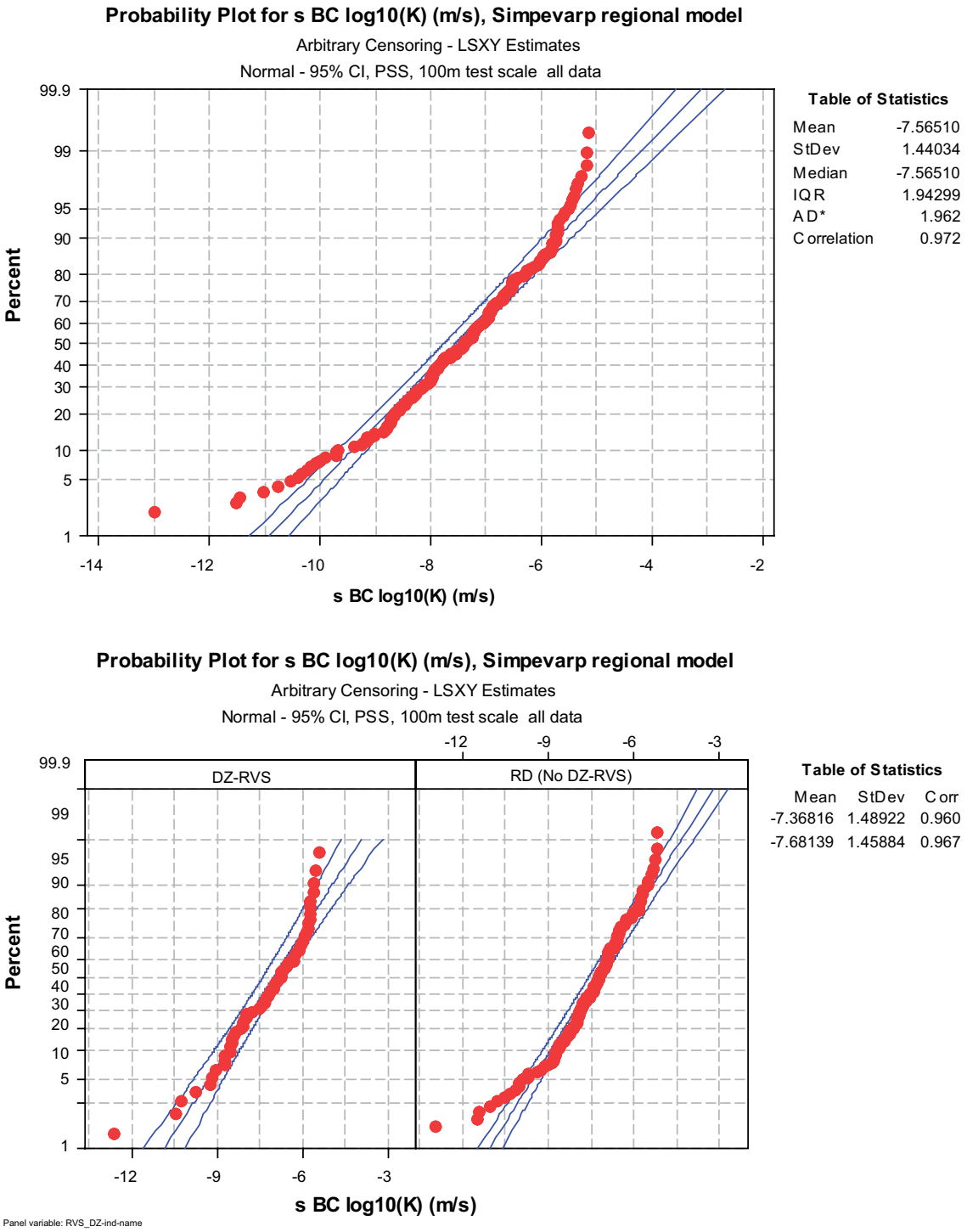

Figure A2-9. *Statistics of the hydraulic conductivity in HRDs. Test scale 100 m. Laxemar, Simpevarp peninsula, Äspö, Ävrö-Hålö-Mjälen. Top: Data representing all data* ***including*** *deterministically defined deformation zones in RVS model version L1.2. Bottom: Data representing all data* ***excluding*** *deterministically defined deformation zones (right) or just the deterministically defined deformation zones (left) in RVS model version L1.2*

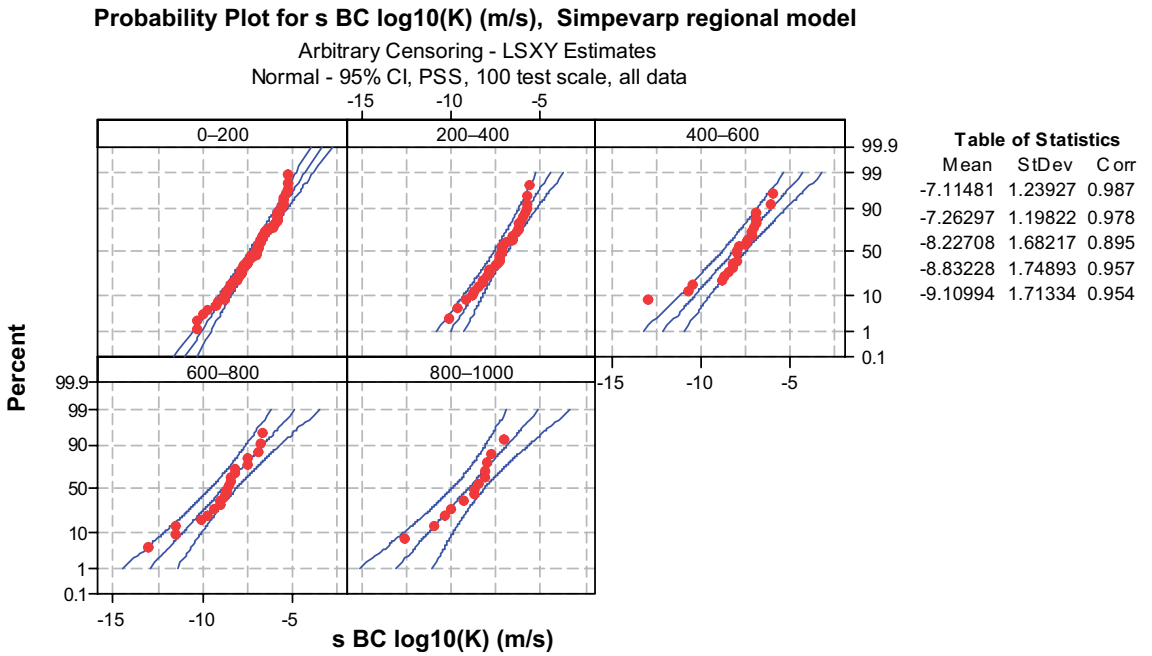

Panel variable: Elev_class_2

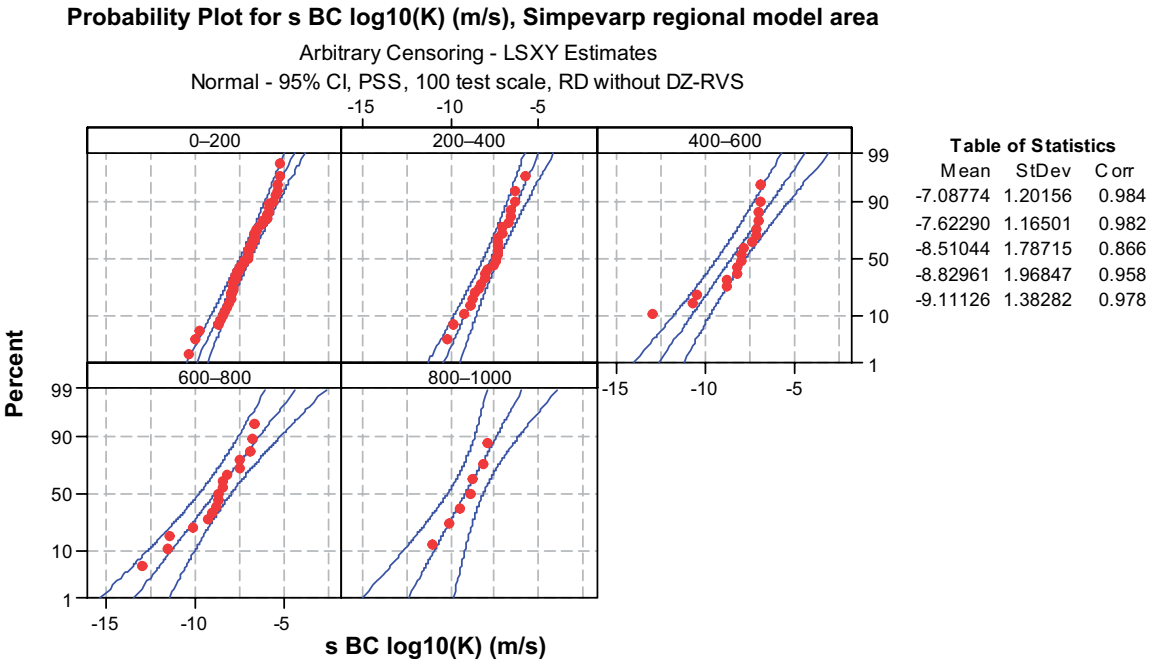

Panel variable: Elev_class_2

Figure A2-10. *Statistics for depth trend of the hydraulic conductivity in HRDs. Test scale 100 m. Laxemar, Simpevarp peninsula, Äspö, Ävrö-Hålö-Mjälen. Top: Data representing all data* ***including*** *deterministically defined deformation zones in RVS model version L1.2. Bottom: Data representing all data* ***excluding*** *deterministically defined deformation zones in RVS model version L1.2. Statistics for elevation interval 200 m.*

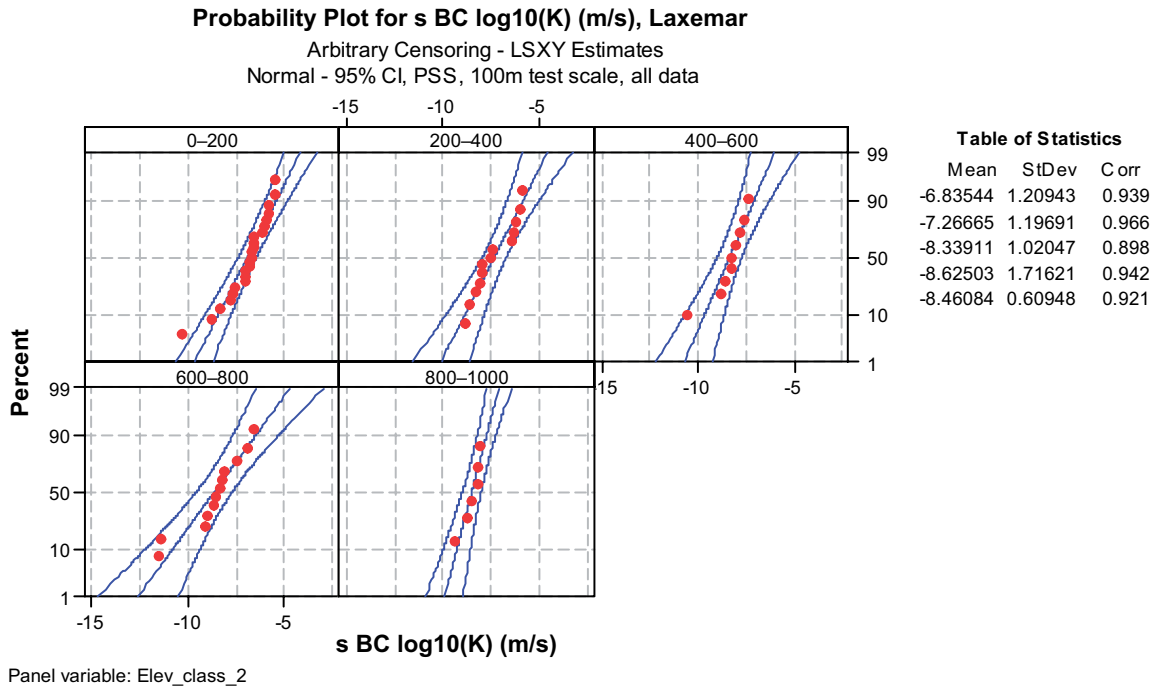

Panel variable: Elev_class_2

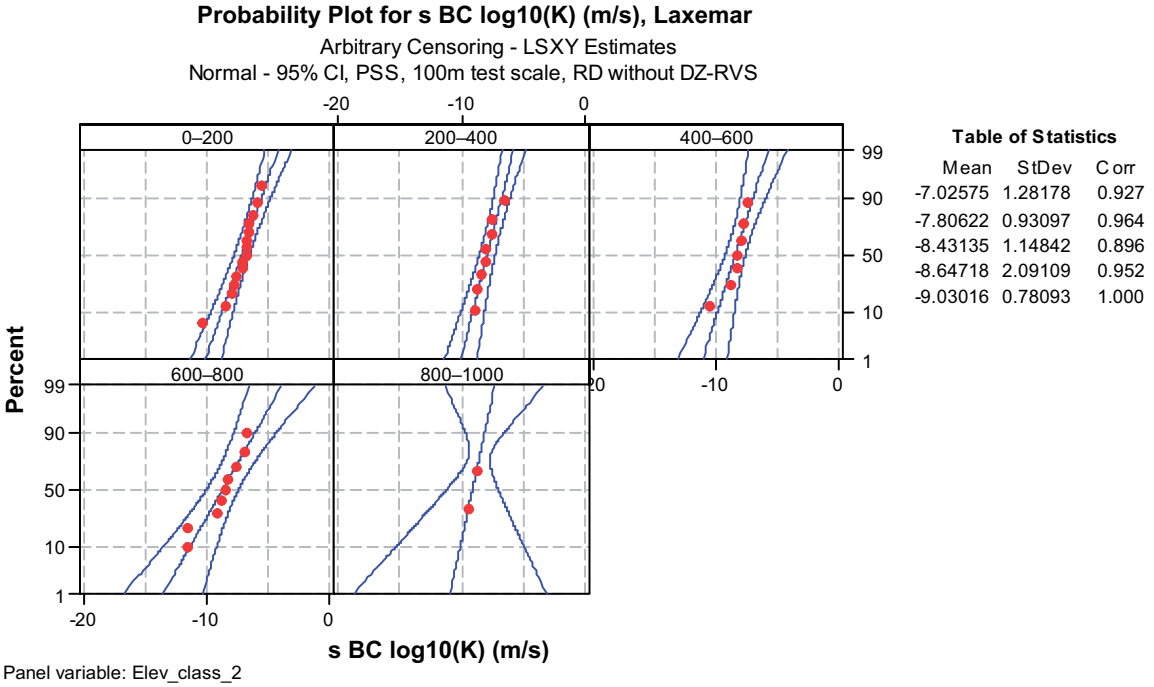

Panel variable: Elev_class_2

Figure A2-11. *Statistics for depth trend of the hydraulic conductivity in HRDs. Test scale 100 m. Laxemar. Top: Data representing all data* ***including*** *deterministically defined deformation zones in RVS model version L1.2. Bottom: Data representing all data* ***excluding*** *deterministically defined deformation zones in RVS model version L1.2. Statistics for elevation interval 200 m.*

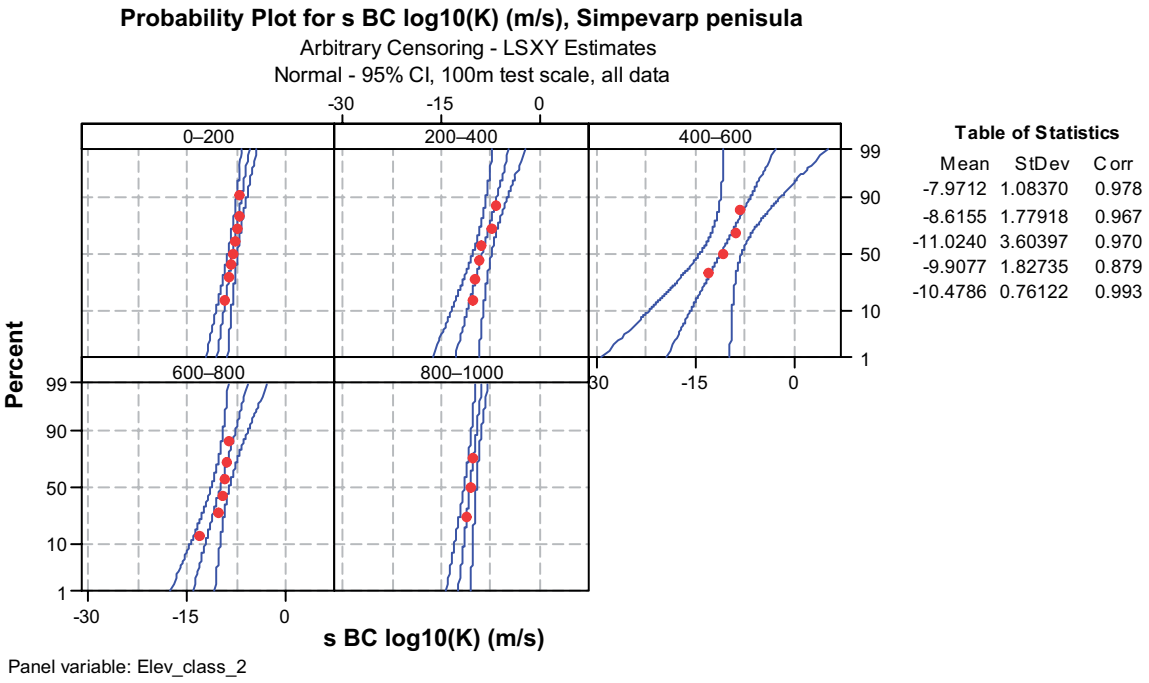

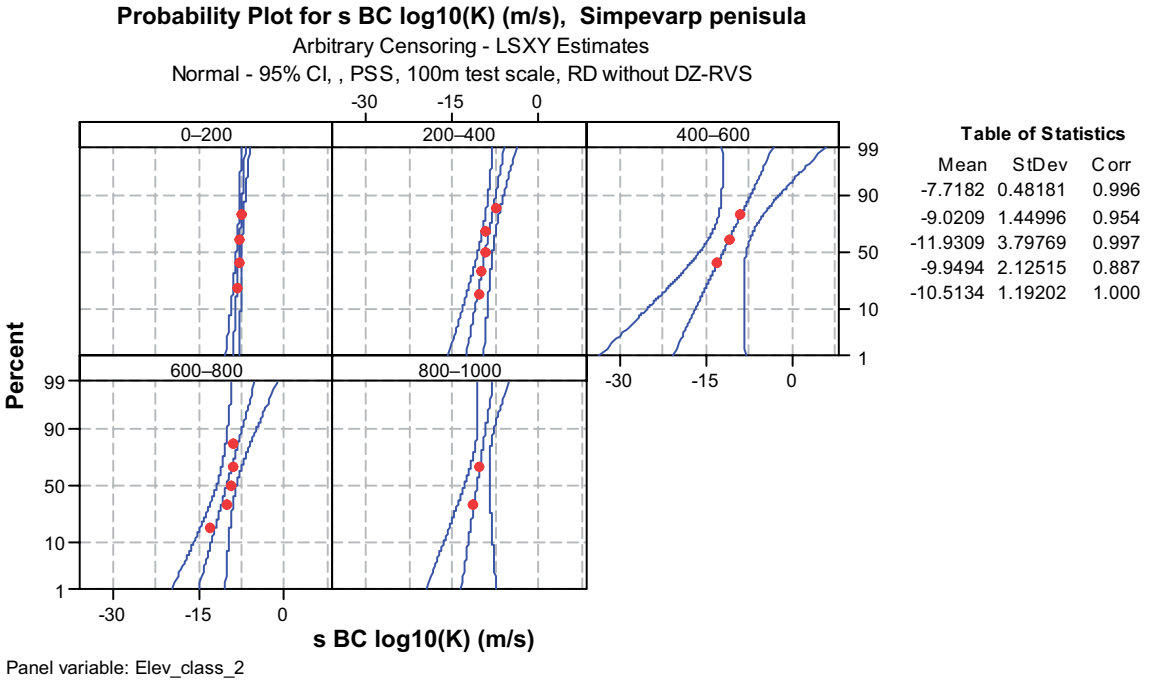

Figure A2-12. *Statistics for depth trend of the hydraulic conductivity in HRDs. Test scale 100 m. Simpevar. Top: Data representing all data* ***including*** *deterministically defined deformation zones in RVS model version L1.2. Bottom: Data representing all data* ***excluding*** *deterministically defined deformation zones in RVS model version L1.2. Statistics for elevation interval 200 m.*

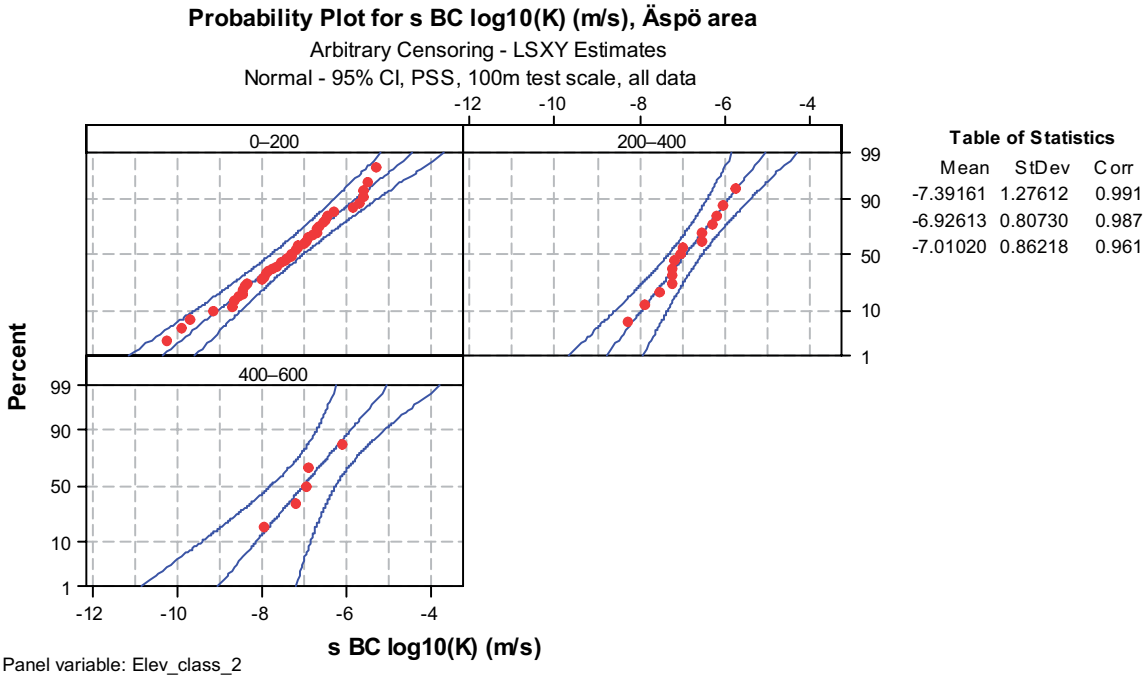

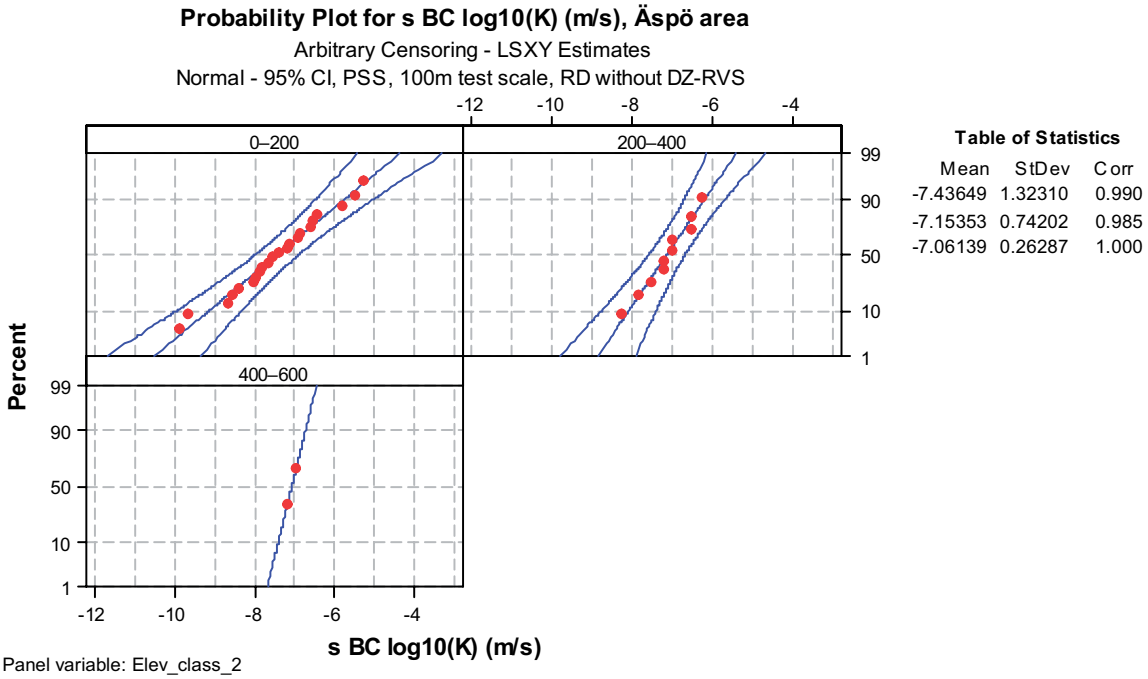

Figure A2-13. *Statistics for depth trend of the hydraulic conductivity in HRDs. Test scale 100 m. Äspör. Top: Data representing all data* ***including*** *deterministically defined deformation zones in RVS model version L1.2. Bottom: Data representing all data* ***excluding*** *deterministically defined deformation zones in RVS model version L1.2. Statistics for elevation interval 200 m.*

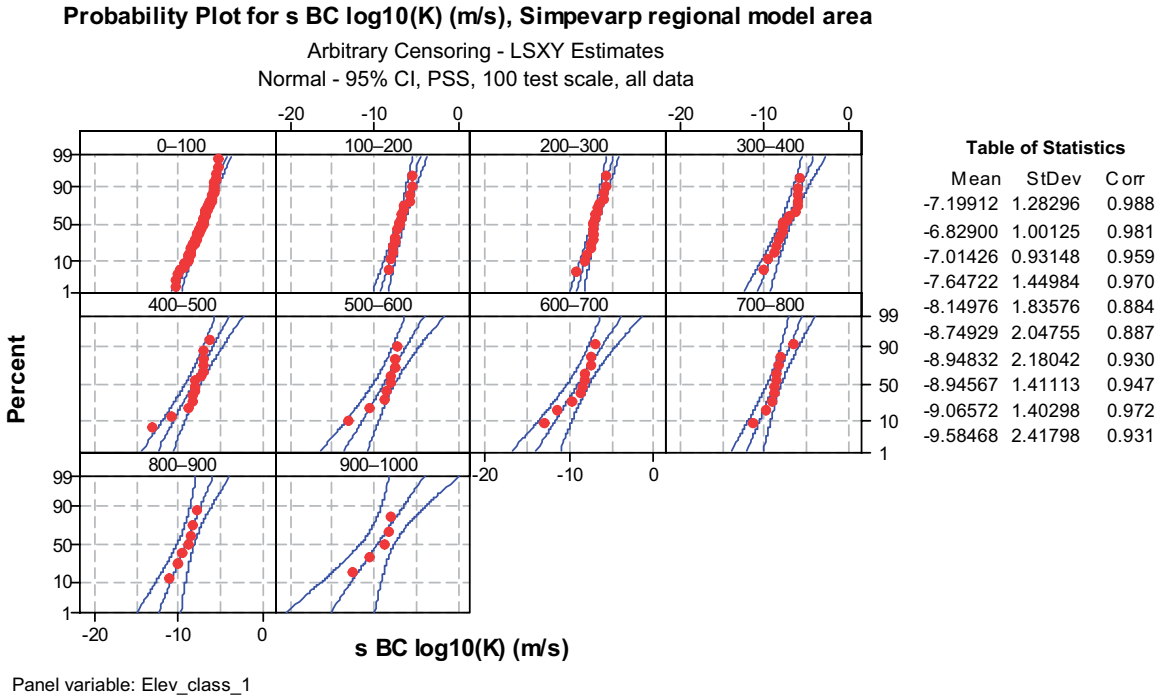

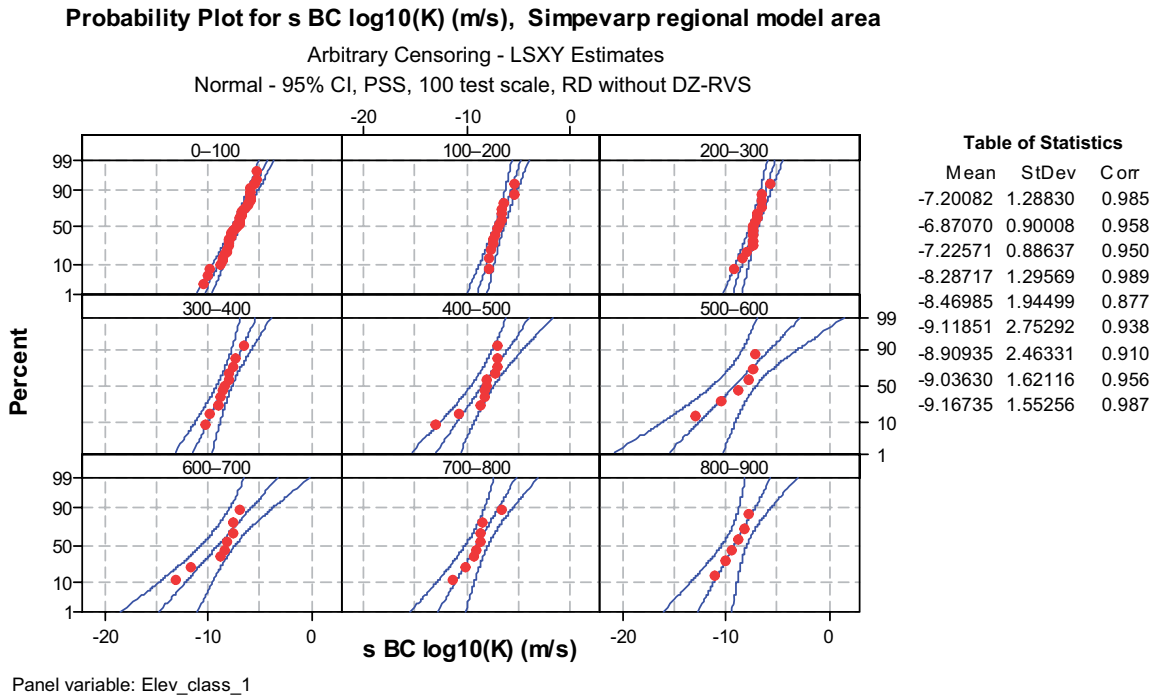

Figure A2-14. *Statistics for depth trend of the hydraulic conductivity in HRDs. Test scale 100 m. Laxemar, Simpevarp peninsula, Äspö, Ävrö-Hålö-Mjälen. Top: Data representing all data* ***including*** *deterministically defined deformation zones in RVS model version L1.2. Bottom: Data representing all data* ***excluding*** *deterministically defined deformation zones in RVS model version L1.2. Statistics for elevation interval 100 m.*

Table A2-1. Univariate statistics for hydraulic tests performed in cored boreholes in the Simpevarp area. Areas: "All": All data for SDM L1.2 , covering Aspö, Ävrö, Hålö, Mjälen Simpevarpand Laxemar, Asp: Äspö, Avr: Ävrö, Mjälen and Hålö, Simp: Simpevarp peninsula, Lax: Laxemar area. Data type: "All": all data for chosen "Area", RD-(DZ): Rock domain with test sections NOT intersecting deterministically modelled deformations zones in RVS, DZ: Rock domain with test sections intersecting deterministically modelled deformations zones in RVS. Elevation shows the interval-classes for the mid-point of the test sections. All tests sections are ca 100 except for a few in KLX02 which are around 300 m. (ch: core drilled holes, ph: percussion drilled holes).

Area	Data type	Test type	Elevation Upper limit (m)	Elevation Lower limit (m)	Test scale (m)	Sample size, all	Sample size, lower meas lim	Lower meas. limit[1] Log10 K (m/s)	K Log10(K) (m/s)	Mean Log10 K (m/s)	Std Log10 K (m/s)	Log10 Conf limits 95% (+/–)
All	All	PSS	0	1,700	100	195	5	(ph≈ –8) (ch≈ –13)		–7.57	1.44	0.203
All	All	PSS	0	200	100	93	1	(ph≈ –8) (ch≈ –13)		–7.11	1.24	0.255
All	All	PSS	200	400	100	39	0	(ph≈ –8) (ch≈ –13)		–7.26	1.20	0.389
All	All	PSS	400	600	100	25	2	(ph≈ –8) (ch≈ –13)		–8.23	1.68	0.694
All	All	PSS	600	800	100	22	1	(ph≈ –8) (ch≈ –13)		–8.83	1.75	0.776
All	All	PSS	800	1,000	100	14	1	(ph≈ –8) (ch≈ –13)		–9.11	1.71	0.987
All	All	PSS	1,000	1,700	100	2	0	(ph≈ –8) (ch≈ –13)		(–7.8)	–	–

Table A2-2. Univariate statistics for hydraulic tests performed in cored boreholes in the Simpevarp area. Areas: "All": All data for SDM L1.2 , covering Aspö, Ävrö, Hålö, Mjälen Simpevarpand Laxemar, Asp: Äspö, Avr: Ävrö, Mjälen and Hålö, Simp: Simpevarp peninsula, Lax: Laxemar area. Data type: "All": all data for chosen "Area", RD-(DZ): Rock domain with test sections NOT intersecting deterministically modelled deformations zones in RVS, DZ: Rock domain with test sections intersecting deterministically modelled deformations zones in RVS. Elevation shows the interval-classes for the mid-point of the test sections. All tests sections are ca 100 except for a few in KLX02 which are around 300 m. (ch: core drilled holes, ph: percussion drilled holes).

Area	Data type	Test type	Elevation Upper limit (m)	Elevation Lower limit (m)	Test scale (m)	Sample size, all	Sample size, lower meas lim	Lower meas. limit[1] Log10 K (m/s)	K Log10(K) (m/s)	Mean Log10 K (m/s)	Std Log10 K (m/s)	Conf.lim Log10(T) Mean±D, conf. level 0.95: D (m/s)
All	RD-(DZ)	PSS	0	1,700	100	134	3	(ph≈ –8) (ch≈ –13)		–7.68	1.46	0.249
All	RD-(DZ)	PSS	0	200	100	59	0	(ph≈ –8) (ch≈ –13)		–7.09	1.20	0.313
All	RD-(DZ)	PSS	200	400	100	28	0	(ph≈ –8) (ch≈ –13)		–7.62	1.17	0.454
All	RD-(DZ)	PSS	400	600	100	19	2	(ph≈ –8) (ch≈ –13)		–8.51	1.79	0.863
All	RD-(DZ)	PSS	600	800	100	18	1	(ph≈ –8) (ch≈ –13)		–8.83	1.97	0.980
All	RD-(DZ)	PSS	800	1,000	100	8	0	(ph≈ –8) (ch≈ –13)		–9.11	1.38	1.154
All	RD-(DZ)	PSS	1,000	1,700	100	2	0	(ph≈ –8) (ch≈ –13)		(–7.8)	–	–

Table A2-3. Univariate statistics for hydraulic tests performed in cored boreholes in the Simpevarp area. Areas: "All": All data for SDM L1.2 , covering Aspö, Ävrö, Hålö, Mjälen Simpevarpand Laxemar, Asp: Äspö, Avr: Ävrö, Mjälen and Hålö, Simp: Simpevarp peninsula, Lax: Laxemar area. Data type: "All": all data for chosen "Area", RD-(DZ): Rock domain with test sections NOT intersecting deterministically modelled deformations zones in RVS, DZ: Rock domain with test sections intersecting deterministically modelled deformations zones in RVS. Elevation shows the interval-classes for the mid-point of the test sections. All tests sections are ca 100 except for a few in KLX02 which are around 300 m. (ch: core drilled holes, ph: percussion drilled holes).

Area	Data type	Test type	Elevation Upper limit (m)	Elevation Lower limit (m)	Test scale (m)	Sample size, all	Sample size, lower meas lim	Lower meas. limit[1] Log10 K (m/s)	K Log10(K) (m/s)	Mean Log10 K (m/s)	Std Log10 K (m/s)	Conf.lim Log10(T) Mean±D, conf. level 0.95: D (m/s)
All	DZ	PSS	0	1,000	100	61	2	(ph≈ –8) (ch≈ –13)		–7.37	1.49	0.382
All	DZ	PSS	0	200	100	34	1	(ph≈ –8) (ch≈ –13)		–7.21	1.36	0.475
All	DZ	PSS	200	400	100	11	0	(ph≈ –8) (ch≈ –13)		–6.45	0.83	0.558
All	DZ	PSS	400	600	100	6	0	(ph≈ –8) (ch≈ –13)		–7.61	1.14	1.196
All	DZ	PSS	600	800	100	4	0	(ph≈ –8) (ch≈ –13)		–9.07	0.88	1.400
All	DZ	PSS	800	1,000	100	6	1	(ph≈ –8) (ch≈ –13)		–9.52	2.42	2.540

Table A2-4. Univariate statistics for hydraulic tests performed in cored boreholes in the Simpevarp area. Areas: "All": All data for SDM L1.2 , covering Aspö, Ävrö, Hålö, Mjälen Simpevarpand Laxemar, Asp: Äspö, Avr: Ävrö, Mjälen and Hålö, Simp: Simpevarp peninsula, Lax: Laxemar area. Data type: "All": all data for chosen "Area", RD-(DZ): Rock domain with test sections NOT intersecting deterministically modelled deformations zones in RVS, DZ: Rock domain with test sections intersecting deterministically modelled deformations zones in RVS. Elevation shows the interval-classes for the mid-point of the test sections. All tests sections are ca 100 except for a few in KLX02 which are around 300 m. (ch: core drilled holes, ph: percussion drilled holes).

Area	Data type	Test type	Elevation Upper limit (m)	Elevation Lower limit (m)	Test scale (m)	Sample size, all	Sample size, lower meas lim	Lower meas. limit[1] Log10 K (m/s)	K Log10(K) (m/s)	Mean Log10 K (m/s)	Std Log10 K (m/s)	Log10 Conf limits 95% (+/–)
Lax	All	PSS	0	1,700	100	70	0	(ph≈ –8) (ch≈ –13)		–7.57	1.37	0.327
Lax	All	PSS	0	200	100	24	0	(ph≈ –8) (ch≈ –13)		–6.84	1.21	0.511
Lax	All	PSS	200	400	100	14	0	(ph≈ –8) (ch≈ –13)		–7.27	1.20	0.693
Lax	All	PSS	400	600	100	10	0	(ph≈ –8) (ch≈ –13)		–8.34	1.02	0.730
Lax	All	PSS	600	800	100	13	0	(ph≈ –8) (ch≈ –13)		–8.62	1.72	1.039
Lax	All	PSS	800	1,000	100	7	0	(ph≈ –8) (ch≈ –13)		–8.46	0.61	0.564
Lax	All	PSS	1,000	1,700	100	2	0	(ph≈ –8) (ch≈ –13)		(–7.8)	–	–

Table A2-5. Univariate statistics for hydraulic tests performed in cored boreholes in the Simpevarp area. Areas: "All": All data for SDM L1.2 , covering Aspö, Ävrö, Hålö, Mjälen Simpevarpand Laxemar, Asp: Äspö, Avr: Ävrö, Mjälen and Hålö, Simp: Simpevarp peninsula, Lax: Laxemar area. Data type: "All": all data for chosen "Area", RD-(DZ): Rock domain with test sections NOT intersecting deterministically modelled deformations zones in RVS, DZ: Rock domain with test sections intersecting deterministically modelled deformations zones in RVS. Elevation shows the interval-classes for the mid-point of the test sections. All tests sections are ca 100 except for a few in KLX02 which are around 300 m. (ch: core drilled holes, ph: percussion drilled holes).

Area	Data type	Test type	Elevation Upper limit (m)	Elevation Lower limit (m)	Test scale (m)	Sample size, all	Sample size, lower meas lim	Lower meas. limit[1] Log10 K (m/s)	K Log10(K) (m/s)	Mean Log10 K (m/s)	Std Log10 K (m/s)	Conf.lim Log10(T) Mean±D, conf. level 0.95: D (m/s)
Lax	RD-(DZ)	PSS	0	1,700	100	48	0	(ph≈ –8) (ch≈ –13)		–7.77	1.42	0.412
Lax	RD-(DZ)	PSS	0	200	100	16	0	(ph≈ –8) (ch≈ –13)		–7.03	1.28	0.682
Lax	RD-(DZ)	PSS	200	400	100	9	0	(ph≈ –8) (ch≈ –13)		–7.81	0.93	0.715
Lax	RD-(DZ)	PSS	400	600	100	8	0	(ph≈ –8) (ch≈ –13)		–8.43	1.15	0.961
Lax	RD-(DZ)	PSS	600	800	100	10	0	(ph≈ –8) (ch≈ –13)		–8.65	2.09	1.495
Lax	RD-(DZ)	PSS	800	1,000	100	3	0	(ph≈ –8) (ch≈ –13)		–9.03	0.78	1.938
Lax	RD-(DZ)	PSS	1,000	1,700	100	2	0	(ph≈ –8) (ch≈ –13)		(–7.8)	–	–

Table A2-6. Univariate statistics for hydraulic tests performed in cored boreholes in the Simpevarp area. Areas: "All": All data for SDM L1.2 , covering Aspö, Ävrö, Hålö, Mjälen Simpevarpand Laxemar, Asp: Äspö, Avr: Ävrö, Mjälen and Hålö, Simp: Simpevarp peninsula, Lax: Laxemar area. Data type: "All": all data for chosen "Area", RD-(DZ): Rock domain with test sections NOT intersecting deterministically modelled deformations zones in RVS, DZ: Rock domain with test sections intersecting deterministically modelled deformations zones in RVS. Elevation shows the interval-classes for the mid-point of the test sections. All tests sections are ca 100 except for a few in KLX02 which are around 300 m. (ch: core drilled holes, ph: percussion drilled holes).

Area	Data type	Test type	Elevation Upper limit (m)	Elevation Lower limit (m)	Test scale (m)	Sample size, all	Sample size, lower meas lim	Lower meas. limit[1] Log10 K (m/s)	K Log10(K) (m/s)	Mean Log10 K (m/s)	Std Log10 K (m/s)	Log10 Conf limits 95% (+/–)
Asp	All	PSS	0	1,700	100	67	0	(ph≈ –8) (ch≈ –13)		–7.18	1.14	0.327
Asp	All	PSS	0	200	100	43	0	(ph≈ –8) (ch≈ –13)		–7.39	1.28	0.394
Asp	All	PSS	200	400	100	16	0	(ph≈ –8) (ch≈ –13)		–6.93	0.80	0.432
Asp	All	PSS	400	600	100	7	0	(ph≈ –8) (ch≈ –13)		–7.01	0.86	0.795

Table A2-7. Univariate statistics for hydraulic tests performed in cored boreholes in the Simpevarp area. Areas: "All": All data for SDM L1.2 , covering Aspö, Ävrö, Hålö, Mjälen Simpevarpand Laxemar, Asp: Äspö, Avr: Ävrö, Mjälen and Hålö, Simp: Simpevarp peninsula, Lax: Laxemar area. Data type: "All": all data for chosen "Area", RD-(DZ): Rock domain with test sections NOT intersecting deterministically modelled deformations zones in RVS, DZ: Rock domain with test sections intersecting deterministically modelled deformations zones in RVS. Elevation shows the interval-classes for the mid-point of the test sections. All tests sections are ca 100 except for a few in KLX02 which are around 300 m. (ch: core drilled holes, ph: percussion drilled holes).

Area	Data type	Test type	Elevation Upper limit (m)	Elevation Lower limit (m)	Test scale (m)	Sample size, all	Sample size, lower meas lim	Lower meas. limit[1] Log10 K (m/s)	K Log10(K) (m/s)	Mean Log10 K (m/s)	Std Log10 K (m/s)	Conf.lim Log10(T) Mean±D, conf. level 0.95: D (m/s)
Asp	RD-(DZ)	PSS	0	1,700	100	39	0	(ph≈ –8) (ch≈ –13)		–7.25	1.10	0.357
Asp	RD-(DZ)	PSS	0	200	100	23	0	(ph≈ –8) (ch≈ –13)		–7.44	1.32	0.571
Asp	RD-(DZ)	PSS	200	400	100	11	0	(ph≈ –8) (ch≈ –13)		–7.15	0.74	0.497
Asp	RD-(DZ)	PSS	400	600	100	4	0	(ph≈ –8) (ch≈ –13)		–7.06	0.26	0.414

Table A2-8. Univariate statistics for hydraulic tests performed in cored boreholes in the Simpevarp area. Areas: "All": All data for SDM L1.2 , covering Aspö, Ävrö, Hålö, Mjälen Simpevarpand Laxemar, Asp: Äspö, Avr: Ävrö, Mjälen and Hålö, Simp: Simpevarp peninsula, Lax: Laxemar area. Data type: "All": all data for chosen "Area", RD-(DZ): Rock domain with test sections NOT intersecting deterministically modelled deformations zones in RVS, DZ: Rock domain with test sections intersecting deterministically modelled deformations zones in RVS. Elevation shows the interval-classes for the mid-point of the test sections. All tests sections are ca 100 except for a few in KLX02 which are around 300 m. (ch: core drilled holes, ph: percussion drilled holes).

Area	Data type	Test type	Elevation Upper limit (m)	Elevation Lower limit (m)	Test scale (m)	Sample size, all	Sample size, lower meas lim	Lower meas. limit[1] Log10 K (m/s)	K Log10(K) (m/s)	Mean Log10 K (m/s)	Std Log10 K (m/s)	Log10 Conf limits 95% (+/–)
Simp	All	PSS	0	1,700	100	34	0	(ph≈ –8) (ch≈ –13)		–9.03	1.77	0.618
Simp	All	PSS	0	200	100	10	0	(ph≈ –8) (ch≈ –13)		–7.97	1.08	0.773
Simp	All	PSS	200	400	100	7	0	(ph≈ –8) (ch≈ –13)		–8.62	1.78	1.646
Simp	All	PSS	400	600	100	6	0	(ph≈ –8) (ch≈ –13)		–11.02	3.60	3.778
Simp	All	PSS	600	800	100	7	0	(ph≈ –8) (ch≈ –13)		–9.91	1.83	1.692
Simp	All	PSS	800	1,000	100	4	0	(ph≈ –8) (ch≈ –13)		–10.48	0.76	1.209
Simp	All	PSS	1,000	1,700	100	0	0	(ph≈ –8) (ch≈ –13)		–	–	–

Table A2-9. Univariate statistics for hydraulic tests performed in cored boreholes in the Simpevarp area. Areas: "All": All data for SDM L1.2 , covering Aspö, Ävrö, Hålö, Mjälen Simpevarpand Laxemar, Asp: Äspö, Avr: Ävrö, Mjälen and Hålö, Simp: Simpevarp peninsula, Lax: Laxemar area. Data type: "All": all data for chosen "Area", RD-(DZ): Rock domain with test sections NOT intersecting deterministically modelled deformations zones in RVS, DZ: Rock domain with test sections intersecting deterministically modelled deformations zones in RVS. Elevation shows the interval-classes for the mid-point of the test sections. All tests sections are ca 100 except for a few in KLX02 which are around 300 m. (ch: core drilled holes, ph: percussion drilled holes).

Area	Data type	Test type	Elevation Upper limit (m)	Elevation Lower limit (m)	Test scale (m)	Sample size, all	Sample size, lower meas lim	Lower meas. limit[1] Log10 K (m/s)	K Log10(K) (m/s)	Mean Log10 K (m/s)	Std Log10 K (m/s)	Conf.lim Log10(T) Mean±D, conf. level 0.95: D (m/s)
Simp	RD-(DZ)	PSS	0	1,700	100	25	0	(ph≈ –8) (ch≈ –13)		–9.27	1.71	0.706
Simp	RD-(DZ)	PSS	0	200	100	5	0	(ph≈ –8) (ch≈ –13)		–7.72	0.48	0.596
Simp	RD-(DZ)	PSS	200	400	100	6	0	(ph≈ –8) (ch≈ –13)		–9.02	1.45	1.522
Simp	RD-(DZ)	PSS	400	600	100	5	0	(ph≈ –8) (ch≈ –13)		–11.93	3.80	4.718
Simp	RD-(DZ)	PSS	600	800	100	6	0	(ph≈ –8) (ch≈ –13)		–9.95	2.13	2.235
Simp	RD-(DZ)	PSS	800	1,000	100	3	0	(ph≈ –8) (ch≈ –13)		–10.51	1.19	2.956
Simp	RD-(DZ)	PSS	1,000	1,700	100	0	0	(ph≈ –8) (ch≈ –13)		–	–	–

Table A2-10. Univariate statistics for hydraulic tests performed in cored boreholes in the Simpevarp area. Areas: "All": All data for SDM L1.2 , covering Aspö, Ävrö, Hålö, Mjälen Simpevarpand Laxemar, Asp: Äspö, Avr: Ävrö, Mjälen and Hålö, Simp: Simpevarp peninsula, Lax: Laxemar area. Data type: "All": all data for chosen "Area", RD-(DZ): Rock domain with test sections NOT intersecting deterministically modelled deformations zones in RVS, DZ: Rock domain with test sections intersecting deterministically modelled deformations zones in RVS. Elevation shows the interval-classes for the mid-point of the test sections. All tests sections are ca 100 except for a few in KLX02 which are around 300 m. (ch: core drilled holes, ph: percussion drilled holes).

Area	Data type	Test type	Elevation Upper limit (m)	Elevation Lower limit (m)	Test scale (m)	Sample size, all	Sample size, lower meas lim	Lower meas. limit[1] Log10 K (m/s)	K Log10(K) (m/s)	Mean Log10 K (m/s)	Std Log10 K (m/s)	Conf.lim Log10(T) Mean±D, conf. level 0.95: D (m/s)
All	All	PSS	0	1,700	100	195	5	(ph≈ –8) (ch≈ –13)		–7.57	1.44	0.203
All	All	PSS	0	100	100	74	0	(ph≈ –8) (ch≈ –13)		–7.20	1.28	0.297
All	All	PSS	100	200	100	19	1	(ph≈ –8) (ch≈ –13)		–6.83	1.00	0.482
All	All	PSS	200	300	100	21	0	(ph≈ –8) (ch≈ –13)		–7.01	0.93	0.423
All	All	PSS	300	400	100	18	0	(ph≈ –8) (ch≈ –13)		–7.65	1.45	0.721
All	All	PSS	400	500	100	15	1	(ph≈ –8) (ch≈ –13)		–8.15	1.84	1.019
All	All	PSS	500	600	100	10	1	(ph≈ –8) (ch≈ –13)		–8.75	2.05	1.466
All	All	PSS	600	700	100	11	1	(ph≈ –8) (ch≈ –13)		–8.95	2.18	1.465
All	All	PSS	700	800	100	11	0	(ph≈ –8) (ch≈ –13)		–8.95	1.41	0.947
All	All	PSS	800	900	100	8	0	(ph≈ –8) (ch≈ –13)		–9.07	1.40	1.170
All	All	PSS	900	1,000	100	6	1	(ph≈ –8) (ch≈ –13)		–9.58	2.42	2.540
All	All	PSS	1,000	1,700	100	2	0	(ph≈ –8) (ch≈ –13)		(–7.8)	–	–

Table A2-11. Univariate statistics for hydraulic tests performed in cored boreholes in the Simpevarp area. Areas: "All": All data for SDM L1.2 , covering Aspö, Ävrö, Hålö, Mjälen Simpevarpand Laxemar, Asp: Äspö, Avr: Ävrö, Mjälen and Hålö, Simp: Simpevarp peninsula, Lax: Laxemar area. Data type: "All": all data for chosen "Area", RD-(DZ): Rock domain with test sections NOT intersecting deterministically modelled deformations zones in RVS, DZ: Rock domain with test sections intersecting deterministically modelled deformations zones in RVS. Elevation shows the interval-classes for the mid-point of the test sections. All tests sections are ca 100 except for a few in KLX02 which are around 300 m. (ch: core drilled holes, ph: percussion drilled holes).

Area	Data type	Test type	Elevation Upper limit	Elevation Lower limit	Test scale	Sample size, all	Sample size, lower meas lim	Lower meas. limit[1] Log10 K	K Log10(K)	Mean Log10 K	Std Log10 K	Conf.lim Log10(T) Mean±D, conf. level 0.95: D
			(m)	(m)	(m)			(m/s)	(m/s)	(m/s)	(m/s)	(m/s)
All	RD-(DZ)	PSS	0	1,700	100	134	3	(ph≈ –8) (ch≈ –13)		–7.68	1.46	0.249
All	RD-(DZ)	PSS	0	100	100	44	0	(ph≈ –8) (ch≈ –13)		–7.20	1.29	0.392
All	RD-(DZ)	PSS	100	200	100	15	0	(ph≈ –8) (ch≈ –13)		–6.87	0.90	0.498
All	RD-(DZ)	PSS	200	300	100	16	0	(ph≈ –8) (ch≈ –13)		–7.22	0.88	0.469
All	RD-(DZ)	PSS	300	400	100	12	0	(ph≈ –8) (ch≈ –13)		–8.29	1.30	0.826
All	RD-(DZ)	PSS	400	500	100	12	1	(ph≈ –8) (ch≈ –13)		–8.47	1.94	1.233
All	RD-(DZ)	PSS	500	600	100	7	1	(ph≈ –8) (ch≈ –13)		–9.12	2.75	2.543
All	RD-(DZ)	PSS	600	700	100	9	1	(ph≈ –8) (ch≈ –13)		–8.90	2.46	1.891
All	RD-(DZ)	PSS	700	800	100	9	0	(ph≈ –8) (ch≈ –13)		–9.03	1.62	1.245
All	RD-(DZ)	PSS	800	900	100	7	0	(ph≈ –8) (ch≈ –13)		–9.17	1.55	1.434
All	RD-(DZ)	PSS	900	1,000	100	1	0	(ph≈ –8) (ch≈ –13)	(–8.8)	–	–	–
All	RD-(DZ)	PSS	1,000	1,700	100	2	0	(ph≈ –8) (ch≈ –13)		(–7.8)	–	–

Appendix 3

Depth trends of hydraulic conductivity in rock mass, test scale 10–20–30 m

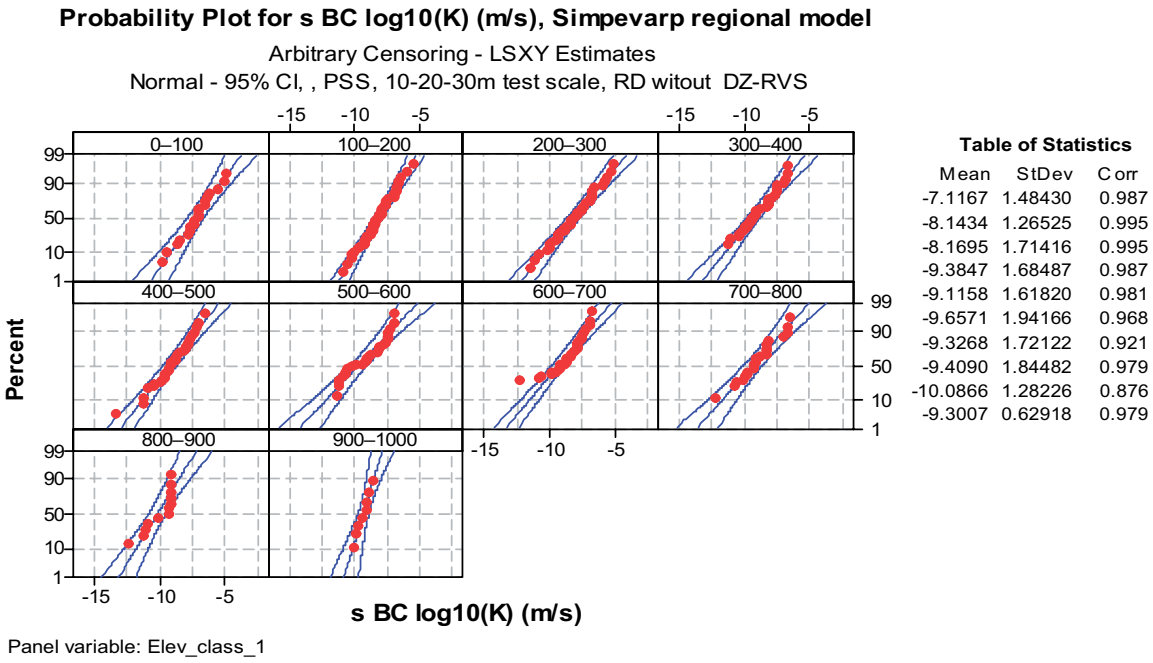

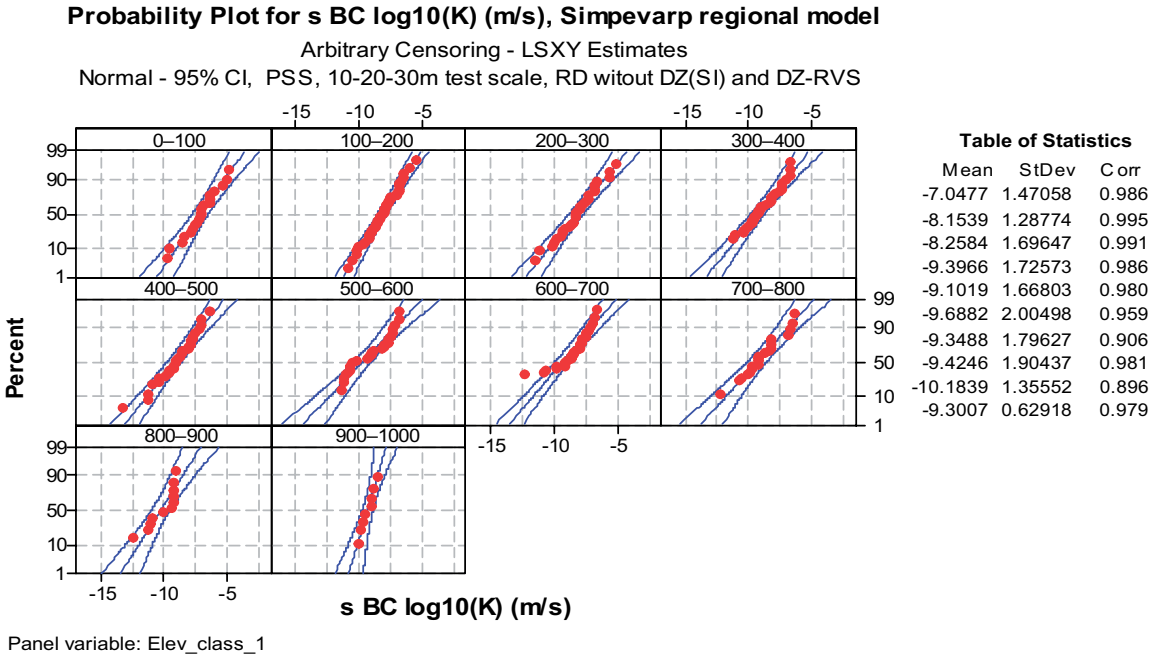

Figure A3-1. *Statistics for depth trend of the hydraulic conductivity in HRDs. Test scale 100 m. Laxemar, Simpevarp peninsula, Äspö, Ävrö-Hålö-Mjälen. Top: Data representing all data* ***excluding*** *deterministically defined deformation zones in RVS model version L1.2. Bottom: Data representing all data* ***excluding*** *deterministically defined deformation zones in RVS model version L1.2and deformations zones in the geological single-hole interpretation.*

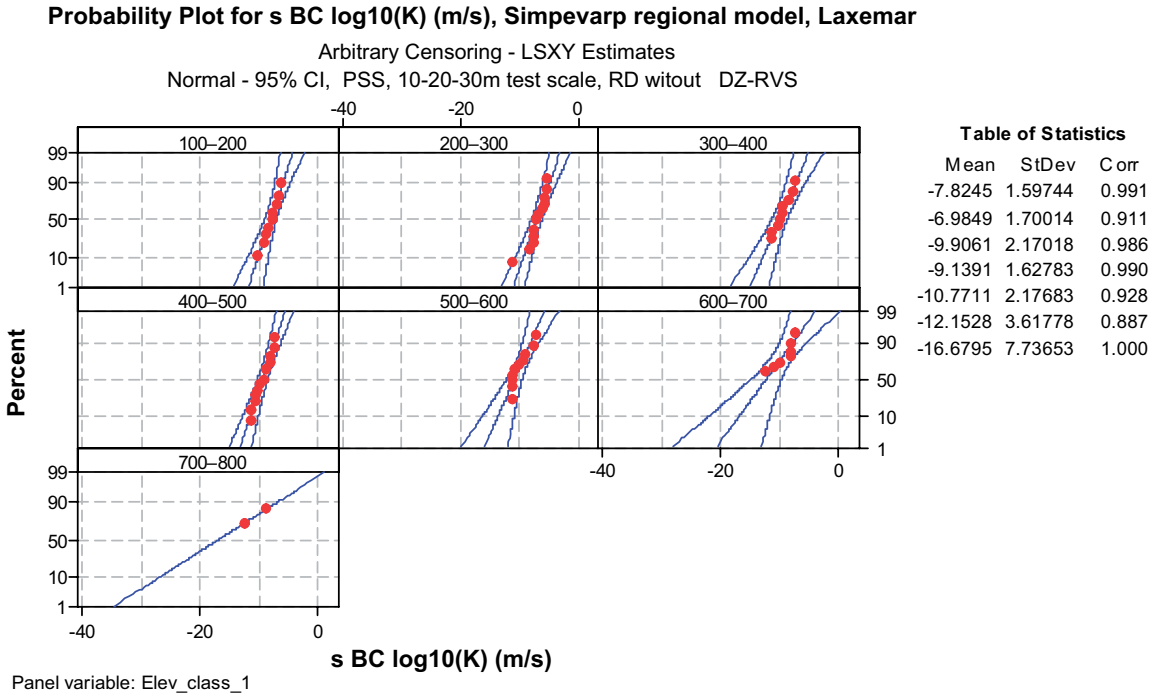

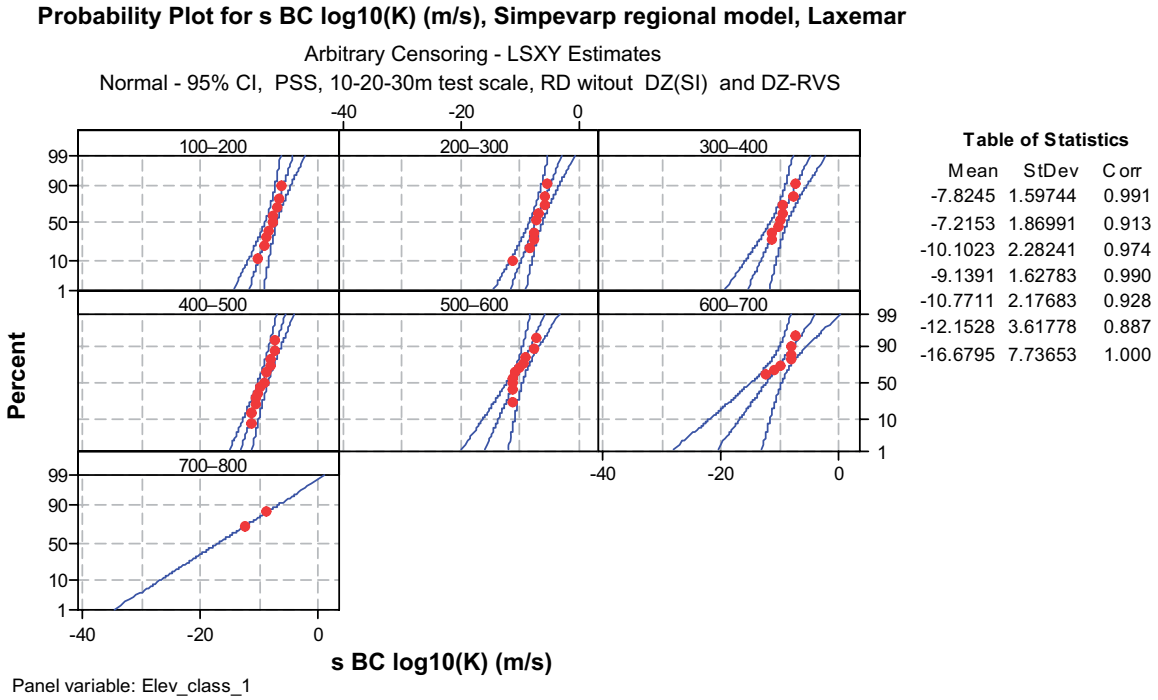

Figure A3-2. *Statistics for depth trend of the hydraulic conductivity in HRDs. Test scale 100 m. Laxemar area. Top: Data representing all data* ***excluding*** *deterministically defined deformation zones in RVS model version L1.2. Bottom: Data representing all data* ***excluding*** *deterministically defined deformation zones in RVS model version L1.2and deformations zones in the geological single-hole interpretation.*

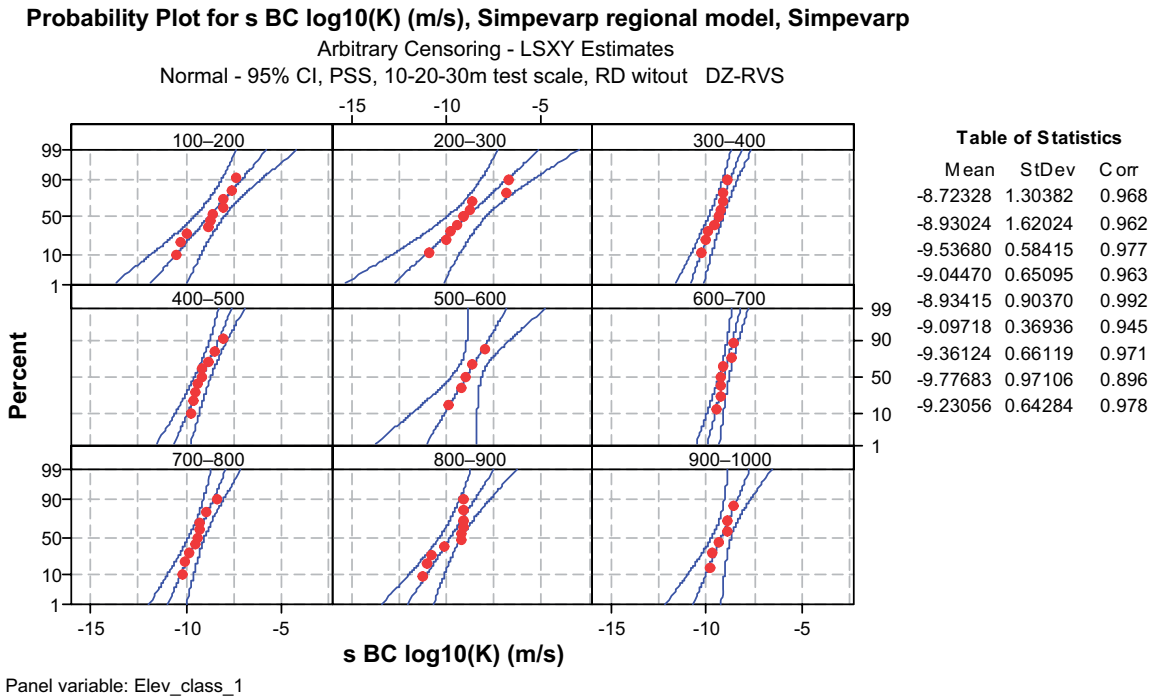

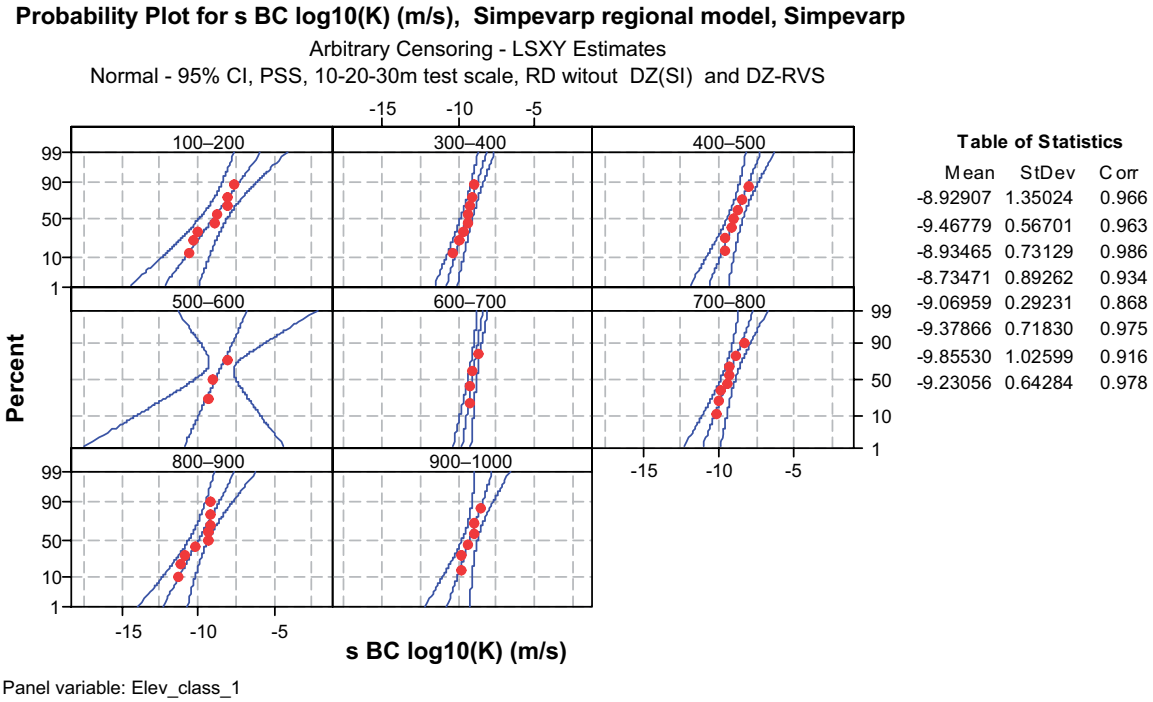

Figure A3-3. *Statistics for depth trend of the hydraulic conductivity in HRDs. Test scale 100 m. Simpevarp peninsula. Top: Data representing all data* ***excluding*** *deterministically defined deformation zones in RVS model version L1.2. Bottom: Data representing all data* ***excluding*** *deterministically defined deformation zones in RVS model version L1.2and deformations zones in the geological single-hole interpretation.*

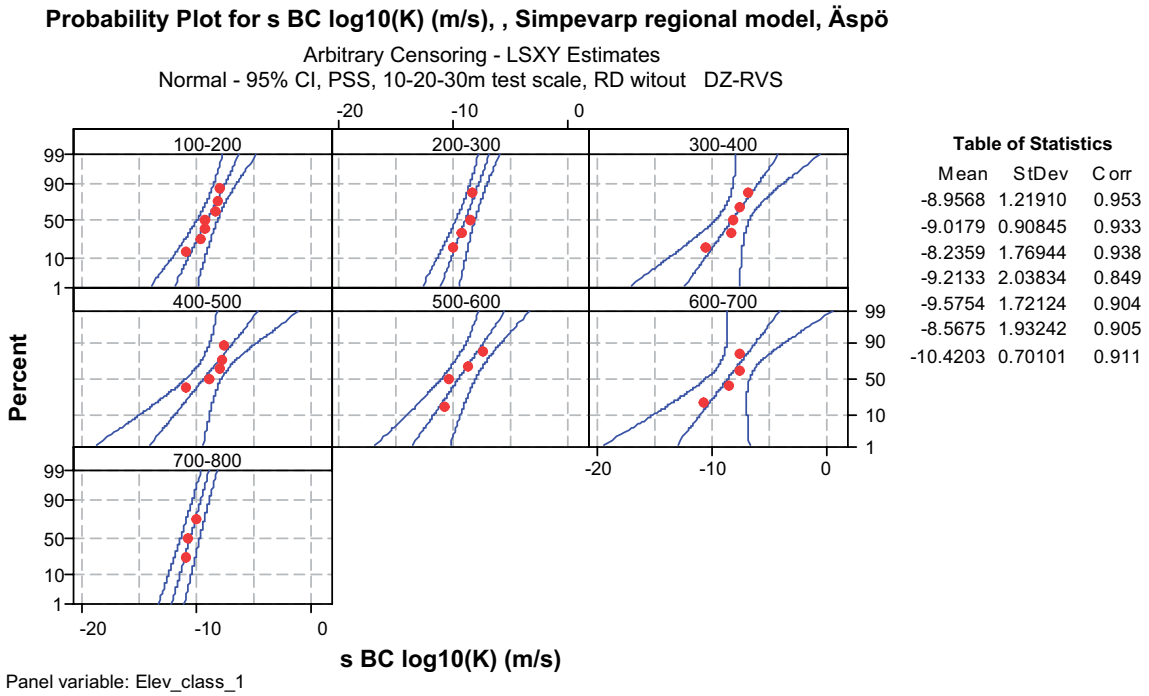

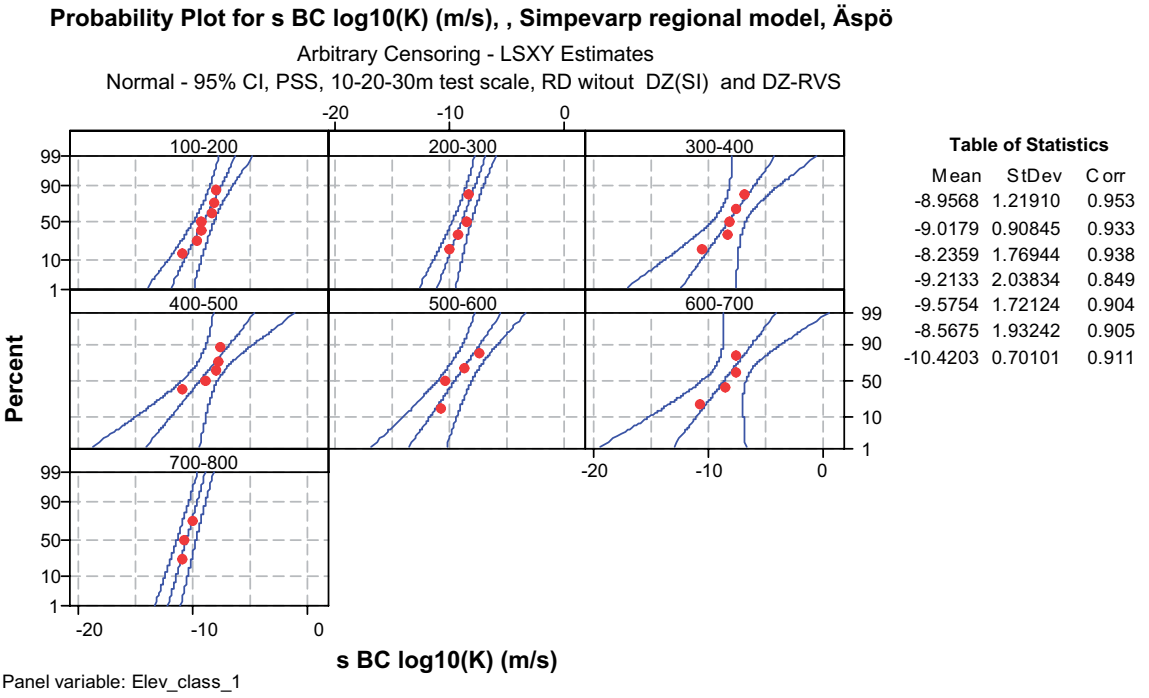

Figure A3-4. *Statistics for depth trend of the hydraulic conductivity in HRDs. Test scale 100 m. Äspö area. Top: Data representing all data* ***excluding*** *deterministically defined deformation zones in RVS model version L1.2. Bottom: Data representing all data* ***excluding*** *deterministically defined deformation zones in RVS model version L1.2and deformations zones in the geological single-hole interpretation.*

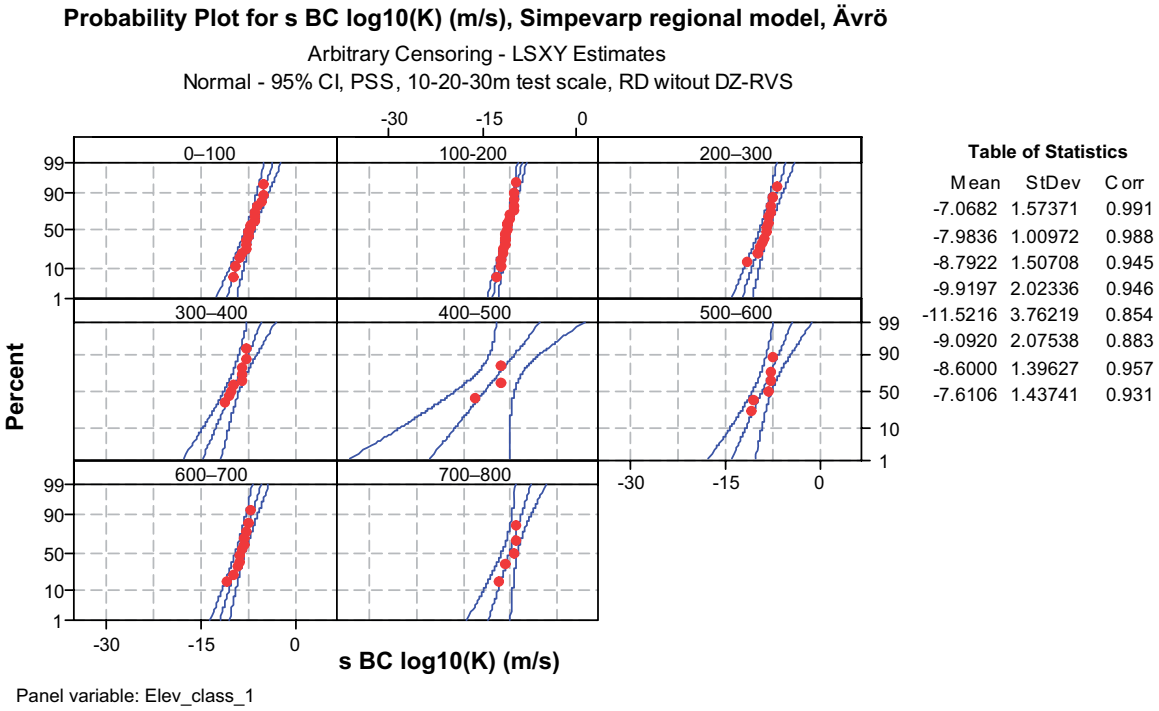

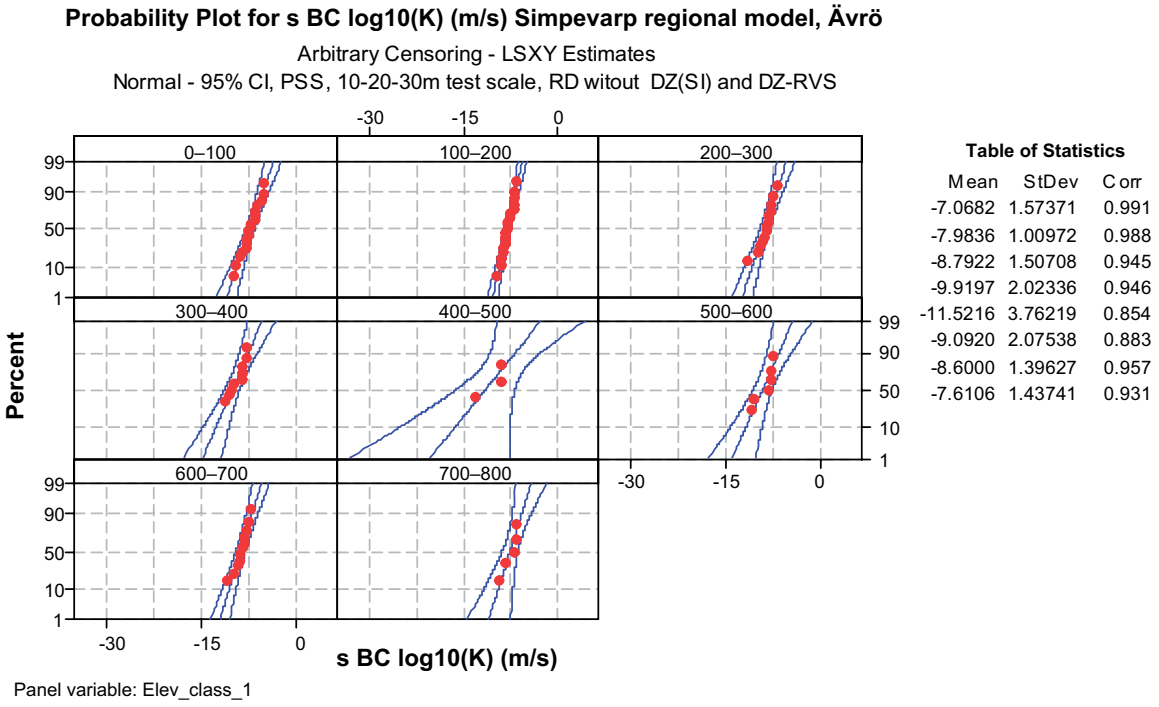

Figure A3-5. *Statistics for depth trend of the hydraulic conductivity in HRDs. Test scale 100 m. Ävrö-Hålö-Mjälen area. Top: Data representing all data* ***excluding*** *deterministically defined deformation zones in RVS model version L1.2. Bottom: Data representing all data* ***excluding*** *deterministically defined deformation zones in RVS model version L1.2and deformations zones in the geological single-hole interpretation.*

Appendix 4

Hydraulic conductivity in rock domains, test scales 100 m and 10–20–30 m

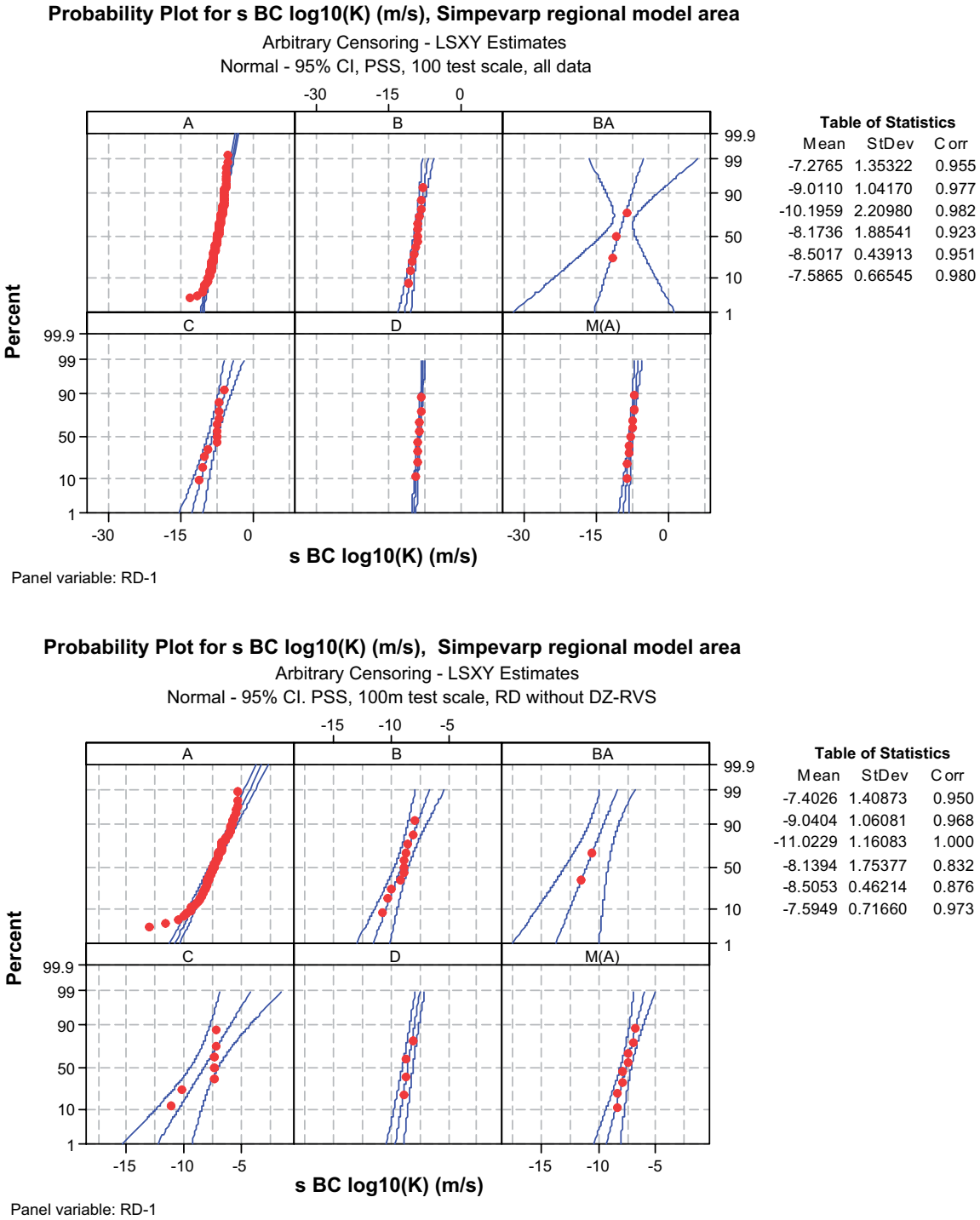

Figure A4-1. *Statistics of the hydraulic conductivity of rock domains. Test scale 100 m. Data from Laxemar, Simpevarp peninsula, Äspö, Ävrö-Hålö-Mjälen. Top: All data, Bottom: Data representing all data* ***excluding*** *deterministically defined deformation zones in RVS model version L1.2.*

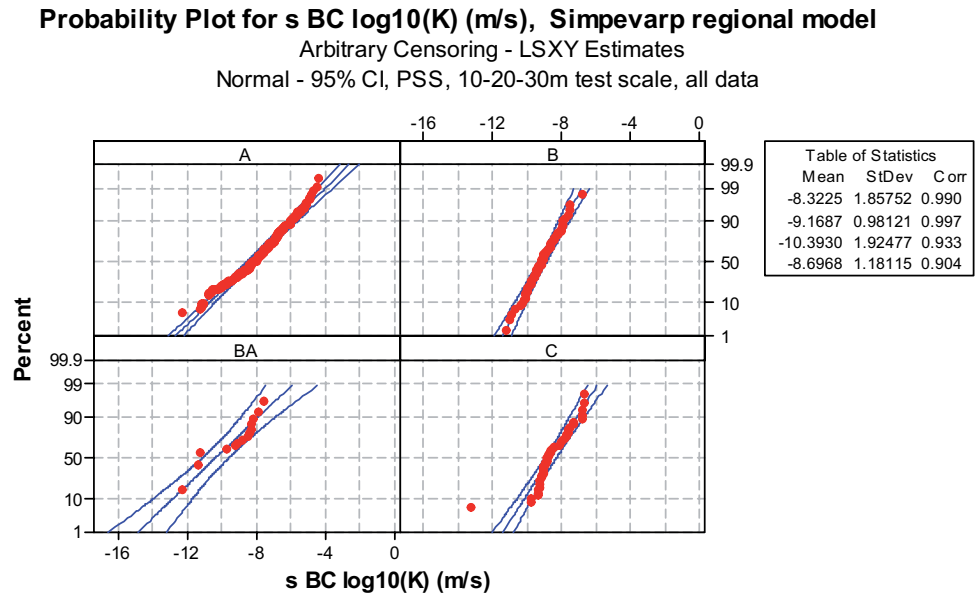

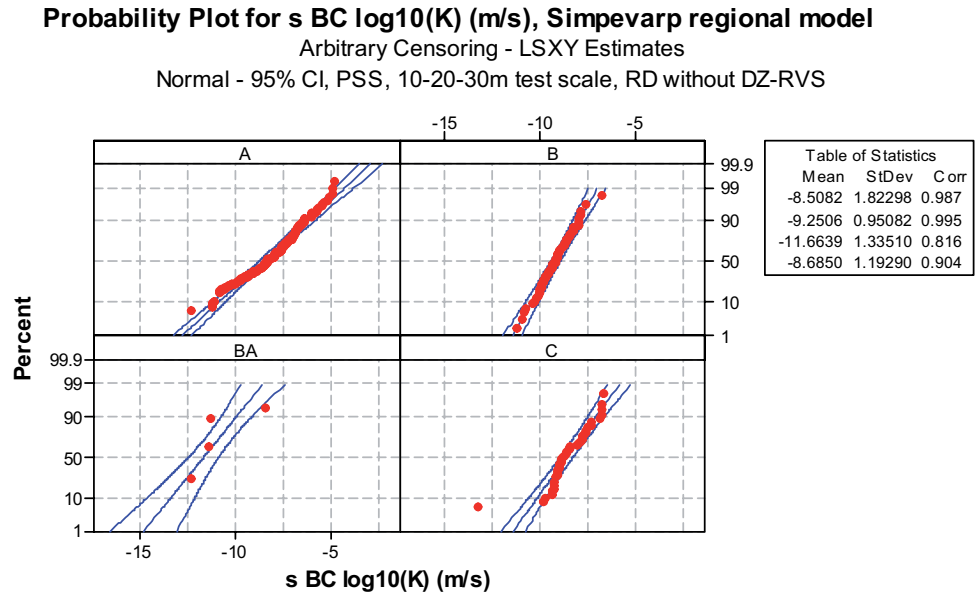

Figure A4-2. *Statistics of the hydraulic conductivity of rock domains. Test scale 10–20–30 m. Data from Laxemar, Simpevarp peninsula, Äspö, Ävrö-Hålö-Mjälen. Top: All data, Bottom: Data representing all data* ***excluding*** *deterministically defined deformation zones in RVS model version L1.2.*

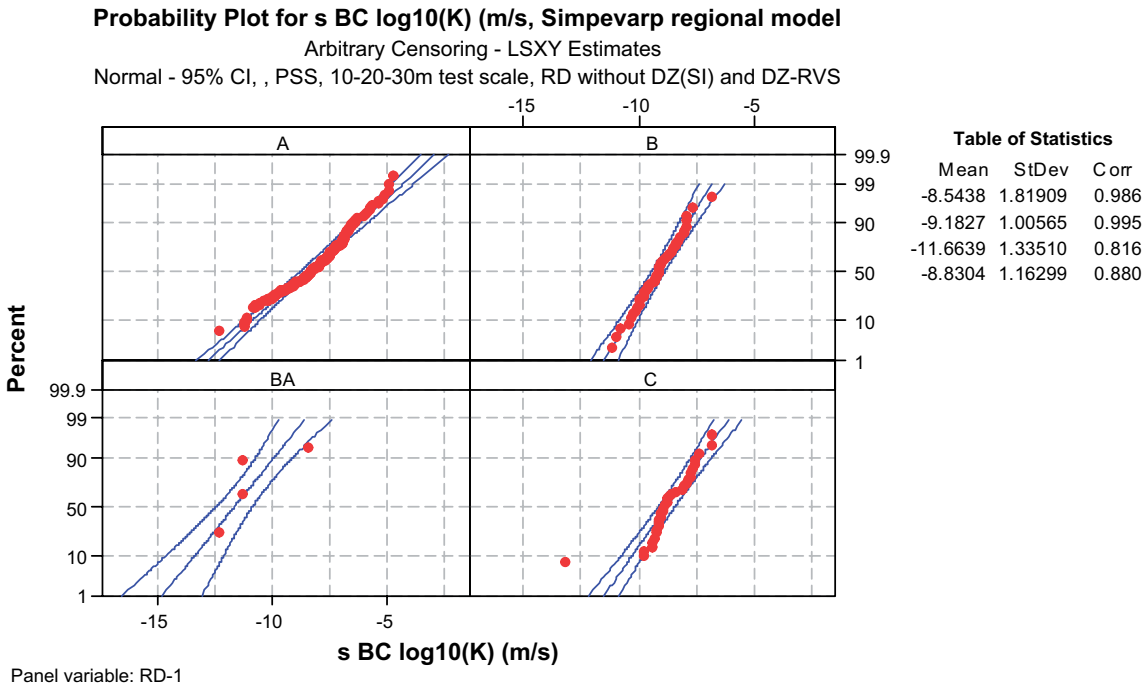

Figure A4-3. *Statistics of the hydraulic conductivity of rock domains. Test scale 10–20–30 m. Data from Laxemar, Simpevarp peninsula, Äspö, Ävrö-Hålö-Mjälen. Top: All data, Bottom: Data representing all data* ***excluding*** *deterministically defined deformation zones in RVS model version L1.2 and deformation zones defined in the geological single-hole interpretation.*

Appendix 5

Götemar granite

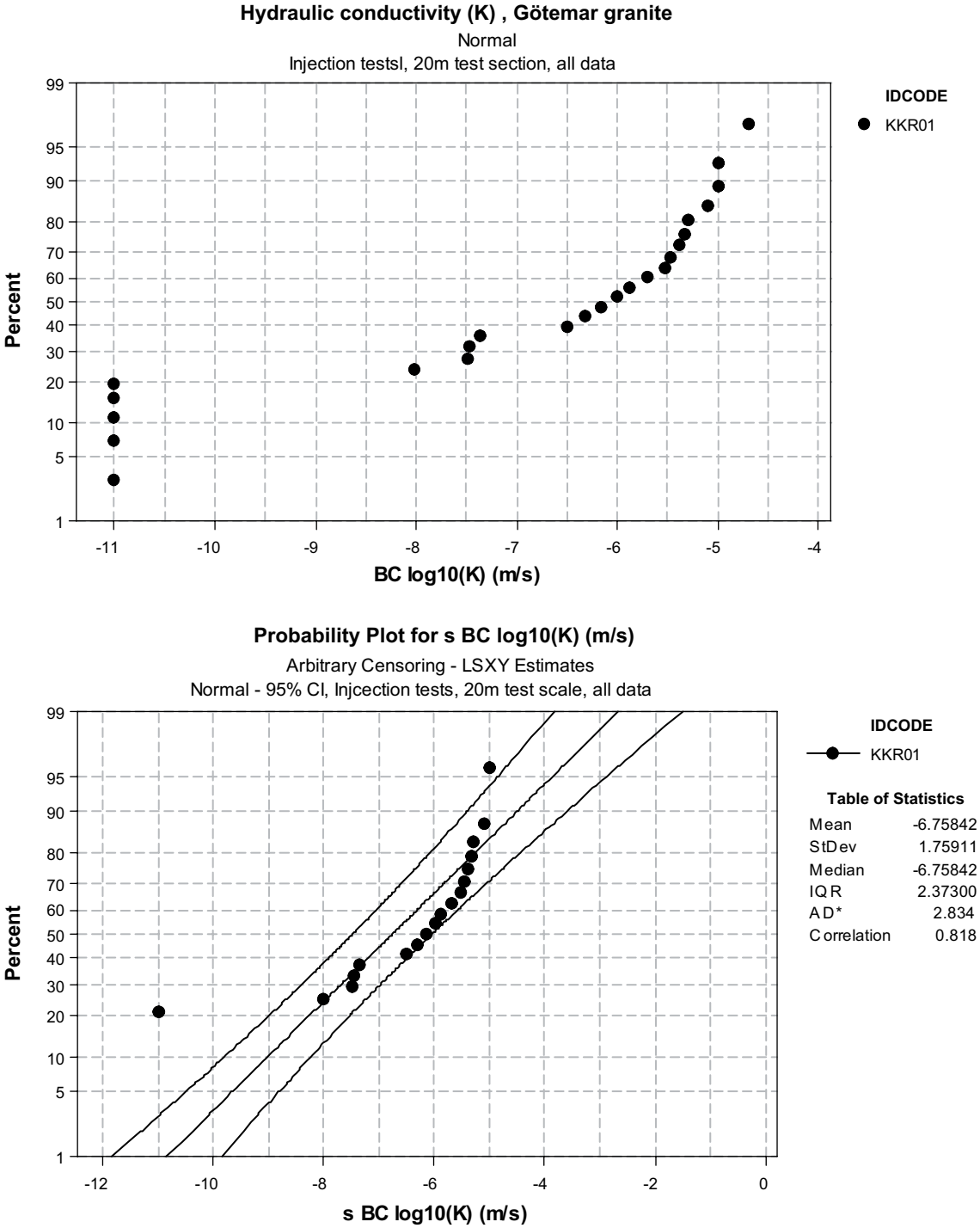

Figure A5-1. *Statistics of the hydraulic conductivity in the Götemar granite. Test scale 20 m. Top: All data. Bottom: Statistical distribution.*

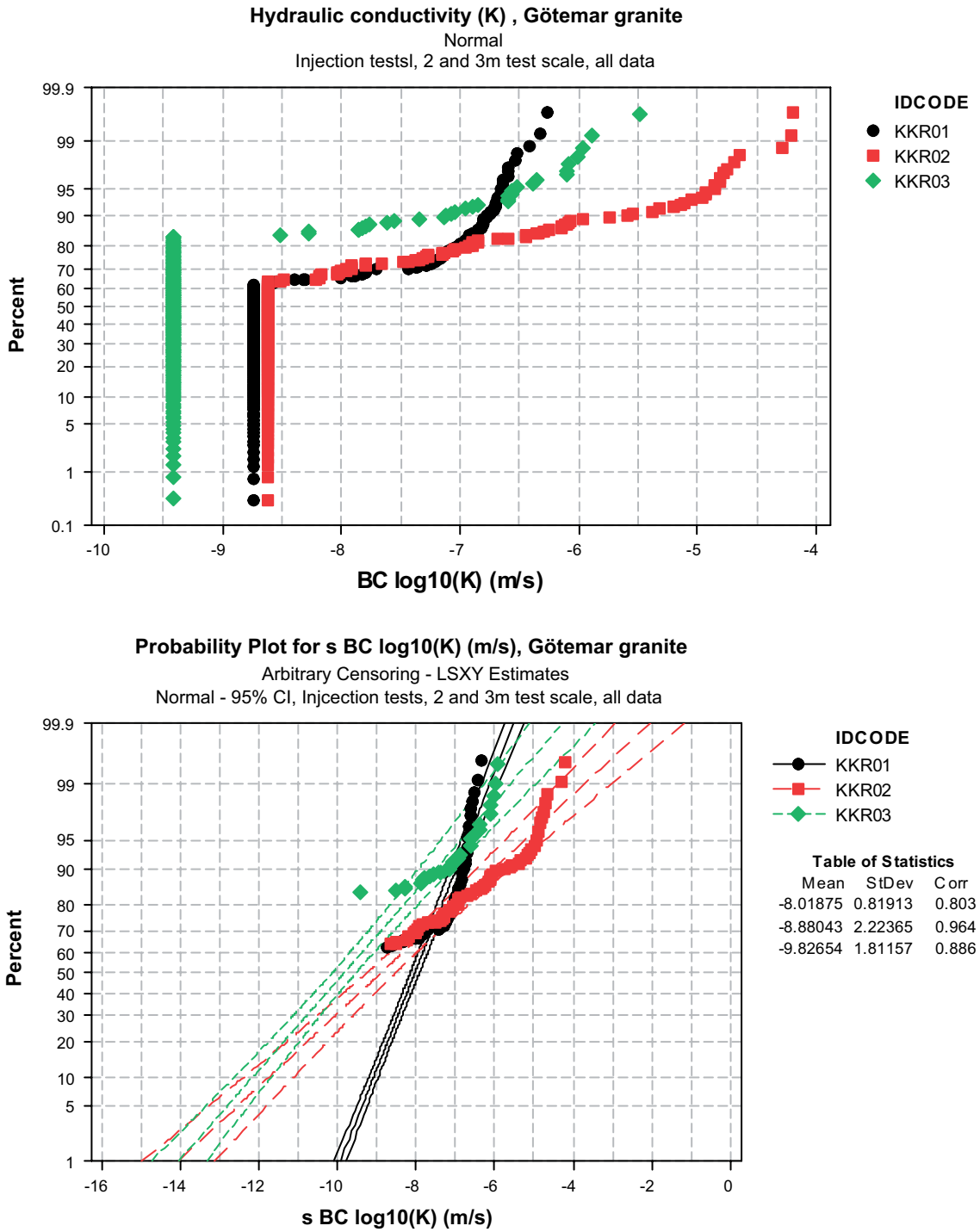

Figure A5-2. *Statistics of the hydraulic conductivity in the Götemar granite. Test scale 2 and 3 m. Top: All data. Bottom: Statistical distribution.*

PFL-f transmissivity

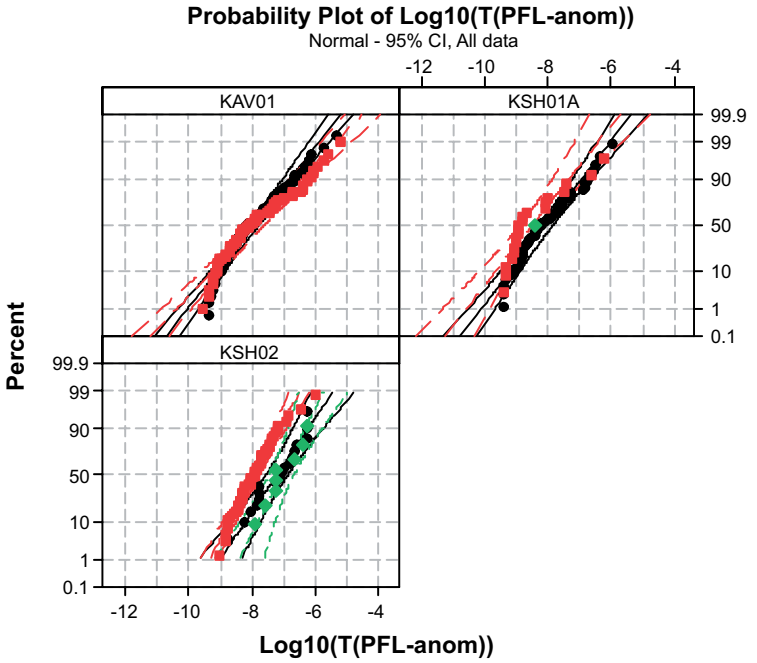

Panel variable: IDCODE

KAV01

Mean	StDev	N	AD	P
-7.940	0.8912	106	1.010	0.011
-7.843	1.086	75	1.193	<0.005
*	*	0	*	

KSH01A

Mean	StDev	N	AD	P
-8.045	0.8813	60	0.784	0.040
-8.484	0.9053	21	1.427	<0.005
*	*	1	*	

KSH02

Mean	StDev	N	AD	P
-7.206	0.7529	18	0.404	0.319
-7.907	0.6020	56	0.350	0.461
-7.057	0.5681	8	0.351	0.371

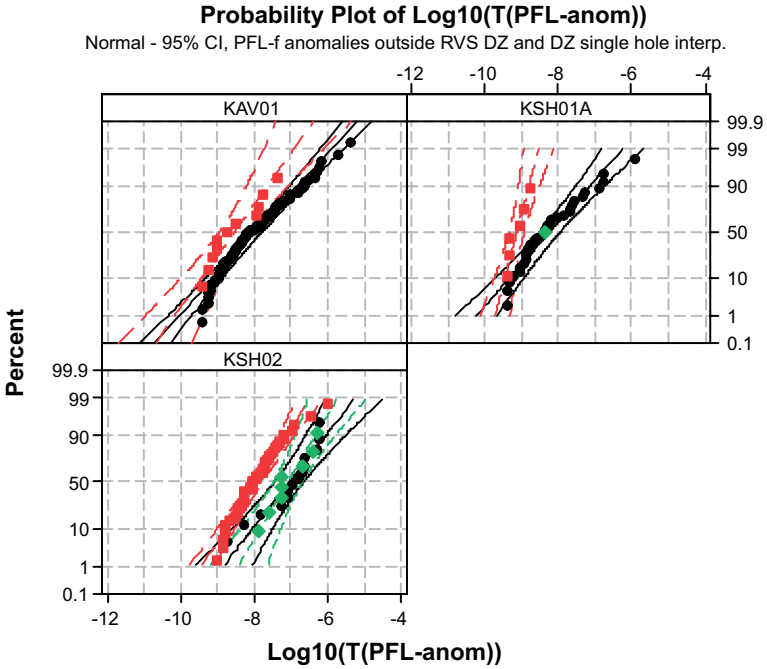

Panel variable: IDCODE

KAV01

Mean	StDev	N	AD	P
-7.940	0.8912	106	1.010	0.011
-8.522	0.6994	11	0.487	0.176
*	*	0	*	

KSH01A

Mean	StDev	N	AD	P
-8.250	0.8574	34	0.687	0.066
-9.144	0.2572	6	0.347	0.340
*	*	1	*	

KSH02

Mean	StDev	N	AD	P
-7.024	0.7589	14	0.598	0.097
-7.926	0.6275	50	0.411	0.329
-7.057	0.5681	8	0.351	0.371

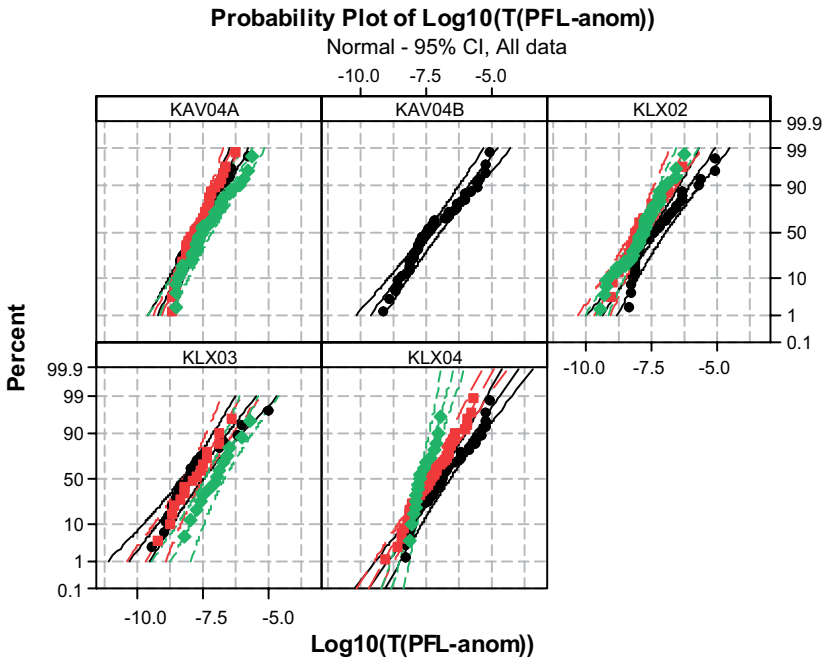

Panel variable: IDCODE

Elevation

Class

0-300

300-700

700-

KAV04A

Mean	StDev	N	AD	P
-7.587	0.6639	43	0.720	0.056
-7.657	0.5748	52	0.450	0.266
-7.289	0.7712	39	0.437	0.283

KAV04B

Mean	StDev	N	AD	P
-7.211	1.044	54	0.891	0.021
*	*	0	*	
*	*	0	*	

KLX02

Mean	StDev	N	AD	P
-7.233	0.9287	37	1.135	<0.005
-7.932	0.7494	21	0.354	0.429
-7.872	0.7448	44	0.426	0.302

KLX03

Mean	StDev	N	AD	P
-7.809	1.046	25	0.848	0.025
-7.773	0.7811	16	0.169	0.920
-6.959	0.7209	14	0.110	0.991

KLX04

Mean	StDev	N	AD	P
-6.824	0.9159	53	0.591	0.117
-7.303	0.7808	59	0.343	0.480
-7.622	0.3779	17	0.698	0.056

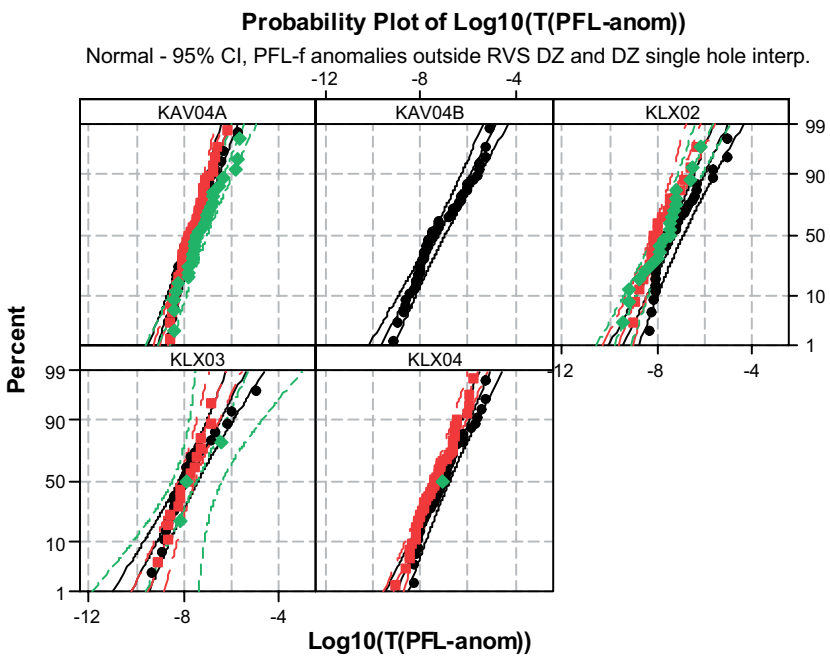

Panel variable: IDCODE

Elev_Class_3

0-300

300-700

700-

KAV04A

Mean	StDev	N	AD	P
-7.587	0.6639	43	0.720	0.056
-7.657	0.5748	52	0.450	0.266
-7.252	0.7792	31	0.370	0.404

KAV04B

Mean	StDev	N	AD	P
-7.211	1.044	54	0.891	0.021
*	*	0	*	
*	*	0	*	

KLX02

Mean	StDev	N	AD	P
-7.237	0.9489	32	1.135	<0.005
-7.932	0.7494	21	0.354	0.429
-7.770	0.8935	21	0.376	0.380

KLX03

Mean	StDev	N	AD	P
-7.809	1.046	25	0.848	0.025
-7.870	0.7020	15	0.211	0.825
-7.437	0.9423	3	0.355	0.174

KLX04

Mean	StDev	N	AD	P
-7.011	0.8459	44	0.496	0.203
-7.347	0.7703	51	0.300	0.570
*	*	1	*	

Appendix 7

Transmissivity in HCD, individual observations

Def_zone	BH	RVS geometrical sec-up m	RVS geometrical sec-low m	Bh-DZ Geol target_ sec-up m	Bh-DZ geol target_ sec-low m	BH-DZ Elev. sec-mid m	BH-DZ Depth sec-mid m	Elevation surface m	Bh-T Hydro sec-up m	Bh-T Hydro sec-low m	Transm. (T) (m^2/s)	Log10(T) (m^2/s)	Comment T
ZSMEW002A	HAS10	49.33	49.33			-37	43.376	6.376	0	125	2.60E-08	-7.59E+00	
ZSMEW002A	HLX02	123.45	123.45			-101	110.035	9.035	0	132	2.20E-06	-5.66E+00	
ZSMEW002A	KAS03	307	495	280	480	-389	397.818	8.818	283	523	5.40E-06	-5.27E+00	Sum 30 inj. tests
ZSMEW002A	KLX06	300	430	300	400	-289	306.68	17.68	307	415	8.00E-05	-4.10E+00	100m WL-test
ZSMEW002A	HLX20	60	185			-96	107.179	11.179	9	202	3.80E-05	-4.42E+00	
ZSMEW007A	KLX01	972	1044	1000	1020	-995	1011.77	16.77	926	1077.99	1.50E-05	-4.82E+00	100m test
ZSMEW007A	KLX02	234	311	265	275	-252	270.4	18.4	204	344	2.22E-04	-3.65E+00	Sum 20m PPS-tests
ZSMEW007A	KLX04	314	391	346	355	-326	350.09	24.09	345.44	365.44	5.60E-05	-4.25E+00	
ZSMEW007A	HLX10	34.39	34.39			-20	31.737	11.737	0	85	1.60E-04	-3.80E+00	
ZSMEW007A	HLX13	14.19	66.01			-17	34.391	17.391	11.87	200	3.47E-07	-6.46E+00	
ZSMEW007A	HLX14	35.43	35.43			-16	33.113	17.113	11.9	115.9	1.17E-05	-4.93E+00	
ZSMEW007A	HLX24					-74	86.7	12.7	9.1	175.2	7.29E-04	-3.14E+00	
ZSMEW007A	HLX22					-70	80	10	9.1	163.2	2.20E-04	-3.66E+00	
ZSMEW009A	HAS14	0.2	49			-22	23.698	1.698			2.50E-05	-4.60E+00	
ZSMEW009A	HAS21	25	57			-33	36.068	3.068			1.60E-05	-4.80E+00	
ZSMEW009A	KAS06	59	76	60	75	-53	58.188	5.188			3.80E-06	-5.42E+00	
ZSMEW009A	TASA			1407	1421	-195.6	195.6	0			1.40E-05	-4.85E+00	Geom mean SA1420A,B, HA1405A,B
ZSMEW013A	KA1755A	188	234	180	230	-341.592	346.592	5	99	297.8	5.00E-05	-4.30E+00	
ZSMEW013A	KAS04	100	185	87	158	-110	121.688	11.688	102	202	5.00E-06	-5.30E+00	
ZSMEW013A	HLX03	0	19			2	8.453	10.453	0	100	2.80E-06	-5.55E+00	
ZSMEW013A	HAS18	110.95	110.95			-92	99.564	7.564	0	150	6.20E-07	-6.21E+00	
ZSMEW013A	HAS01	4	100			-39	45.408	6.408	0	100	5.80E-09	-8.24E+00	
ZSMEW014A	HLX02	5.16	5.16			4.5	4.535	9.035	0	132	2.20E-06	-5.66E+00	
ZSMEW038A	HAV05	20	38			-16.9	23.758	6.858	0	100	1.10E-06	-5.96E+00	
ZSMEW038A	KAS09	220	239	249	253	-193	197.108	4.108	303	450	2.90E-04	-3.54E+00	
ZSMEW038A	KBH02	538	547			-175	180.528	5.528	408	706.35	4.32E-04	-3.36E+00	Assumed that T for NE-1 (2.18E-4) can be subtracted
ZSMEW038A	TASA			1180		-162.835	162.835	0			1.58E-03	-2.80E+00	Sum of pair- mean SA-holes
ZSMEW039A	HLX05	24	24			-5.247	20.954	15.707	0	100	5.50E-07	-6.26E+00	
ZSMEW900A	HLX25	169	182	166	185	-135	155.656	20.656	6.12	202.5	2.20E-04	-3.66E+00	
ZSMEW900A	HLX14	11	29			-1	18.113	17.113	11.9	115.9	1.17E-05	-4.93E+00	
ZSMNE004A	TASA			302	334	-43.676	43.676	0	289	327	2.80E-06	-5.55E+00	Sum SA0289A, SA327A
ZSMNE005A	KA1755A	22	288	95	140	-292.627	297.627	5	99	201.7	4.90E-05	-4.31E+00	
ZSMNE005A	KA1754A	26	160 (Base)	90	115	-278.371	283.371	5	0	159.9	4.20E-06	-5.38E+00	
ZSMNE005A	KA1751A	45	150 (Base)	110	114	-245.789	250.789	5	0	150	2.60E-05	-4.59E+00	
ZSMNE005A	KAS04	2	464	131	437	-187.5	199.188	11.688	0	481	2.40E-05	-4.62E+00	
ZSMNE005A	KA3590G02	20	30 (Base)	19	30	-465.363	470.363	5	0.39	30.05	1.90E-07	-6.72E+00	IPR-01-65
ZSMNE005A	KAS02			795	924	-849	856.7	7.7	802	924.04	2.50E-04	-3.60E+00	
ZSMNE005A	KAS12	0 (Top)	269	19	286	-120	124.858	4.858	0	303	3.40E-05	-4.47E+00	sum 100 tests
ZSMNE005A	HLX09	99	151 (Base)			-108	111.31	3.31	0	151	2.70E-04	-3.57E+00	
ZSMNE006A	HLX18	105.38	105.38			-85	89.036	4.036	15.12	181.2	4.58E-05	-4.34E+00	
ZSMNE006A	KA1061	94	209 (Base)	198	209	-143.076	143.076	0	160	208.5	4.80E-04	-3.32E+00	
ZSMNE006A	KA1131B	47	203 (Base)	173	203	-184.078	184.078	0	92.1	203.1	4.00E-05	-4.40E+00	
ZSMNE006A	KAS07	402	602 (Base)	497	602	-422	426.608	4.608	462	604	1.60E-05	-4.80E+00	
ZSMNE006A	KAS08	440	590	537	601	-412	419.688	7.688	447	601	1.30E-04	-3.89E+00	
ZSMNE006A	KAS09	53	225	50	112	-116	120.108	4.108	0	305	1.00E-03	-3.00E+00	sum 100m tests
ZSMNE006A	KAS11	115	249 (Base)	156	220	-177	181.25	4.25	99	249	4.10E-04	-3.39E+00	
ZSMNE006A	KAS14	38	194	51	91	-96	99.378	3.378	0	212	9.60E-04	-3.02E+00	
ZSMNE006A	KBH02	543	706 (Base)	667	706	-192	197.528	5.528	408	706.35	4.32E-04	-3.36E+00	Assumed that T for NE-1 (2.18E-4) can be subtracted
ZSMNE006A	KAS02	740	924 (Base)	806	914	-821	828.708	7.708	802	924.04	2.50E-04	-3.60E+00	
ZSMNE006A	KAS16	228	439	380	430	-324	327.688	3.688	302.6	501.18	4.20E-04	-3.38E+00	sum 100m tests
ZSMNE006A	TASA			1240	1325	-177.185	177.185	0	1273	1286	4.13E-04	-3.38E+00	7 HA-probeholes
ZSMNE012A	HAV02	90	163 (Base)	90	150	-120	126.108	6.108	0	93	1.40E-04	-3.85E+00	
ZSMNE012A	HAV13	0	121			-50	52.215	2.215	11.87	200	3.47E-07	-6.46E+00	
ZSMNE012A	HLX018	0 (Top)	181 (Base)	16	181	-72	76.036	4.036	15.12	181.2	4.58E-05	-4.34E+00	
ZSMNE012A	HMJ01	0 (Top)	46 (Base)			-18	19.413	1.413	0	46	3.34E-04	-3.48E+00	
ZSMNE012A	KAV01	401	630	400	580	-501	515.1	14.1	401.78	582.1	2.55E-05	-4.59E+00	Sum of 5m PFLtests
ZSMNE012A	KAV03	188	248	164	232	-209	217.738	8.738	160	225	6.91E-04	-3.16E+00	Sum of 5m Inj.tests
ZSMNE012A	KAV04A	745	947	840	900	-833	843.35	10.35	840.84	895.95	1.72E-06	-5.76E+00	Sum of 5m PFLtests
ZSMNE012A	KBH02	107	245	140	194	-87	92.528	5.528	192	304	3.00E-05	-4.52E+00	
ZSMNE012A	TASA			827		-113.416	113.416	0	813	850	1.27E-04	-3.90E+00	Sum of pair- mean SA-holes, SA0792A -SA850B
ZSMNE015A	KSH01A	974.12	974.12			-936	941.32	5.32	899	999	3.90E-09	-8.41E+00	
ZSMNE016A	SA0344A					-49	49	0			8.50E-06	-5.07E+00	
ZSMNE016A	SA0344B					-49	49	0			1.50E-07	-6.82E+00	
ZSMNE024A	KSH01A	542	669	540	631	-583	588.32	5.32	540	640	1.43E-06	-5.84E+00	Sum 20m tests
ZSMNE024A	KSH03A	175	258	162	275	-178	182.17	4.17	102.5	301	3.64E-04	-3.44E+00	Sum 100m tests
ZSMNE024A	KAV01A	674	757 (Base)	680	757	-100	114.1	14.1	677	732	1.00E-08	-8.00E+00	PFL 5m, Low values, uncertain property.
ZSMNE024A	KAV04A	937	1004 (Base)	940	1004	-956	966.35	10.35	936	996	1.00E-09	-9.00E+00	PFL 5m, Low values, uncertain property.
ZSMNE031A	KSH01A	682	704	687	693	-668	673.32	5.32	680	700	8.20E-09	-8.09E+00	20m test
ZSMNE031A	KSH03A	282	297	287	292	-240	244.17	4.17	201	301	1.58E-04	-3.80E+00	Impossible to separtae from ZSMNE024A. Highly uncertain value
ZSMNE040A	HLX04	21	82			-38	48.361	10.361	0	125	5.89E-09	-8.23E+00	
ZSMNE040A	HLX01	0	30			-4	12.9	8.9	0	100	9.00E-05	-4.05E+00	
ZSMNS017B	HA1960A					-267	272	5			8.60E-05	-4.07E+00	
ZSMNS017B	SA1997A					-272	277	5			1.10E-04	-3.96E+00	
ZSMNS017B	SA2009A					-273	278	5			2.20E-08	-7.66E+00	
ZSMNS017B	SA2025B					-276	281	5			2.10E-04	-3.68E+00	
ZSMNS017B	SA2074B					-281	286	5			1.30E-03	-2.89E+00	
ZSMNS017B	SA2090B					-283	288	5			7.00E-04	-3.15E+00	
ZSMNS017B	SA2109B					-285	290	5			2.90E-05	-4.54E+00	
ZSMNS017B	KC0045F					-439	444	5	249	266.7	1.10E-04	-3.96E+00	
ZSMNS017B	KA2048B	6	67	28	46	-281.905	286.905	5	28	29	1.00E-04	-4.00E+00	Est. From Q and T from deeper part of bh. PR25-94-06
ZSMNW025A	HSH01A	170	197	160	171	-170	172.864	2.864	12.03	200	1.16E-07	-6.94E+00	
ZSMNW028A	HAV09	72	96	75	105	-81	83.172	2.172	14.9	200	3.55E-07	-6.45E+00	
ZSMNW042A	KLX05	747	960			-672	689.63	17.63	692.95	905.05	4.25E-07	-6.37E+00	
ZSMNW048A	HLX07	44	44			-30.272	38.884	8.612	0	100	3.00E-05	-4.52E+00	
ZSMNW928A	KLX02	764.8	764.8			-746	764.4	18.4	704	804	6.90E-07	-6.16E+00	
ZSMNW928A	KLX04	898.56	898.56			-869	893.09	24.09	886.11	986.11	8.20E-07	-6.09E+00	
ZSMNW929A	KLX02	778	935	770	960	-832	850.4	18.4	704	1004	1.95E-06	-5.71E+00	Sum 100m tests
ZSMNW929A	KLX04	861	986	873	973	-895	919.09	24.09	886.11	986.11	8.20E-07	-6.09E+00	
ZSMNW932A	KLX03	505				-470	488.49	18.49	497.02	599.89	3.11E-06	-5.51E+00	
ZSMNW932A	KLX05	624				-549	566.63	17.63	614.65	695.46	2.48E-07	-6.61E+00	